THE AMPLIFICATION OF TSUNAMIS BY MERCURY BAY, NEW ZEALAND

A thesis

submitted in fulfilment

of the requirements for the degree

of

Master of Philosophy

In Earth and Ocean Sciences

at

The University of Waikato

by

ANDI YULIANTI RAMLI

THE UNIVERSITY OF
WAIKATO
Te Whare Wānanga o Waikato

2012

ABSTRACT

The east coast of New Zealand is exposed to tsunami hazards, which are generated by both distant and near tsunamigenic sources. The impact of tsunami varies along the coast depending on the source region and the amount of local attenuation or amplification. Some regions have consistently amplified historic tsunami, including Mercury Bay on the east coast of the Coromandel Peninsula. Whitianga, located in the Mercury Bay, is now the fastest growing population centre in the Coromandel Region; hence, tsunami hazard is of particular concern. The natural resonance periods (*eigen* periods) of Mercury Bay are determined by its geometry and depth, and tsunami waves that enter the Bay will be amplified when their frequencies match the resonant frequencies of the Bay. The combination of tide levels with the amplified tsunami waves may lead to a destruction of the moored vessels and many coastal facilities. To date, amplification within the bay has mostly increased the trough depth, while having little effect on the crest height.

This study assesses the tsunami hazard in Mercury Bay in response to a tsunami generated along the Kermadec subduction margin (Kermadec Trench). Even though historically, the Kermadec Trench has never produced a hazardous tsunami affecting the eastern coast of New Zealand, it is still important to develop an assessment of the worst scenarios of earthquake generated tsunamis from this source. In particular, the Sumatra 2004 and Tohuku 2011 tsunami events have suggested that a magnitude M_w 9 to 9.5 subduction megathrust earthquake is a plausible scenario.

Merian's formula was used to obtain the natural resonant period of Mercury Bay and 17 scenarios of tsunamigenic earthquakes were simulated using the tsunami model COMCOT version 1.7. Those scenarios included the recent various combination of the Kermadec earthquake, and hypothetical earthquakes that rupture the northern, middle, southern parts of Kermadec Trench. The results demonstrate that most of the initial tsunami waves generated by Kermadec Trench earthquakes are negative waves that arrive in the Bay within 56 to 158 minutes of the earthquake. This may explain the observed historical pattern of enhanced amplification of the troughs. However, significant amplification of the crests, producing waves that would threaten Whitianga Township, are generated by Kermadec earthquakes with magnitudes greater than M_w 8.5.

From the spectral analysis of each tsunami model, Mercury Bay showed a consistent response of about 52 minutes dominant period. This period is also shown as the period of the Mercury Bay when tsunami is absent. In response to distant tsunamis, it seems that the geometry of the Mercury Bay control their periods as they enter the bay. Both the 2011 Tohoku and 2010 Chilean Events have the dominant periods close to the Mercury Bay period at 47 and 51 minutes respectively.

ACKNOWLEDGEMENTS

All praises to Allah, the Almighty for I have successfully completed my MPhil study.

I would like to express my gratitude to all those who gave me the possibility to complete this thesis.

Firstly, I am deeply indebted to my Chief Supervisor Dr. Willem P. de Lange who was abundantly helpful, invaluable assistance and encouragement in completing my research and writing of this thesis. I also thank my Secondary Supervisor Dr. Karin Bryan for her comments and suggestions in refining my thesis.

My deepest gratitude to Dr. Gegar Prasetya for his helps in COMCOT model and for his countless supports to me and my family here in New Zealand. May Allah bless you and your family, Amien.

Thanks to graduate fellows Rafael Guedes and Bryna Flaim for the MATLAB tips. I really appreciate you guys for your patient in assisting me and answering my excessively silly questions. I thank Catherina Liu for helping me with the maps. Without all of you guys, this study would not have been successful. Special thanks also for my friend Varvara Vetrova who's always there for my mathematical questions and be patient for my jokes.

Thanks also due to the Department of Earth and Sciences, University of providing the laboratory facilities. I thank Sydney Wright for her kindness and being very helpful with my queries and various requests.

To the families of Pak Deni Sidharta, Pak Eryansyah, Pak Agung Sedayu, van Wering, Pak Dede Sumirat, Pak Ilham Junaid and the Indonesian Family Society in Hamilton, Ibu Afina Burhanuddin in Wellington and Charlotte Esser in Auckland, from my first days in New Zealand, thank you for the supports, togetherness and friendship among us.

Especially, I would like to present my deepest appreciation to my mother and my in-law; my life would not be successful without your sincere prays. I am forever grateful to my husband the most patient person in my hard days; his help and of his understanding that I can finish my study, and my beloved sons Farrel, Mikhail and Omar for their unconditional affection to me .

This thesis is dedicated to my father; he is the role model of my life.

TABLE OF CONTENTS

LIST OF FIGURES

LIST OF TABLES

Chapter 1 - INTRODUCTION

The tragedy of 2004 Indian Ocean tsunami, the 2010 Chilean Earthquake, and the 2011 Tohoku tsunami made obvious the vulnerability of coastal populations to this deadly natural disaster and illustrated the need for effective forecasting. In the aftermath of the tsunami, the acceleration of development and implementation of more advanced tsunami forecast system worldwide has become a major priority in the scientific and disaster management communities. Predicting when and where the next tsunami will strike is currently impossible. Once the tsunami is generated, forecasting tsunami arrival and impact is possible through modelling and measurement technologies. Various forecast systems are being developed and implemented in many coastal nations.

The eastern coast of New Zealand is the region which is most exposed to tsunamis threats from several sources. Historically, this country has been affected by more than 40 tsunamis in the last 165 years (Berryman, 2005). Even though the heights of historic tsunami waves that struck New Zealand region was generally small, people still need to be warned and prepared. Any increase in maximum water level might cause an impact to coastal structures and habitats. Therefore, it is important for the emergency managers and coastal planners to incorporate tsunami in risk management and community education, as the limited inundation observed for historic events is likely to be repeated.

The study area, Whitianga, is located on the east coast of the North Island, within the Mercury Bay on the Coromandel Peninsula, and has experienced 7 large tsunamis and several smaller ones since 1840. The large events include sources in South America (1868, 1877, 1960 and 2010), Indonesia (1883) and the North Pacific (1952 and 1964). Larger tsunami amplitudes in Mercury Bay than the adjacent open coastline characterized all of these events. Whitianga is now the fastest growing population centre in the Coromandel Region, but remains relatively isolated, so that tsunami inundation is considered a major threat.

This study will refer to the worst-case scenario a near-field tsunami source generated by an earthquake at the Kermadec Subduction Zone, and two recent far-field tsunamis the 2010 Chilean and 2011 Tohoku events. The COrnell Multi-grid COupled Tsunami (COMCOT) model will be employed for simulating scenarios, and the results will be used to examine the hazard to the area around Mercury Bay. The tsunami initial condition, maximum wave height, arrival time, wave period, and tsunami characteristics in Mercury Bay area is addressed and discussed.

1.1. Aim and Objectives

The aim of this research is to model the response of Mercury Bay due to a hypothetical earthquake generated tsunami from the Kermadec Subduction Zone, as proposed by Power et al. (2011), for magnitude 8.5 to 9.5 earthquakes scenarios. Specific objectives include:

1) Collate instrumental data of the tidal gauge in Whitianga Wharf, Mercury Bay.
2) Identify the seiche modes and periods for Mercury Bay.
3) Utilize existing numerical models for Mercury Bay and Whitianga to simulate the interaction of tides and tsunami waves by the worst-scenario earthquake.
4) Conduct spectral analysis for the modelled and measured tsunamis and compare them with the background spectra of Mercury Bay.

1.2 Study Area

Mercury Bay is a large V-shaped bay on the eastern coast of the Coromandel Peninsula on the North Island of New Zealand (Figure 1-1). The mouth of Mercury Bay is about 3.7 km across, and the coastline extends some 20 km. On the shore of this bay is the resort town of Whitianga, and a natural harbour is formed by an arm of the bay which extends inland a further six kilometers southward. Several small islets are located at the southern and northern extremities of the bay, and the Mercury Islands are 10 km to the north.

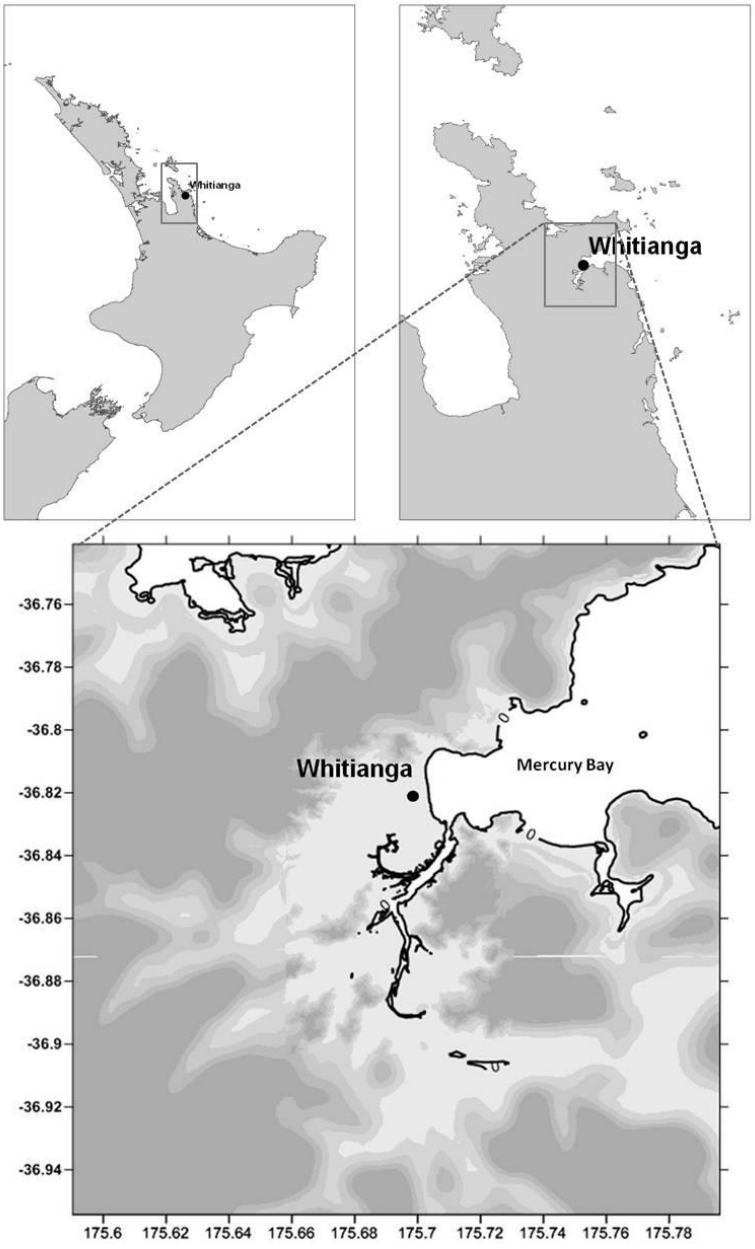

Figure 1-1. Mercury Bay and Whitianga Township location map.

The study area, Mercury Bay is a headland controlled semi-enclosed composite embayment within the greater Mercury Bay (Smith, 1980) (Figure 1-2). The Bay is exposed on the northeast and east to the Pacific Ocean, while to the southeast, south and southwest it is backed by the Purangi Estuary, the larger Whitianga Estuary, hill county, then the rugged Coromandel Ranges.

The bathymetry of Mercury Bay terminates a wide low angled (approximately 0.3^{o} slope) continental shelf and is controlled in part by that of the outer greater Bay.

Bathymetric contours in the greater Bay are cresentic and parallel the coastline, with minor fluctuations about the islands. The Bay itself has length at about 5.46 km and 3.73 km - 5.41 km width. Within Mercury Bay bathymetric contours are headland controlled and cresentic across the Bay (Smith, 1980). Bay depths are shallow, averaging 30 m below chart datum across the front of the Bay, and 8 m over the widest central area (Figure 1-2).

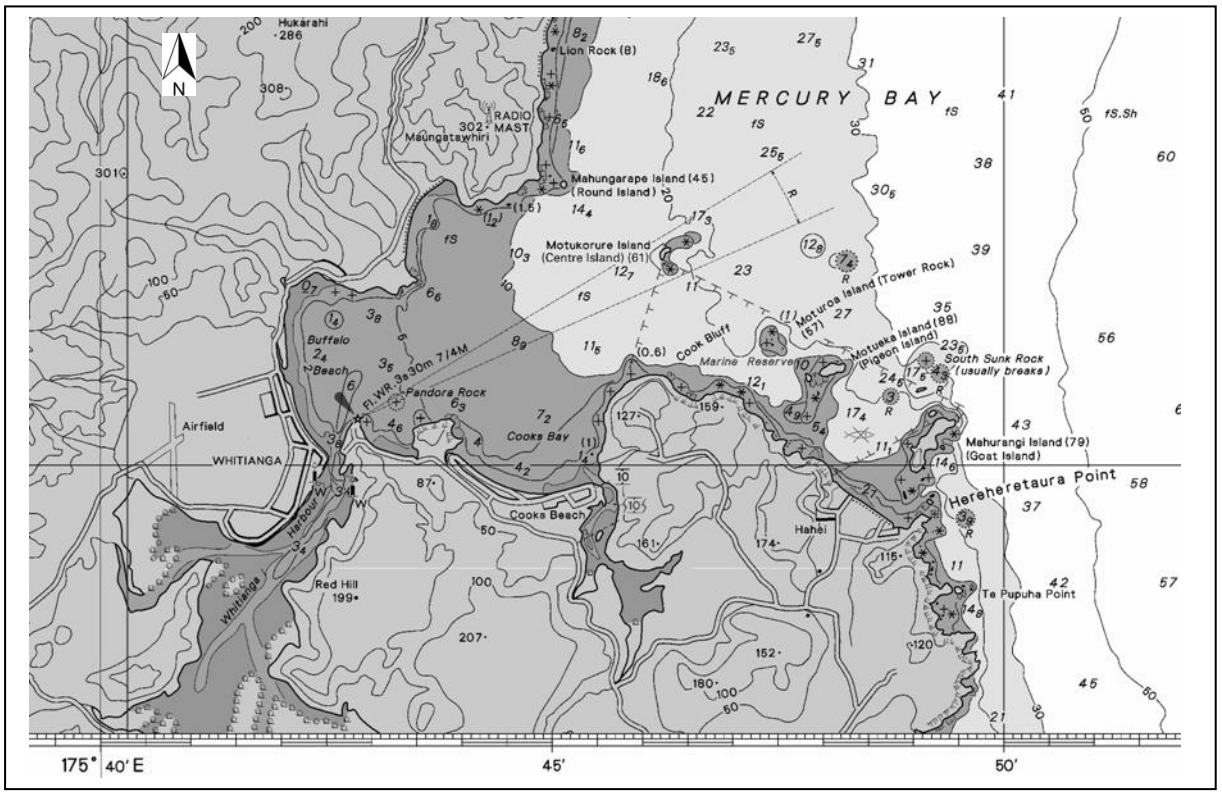

Figure 1-2. Bathymetry map of Mercury Bay (LINZ, 1999).

Within Mercury Bay lie Buffalo Bay and the Whitianga tidal inlet. Both have been undergoing high levels of sedimentation due to a combination of naturally high sediment inputs and increased sediment inputs caused by changing and intensifying land use. This high rate of sedimentation has caused shallowing within Mercury Bay (Steeghs & Healy, 2007).

1.3 Summary of the Thesis

This research study consists of seven chapters which are constructed to achieve the objective of the research as follow:

CHAPTER 1 : Explain the background of the research, aim and objectives, and the study area.

CHAPTER 2 : Describe the generation of a tsunami, tsunami propagation on the open sea and its interaction with the coast. Includes the overview of previous study of tsunami sources.

CHAPTER 3 : Describe the tectonic setting and seismicity of the Kermadec Trench subduction zone that pose tsunami to Mercury Bay.

CHAPTER 4 : Define seiches and harbour oscillations, and indentify seiche modes and periods that developed in Mercury Bay.

CHAPTER 5 : Explain the methods used in this research,

CHAPTER 6 : Results and discussion.

CHAPTER 7 : Conclusions and recommendation for further research.

Chapter 2 -TSUNAMI HAZARDS

2. 1 Introduction

A tsunami is a wave, or series of wave in a wave train, generated by the sudden vertical displacement of a column of water. This displacement can be due to seismic activity, explosive volcanism, landslide above or below water, an asteroid impact, or certain meteorological phenomena. These waves can be generated in oceans, bays, lakes, rivers, or reservoirs. The term *tsunami* is Japanese and means harbour (tsu) wave (nami), because such waves often developed as resonant phenomena in harbours after offshore earthquakes (BRYANT, 2008).

Earthquakes that occur on the seafloor and at coastal regions are the most common factors that generate tsunamis. Other factors are submarine landslide, volcanic eruptions, meteorite (bolide) splashdown (de LANGE, 2003), large explosions (CAMFIELD, 1980), and two further mechanism which may generated tsunami, or tsunami-like long period waves; diapiric intrusions (EIBY, 1982 in de LANGE, 1983) and gas hydrates (Mc IVER, 1982 in de LANGE, 1983). Some of these mechanism can produce transoceanic tsunamis, whereas others only produce very localised tsunamis (de LANGE, 1983). Meteorite or bolide impact as a tsunamigenic process will not be further discussed in this study since its probability to occur is very small, at about 0.002% chance of an impact each year (de LANGE in press, 2001).

In New Zealand the written historical record started after the European settlement (post-1840). From this record, it is known that there have been 51 tsunami events generated regionally (11), locally (19) and distant sources (21) (DOWNES, pers com.).

2.2 Tsunami Generation

2.2.1 Earthquakes

Most shallow large earthquakes in subduction zones cause tsunamis (SATAKE & TANIOKA, 1999)which frequently occur in the Pacific, where dense oceanic plates slide under the lighter continental plates (subduction zones). When these plates fracture they provide a vertical movement of the seafloor that allows a quick and efficient transfer of energy from the solid earth to the ocean (BRYANT, 2008).

Base on the source location, SATAKE & TANIOKA (1999) classified tsunamigenic earthquakes in subduction zone into three types (Figure 2.1); earthquakes at the plate interface (typical interplate events), earthquakes at the outer rise, within the subducting slab or overlying crust (interpolate events), and "tsunami earthquakes" that generate considerably larger tsunamis than expected from seismic waves.

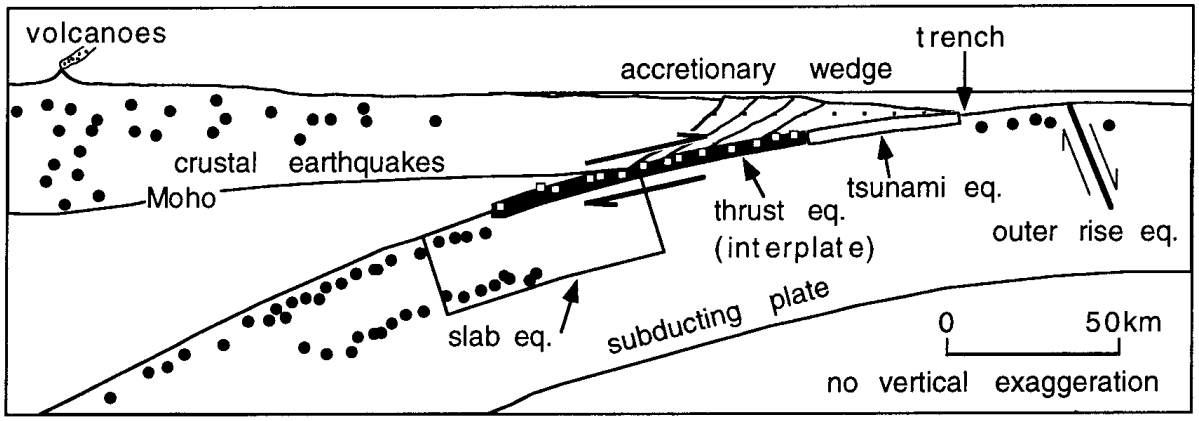

Figure 2.1. Schematic cross section of a subduction zone. "Typical" interplate earthquakes occur at the seismogenic boundary between the subducting and overlying plates. Interplate earthquakes include outer-rise events, slab events and crustal earthquakes. The source region of "tsunami earthquakes" is beneath the most trenchward part of the accretionary wedge (adapted from SATAKE & TANIOKA, 1999).

The size and behaviour of a tsunami generated by a subduction zone earthquake depends on a number of factors including the magnitude, source geometry and location of the event (BRYANT, 2008), source-to-locality distance, local seabed and coastal margin topography and the "birds-eye" plan shape of the

coastline (BELL *et al*., 2004). The magnitude and source geometry of the earthquake determine the surface deformation, which, in turn, determines the overall size and length scale of the tsunami. The representative source geometry can be calculated via an empirical formula that takes fault length, width, slip and moment magnitude into account (BRYANT, 2008). The moment magnitude (M_w) can be determined using equations 2.1 and 2.2, which explain its relation to seismic moment. The seismic moment (M_0) number depends on the rigidity of the crustal rock (μ), average displacement of the fault plane (D), and the area of the fault surface (S).

$$M_w = \frac{2}{3}\,(log_{10}\,M_0 - 9.1) \qquad (2.1)$$

and $$M_0 = \mu.\mathrm{D}.S \qquad (2.2)$$

where the units are : M_0 = N.m; μ = kg/ms^2; D = m, and S = m^2

For tsunami warning purposes where rapid evaluation of the tsunami potential is required, ABE (1994) estimates tsunami run-up height for both near and far-field tsunamis using the value of tsunami magnitude M_t, maximum tsunami amplitude of tsunami waves measured by tide gauges H (metres), distance from the source R (km), and a and D site specific constants (equation 2.3). Unfortunately, due to the tsunami amplitude data limitation and short record of historical tsunami makes still difficult to provide reliable predictions in New Zealand (de LANGE & HEALY, 1999).

$$M_t = \log H + a \log R + D \qquad (2.3)$$

New Zealand has frequent shallow earthquakes, and about a third of them occur on submarine faults offshore. From Canterbury to East Cape and beneath Cook Strait, New Zealand's continental shelf is fractured by active faults. Movement along these faults caused major tsunamis in 1855 and 1947 (de LANGE and McSAVENEY, 2009). The West Coast is vulnerable from movement along the Alpine Fault and offshore faults. The recent Canterbury earthquake on February 22, 2011 was 6.3 in magnitude causing widespread damage and multiple fatalities around Christchurch. The earthquake was centred 2 kilometres west of the town of Lyttelton, and 10 kilometres south-east of the centre of Christchurch, New Zealand's second-most populous city. It followed nearly six months after the 7.1 magnitude 2010 Canterbury earthquake that caused significant damage to the region but no direct fatalities. Both

of these recent earthquakes did not trigger tsunami since the earthquakes centre were on land. Notable local-source tsunami include those caused by the 1855 Wairarapa Fault earthquake (GRAPES and DOWNES, 1997) and those caused by tsunami-earthquakes (KANAMORI, 1972) near Gisborne n March and May 1947 (DOWNES *et al*., 2001; BELL *et al*., 2010).

The submarine earthquakes that generate tsunami hazard to New Zealand mostly occur in the Pacific Ocean and at the subduction zone between Pacific and Australian Plates (WALTERS, 2006; POWER *et al*, 2010; POWER and GALE, 2011).

2.2.2 Submarine Landslides

Submarine landslides can dislocate a water mass from its equilibrium position and generate “surprise tsunami” (WARD, 2000) because they are harder to predict. Submarine landslides often accompany large earthquake as well as collapses during volcanic eruptions. Submarine landslides associated with earthquakes, can initiate tsunami far outside the epicentral area, or far larger than expected given the earthquake size (WARD, 2000). The size of tsunami generated by submarine landslide depends on the volume of the landslide itself and its geometry will determine the direction of tsunami wave’s propagation.

In 2003, the Fiordland earthquake generated a local scale tsunami, a landslide into Charles Sound created a wave that inundated forest 4 to 5 metres above high tide, and damaged a helipad and wharf. Much larger tsunamis may have been triggered by huge submarine landslides off the edges of New Zealand’s continental shelf, revealed by recent sonar mapping (de LANGE and McSAVENEY, 2009).

2.2.3 Underwater Volcanoes and Sector Collapses

Volcanic activity approximately contributes around 5 percent of tsunamigenic sources in the world (TANGUY *et al*, 1998). Volcanic tsunami would generate within a limited source area and they would dissipate rapidly with distance from source (GOFF, 2001). The Krakatoa eruption in 1883 generated destructive tsunami that have been extensively reported in many scientific reports is an example of underwater volcano generated tsunami. The circum-Pacific plate boundaries-sometimes known as the Ring of Fire because of the relentless and dramatic

volcanic activity-alone account for about 75 percent of seismic energy released worldwide (HOUGH, 2004). New Zealand, which lies in the boundary of Pacific and Australia plates, has a wide range of potential tsunamigenic sources including those generated by volcanic activity. Underwater volcanic activity may form tsunami from; undersea eruption, pyroclatic flows impacting on water, landslide and avalances of cold rocks, lahars, phreatomagmatic eruptions, lava bench collapse, airwaves from large explosions, atmospheric acoustic and gravity waves as produced by 1833 Krakatoa eruption (PRESS and HARKRIDER, 1966), and collapse of the volcano caldera (de LANGE, 1983).

Offshore volcanoes, including Tūhua/Mayor Island, Whakaari/White Island, and numerous submarine volcanoes between New Zealand and Tonga, present a tsunami hazard. Modeling studies conducted by de LANGE and PRASETYA (1999), showed that the pyroclastic eruptions of $1km^3$ flows, even though is considered low, is able to generate wave of 0.5 m of height and a pyroclastic flow of Krakatoa scale ($10\ km^3$) would rise the wave that peak around 5 m at the coast.

It is recorded that there are 28 offshore volcanoes along the active Taupo-Kermadec-Tonga arc that are >10 km in diameter and lie within 1000 km of Auckland City (GOFF *et al*., 2005), which could generate regional/local tsunami to the northern part of New Zealand.

Some tsunami deposits in the Bay of Plenty appear to be related to the eruption of submarine Healy Volcano around 1400 AD. Even inland volcanic eruptions can create atmospheric pressure waves that cause tsunamis – some New Zealand deposits are the same age as a catastrophic eruption of Taupō around 1,800 years ago (de LANGE and McSAVENEY, 2009).

2.3 Tsunami Progation and Nearshore Response

Tsunami waves travel outward from the source region as a series of waves, their speed depends upon the depth of the water. Initially, tsunami waves propagate as wave that has small size in height compared to its wave length and the ocean depth. The speed of a tsunami wave, in the deep ocean can range from 500 to 1,000

kilometres per hour. This speed will decrease as the depth of the ocean decreases. As tsunami approaches the shore or land, the water depth decreases and the tsunami wave undergoes shoaling, refraction and diffraction (BRYANT, 2008). By this process the direction of wave propagation can become focused or defocused. At the shoreline, tsunami wave height increases and its energy is concentrated in the vertical direction by the reduction in water depth, and in the horizontal direction by a shortening the wavelength due to the wave slowing down (ITIC-UNESCO.org). Shallow or shallowing areas also serve to reflect energy back away from the coast, as is the case with New Zealand's continental slope (GOFF, 2001).

The periods of tsunami waves may range from a few minutes to as much as one hour. When it interacts with the shore, the tsunami wave will react in many different ways according to the size and period of the waves, near-shore bathymetry and shape of coastline, the state of tide, and other factor. GOFF (2006) indicates there are three primary factors that determine the response of New Zealand to tsunamis that travel across the Pacific Ocean: source location and geometry, wave transformations that occur when the tsunami crosses the ocean and the effects of bathymetry and geometry of the continental shelf and coastal region.

Landslide tsunami will not propagate far for more than 1000 km from its point source and considered as not hazardous, unless the landslide is large (GOFF, 2001).

2.4 Tsunamigenic Sources in New Zealand

The geographical position of New Zealand occupies the southwest Pacific between 34^0 and 48^0 south and 166^0 and 179^0 east. The country is located within the Pacific 'Ring of Fire", which is formed along the boundary between the Pacific oceanic plate and the adjacent continental plates of Australia (Figure 2-2). New Zealand is vulnerable to tsunami hazards because of its long coastline, and also because 80% of all tsunamis occur in the Pacific Ocean (Figure 2-3). This country is not only vulnerable to the tsunami from the Pacific Ocean, but also local-source tsunamis which usually affect limited stretches of coastline. Of all parts of the country, the eastern coast of New Zealand has the greatest exposure to tsunami,

BERRYMAN (2005) plotted the locations that had been affected by some large tsunamis shown in Figure 2-4 A and B.

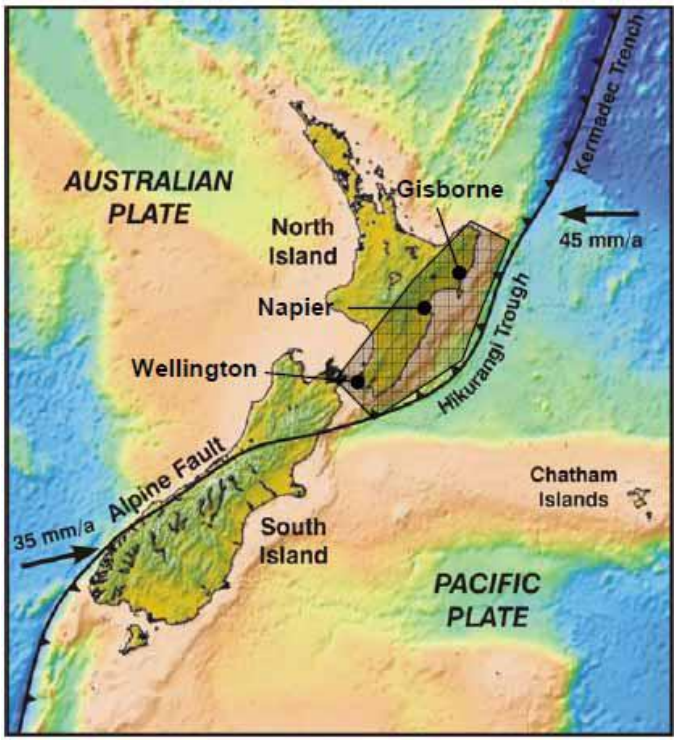

Figure 2.2 Tectonic setting of New Zealand that formed and influenced by the relative motion of Pacific oceanic plate and Australian plate (POWER and GALE, 2010).

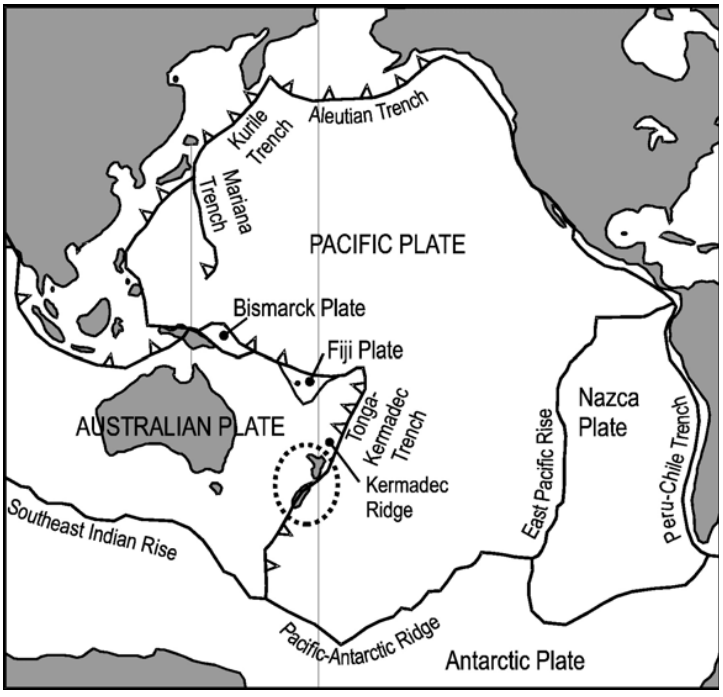

Figure 2-3. New Zealand's position in the Pacific Ocean with relation to the major lithospheric plate boundaries (McFADGEN & GOFF, 2007).

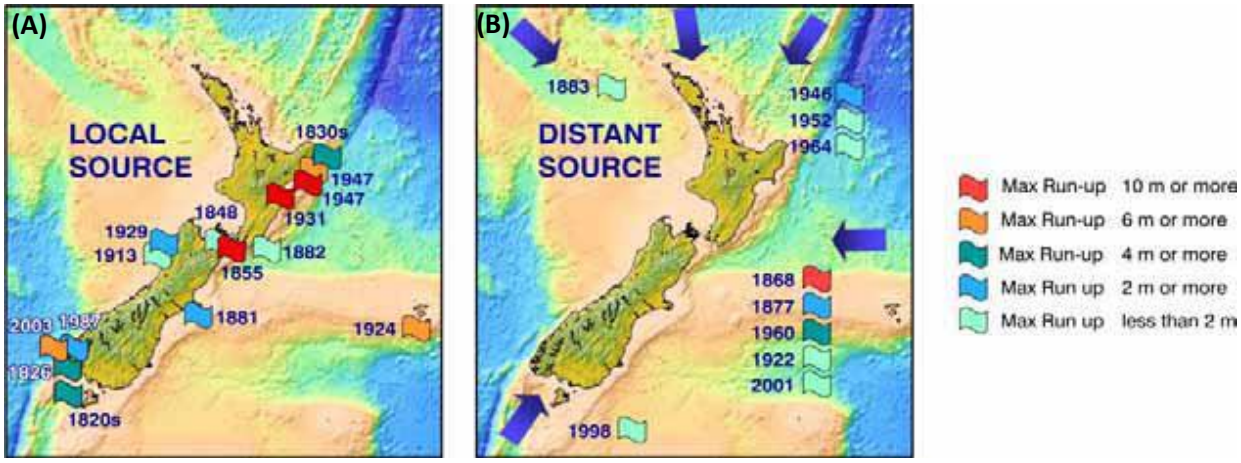

Figure 2-4. Largest tsunami recorded in New Zealand (BERRYMAN, 2005, extracted from SAUNDERS *et al.*, 2011)

BERRYMAN, 2005, also indicates tsunami sources that struck New Zealand in three categories as follow:

- Distant source – more than 3 hours travel time from New Zealand
- Regional source – 1 to 3 hours travel time from New Zealand; and
- Local source – 0 to 60 minutes travel time to the nearest New Zealand coast (most sources are more than 30 minutes travel time).

Locations of main tsunami sources that may pose hazards to New Zealand are shown in Figure 2-5.

The historical tsunami record that affected New Zealand only covers the last 165 years. Of these (GNS, 2005), there were:

- 14 distant earthquake sources
- 7 regional earthquake sources
- 9 local earthquake sources
- 4 local earthquakes accompanied by coastal landslides
- One was a spontaneous landslide without an earthquake
- 8 others were from unknown sources, one of which was possibly a submarine landslide.

GOFF *et al*. (2010) developed a paleotsunami data base of New Zealand and mentioned that the country has experienced at least four historical tsunamis with run-up heights of about 10 m or more. Three were local events (Palliser Bay: 1855A.D., ~ 10m; Waikari River: 1931A.D., ~ 15m; Gisborne: 1947A.D., ~ 10m), and the fourth

was a distant event (South America: 1868A.D., ~ 10 m). The Aleutian Islands and Alaska are also potential sources. A list of some potential local and regional tsunami sources around Bay of Plenty and Eastern Coromandel Peninsula is given in BELL *et al*., (2004).

In New Zealand, the fluctuation in sea level due to the propagation of tsunami wave will be recorded by a network of gauges installed around the country. These sea-level gauges are operated by various agencies including NIWA, port companies, regional and district councils and complement the operational real-time monitoring undertaken by GNS Science through GeoNet (NIWA, 2011). Figure 2-6, shows the locations of open coast stations around New Zealand and their coordinates position are given in table 2.1**.**

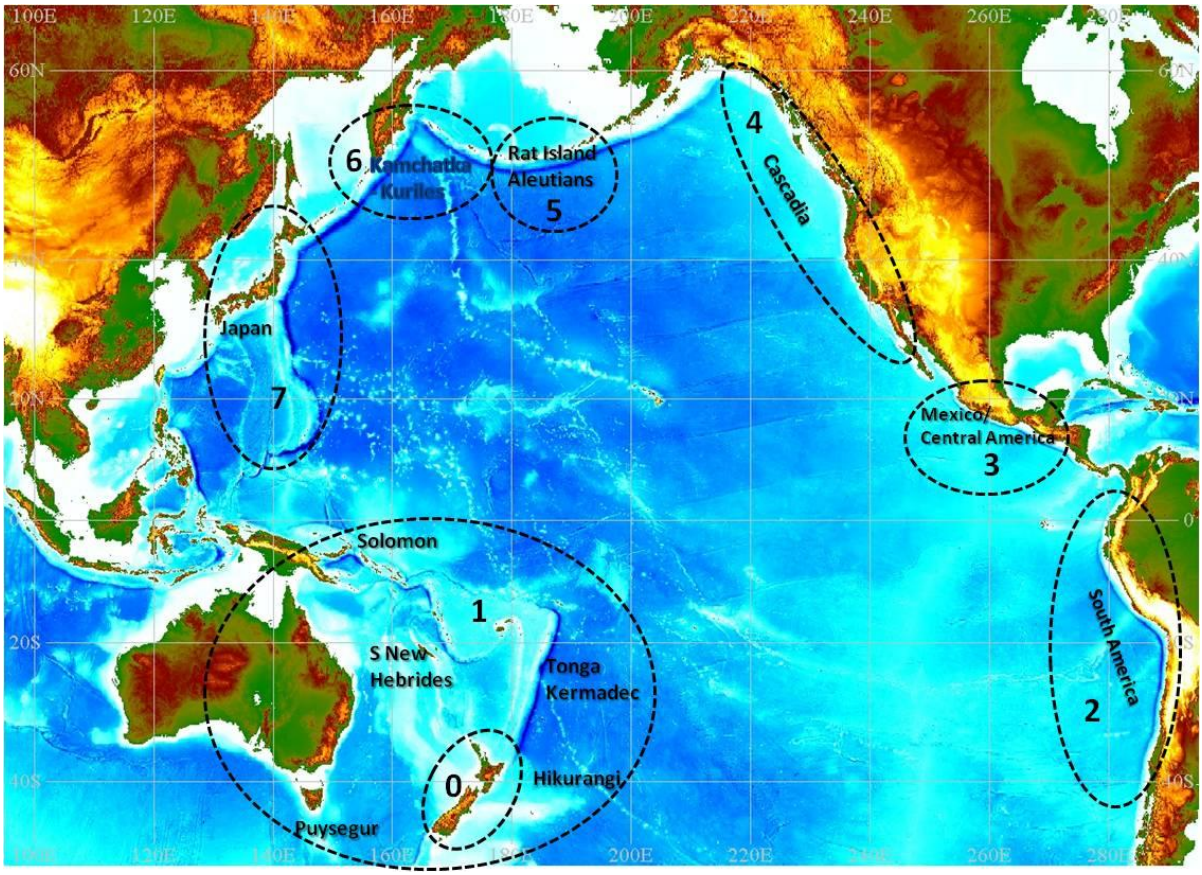

Figure 2-5. The main tsunami sources: 0 = local sources, 1 = regional sources, and 2-7 = distant sources (GNS Science).

Table 2.1 Location of source of New Zealand sea-level gauge datasets. Shaded rows show gauges that record at 5 minute intervals, all other gauges record sea-levels each minute. (NIWA, 2011)

Station	Latitude (°N)	Longitude (°E)	Operating agency
Kaingaroa Chatham Is.	–43.7315	183.733	NIWA
Moturiki Is.	–37.6304	176.186	NIWA
Little Kaiteriteri	–41.048	173.027	Tasman District Council
Marsden Pt.	–35.842	174.5	Northland Regional Council
Whitianga	–36.833	175.709	Environment Waikato
Sumner Head	–43.570	172.773	NIWA
Lyttelton Port	–43.6058	172.7222	Lyttelton Port Co. Ltd
Timaru Port	–44.392	171.254	PrimePort Timaru Ltd
Green Is.	–45.9523	170.3867	NIWA
Dog Is.	–46.652	168.412	NIWA
Jackson Bay	–43.957	168.616	NTC, Bureau of Meteorology
Charleston	–41.908	171.433	NIWA
Port Taranaki	–39.055	174.033	Port Taranaki Ltd
Kapiti Is.	–40.842	174.938	NIWA
Kawhia Wharf	–38.0659	174.8232	Environment Waikato
Anawhata	–36.921	174.461	NIWA
Poutu Pt.	–36.362	174.182	Northland Regional Council
Tararu (Firth Thames)	–37.128	175.521	Environment Waikato
Kaikoura	–42.415	173.703	NIWA
Scott Base (Ross Sea)	–77.85	166.767	NIWA/Antarctica NZ

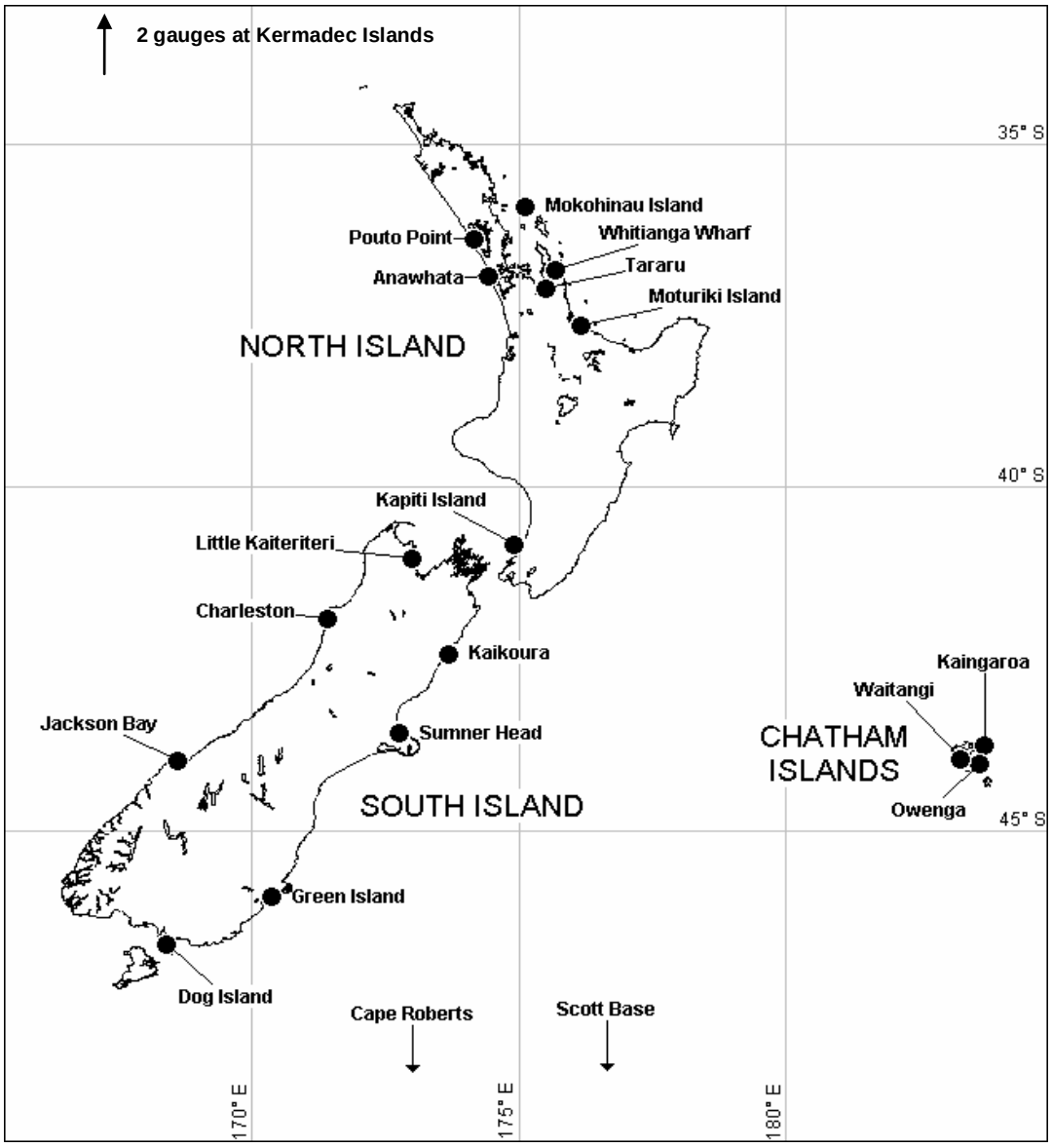

Figure 2-6. The map of open coast sea-level gauge stations in New Zealand (NIWA, 2011).

2.4.1 Distant Source

Within the Pacific Rim, tsunamigenic sources mostly located to the east and northeast of New Zealand pose the greatest threat based on the computer modelling and historical record (POWER & GALE, 2010). From this location, tsunami waves travel to New Zealand in more than 12 hours. Meanwhile, tsunami energy from the northwest Pacific is partly prevented from propagating directly towards New Zealand by reflection and refraction from the chain of island arcs between Papua New Guinea

and Samoa (POWER & GALE, 2010). A data base of distant tsunamigenic sources around Pacific Rim is given by POWER & GALE (2010), which forecast the potential location of earthquakes of magnitude more than M_w = 8.7.

The most significant event of distant source of earthquake generated tsunami that affected New Zealand were the 1968 Peru, 1877 and 1960 Chile (de LANGE & FRASER, 1999; POWER *et al*., 2007). Another distant tsunami source that may hit New Zealand is the Cascadia Fault in North America (THOMPSON, 2011).

2.4.2 Regional and Local Sources

Earthquakes posed by the subduction zone in New Hebrides Trench (POWER *et al.*, 2011) and earthquakes that occur in Kermadec Trench and undersea volcanism in the Kermadec-Tonga system (GOFF *et al*., 2006; PRASETYA *et al*., 2011; POWER *et al*., 2007; POWER *et al*., 2011) are potential regional tsunami source that impacting New Zealand. POWER *et al*., (2011) suggests from the GPS data installed in Matthew and Hunter Islands, that large subduction thrust earthquakes on the east-west trending portion of the southern New Hebrides subduction margin (between 169°E and 174°E) could trigger tsunami that impact New Zealand coastline.

The earthquakes that occur in the northern part of Kermadec Subduction Zone (segment C - see Figure 2-7) can be classified as regional tsunami sources, meanwhile, the middle (segment B), the southern part (segment A) and volcanic arch at the southern end of the trench are classified as regional/local tsunami sources that threaten Mercury Bay (PRASETYA *et al*., 2011; de LANGE *et al*., 2007). Numerical modelling by POWER *et al*., (2011) show that tsunami generated from the southern and/or middle segments of Kermadec Subduction Zone impose a larger hazard to the coast of New Zealand than tsunami generated along the northern Kermadec Subduction Zone.

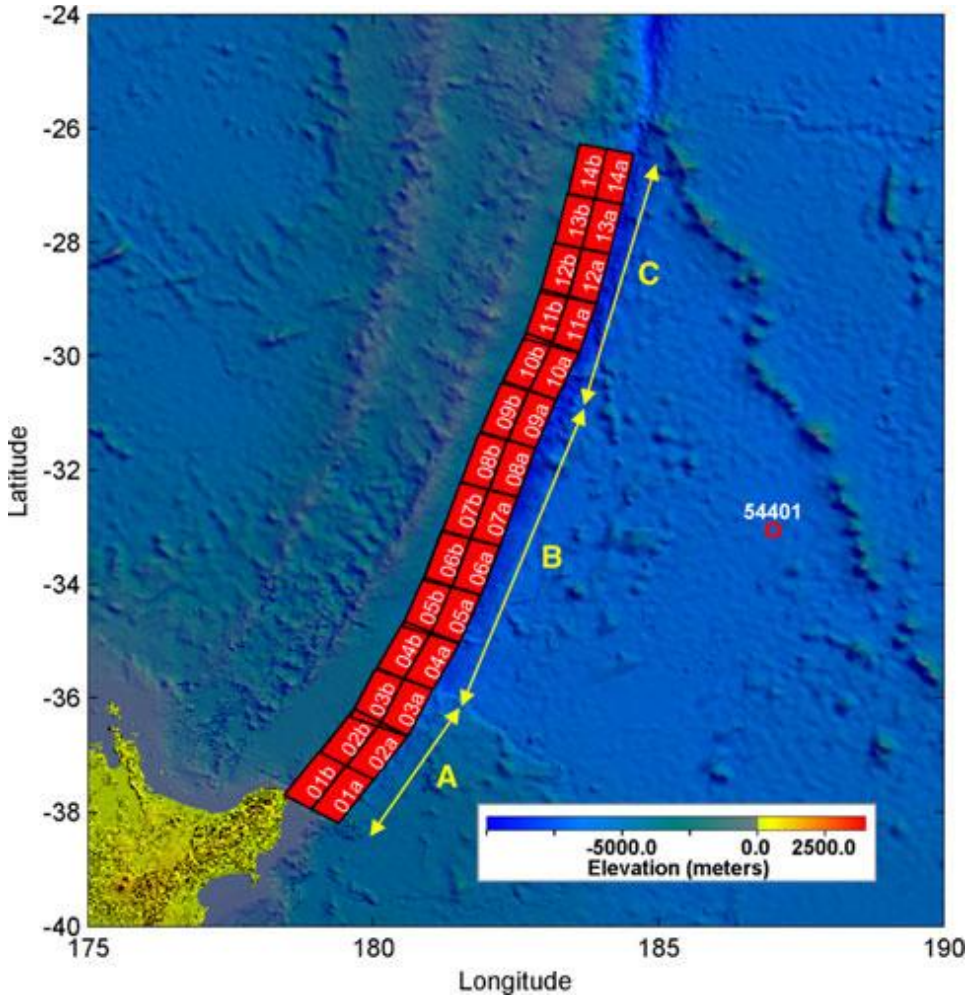

Figure 2-7. The region of Kermadec Subduction Zone is divided into 3 segments that each one consists of 100 km by 50 km unit sources of patches in order to account for the down-dip and along strike variation of the plate interface (POWER *et al*., 2011). The A, B, and C are the southern part, middle part and the northern part of the Kermadec Subduction Zone respectively.

Tsunamis that are generated close to the coastline and require less than 1 hour to arrive at the New Zealand's coastline, and are considered as local tsunami sources. This study focuses on local tsunami sources that may threaten Mercury Bay. However, the historical record, that only covers tsunami history from 1840, does not mention any regional/local tsunami sources that have affected Whitianga within the Mercury Bay (PRASETYA *et al*., 2008). This is probably because some tsunami events have been small when they arrived in Mercury Bay (less than 0.5 m in wave height), where small amplitude of waves only can be recorded by sea level gauges, which were not installed at the time when the tsunami waves arrived in the study area (Mercury Bay).

BELL *et al*., (2004) identified potential tsunamigenic sources (with potential local and regional scale impacts), which are summarized in table 2-2.

Table 2-2. Potential tsunamigenic sources that may impact Bay of Plenty region (BELL, 2004). Note that these sources are classified as local/regional when they have travel time 30 to 60 minutes (local impact) and up to 2-3 hours (regional impact) travel time to coast.

No.	Potential tsunamigenic sources	Possibility to generate tsunami
1	Subduction interface earthquakes that occur in the Tonga-Kermadec-Hikurangi region associated with the Pacific/Australian plate boundary.	It is uncertain if the entire subduction zone is a potential tsunamigenic hazard.
2.	Upper plate faults in the northern Hikurangi continental shelf margin from Mahia to Ruatoria.	Earthquakes in this region are unlikely to cause large tsunami impacts in Bay of Plenty as coastal-trapped waves propagating northwards along the coast dissipated as they moved around East Cape into the BOP.
3.	Landslide sources in the Hikurangi margin off East Cape, Matakaoa and Ruatoria.	Further study to define the landslide dimension, mechanism and its frequency to occur.
4.	Undersea volcanism in the Tonga-Kermadec system.	The volcanic sector collapses that potentially generate tsunami are still unknown whether they are large single catastrophic events of small repetitive movements.
5.	Regional active faults; normal faults in the offshore Taupo Volcanic Zone.	It is still uncertain whether fault rupture with modest displacement is capable of generating destructive tsunamis.
6.	Offshore volcanic sources include Tuhua/Mayor Island, Whakaari/White Island and numerous smaller submarine volcanoes occur on the BOP continental shelf and slope (100-150 km to the coast).	Further investigation using newest technology, high resolution tsunami models and the additional knowledge on fault characteristic and deformation patterns is needed.
7.	Atmospheric pressure-waves or pyroclastic flows from large onshore volcanic eruptions in the Taupo Volcanic Zone (TVZ), or Mt Taranaki.	Potential to generate tsunamis is still little known.

2.5 Tsunami Records in Mercury Bay

There are only few publications of tsunami history that discusses the Mercury Bay in detailed. Most of the publications cover the larger area of Bay of Plenty and Eastern Coromandel. BELL *et al*., (2004), summarized the tsunamis that have been recorded in the Bay of Plenty (BOP) and Eastern Coromandel area in the historical era (1840-1996). Table 2-3 shows the tsunami events that have been recorded in the study area of Whitianga, Mercury Bay.

The oldest tsunami history recorded in Whitianga is the effect of 1883 Krakatau eruption, which de LANGE and HEALY (1986a) concluded that Whitianga experienced sudden increase in water level 36 hours after the largest explosion. The water level rose 1.8 m at low tide then receded, leaving vessel high and dry before the water rose again.

Table 2-3. Tsunami records in Whitianga, Mercury Bay. Records of tsunami 1883 and 1922 are taken from Bell et al., (2004).

Year	Run-up (m)	Tsunami Source Data	Tsunami Impact: Descriptive accounts/comments
1883	1.8	Pressure-wave tsunami, attributed to eruption of Krakatau	The water rose 1.8 m during ebb flow (Fraser database, 1998).
1922	0.9	M8.3 – 8.5 earthquake, Chile	Maximum rise to HWM. Rises and falls at intervals of 20 minutes throughout day, diminishing towards evening. Fluctuations on lesser scale next morning (13th) (GNS, unpublished data).
1960	~ 5 m	Tsunami waves, magnitude 9.5 off the coast of Chile	The tsunami arrived at Whitianga at about 12.5 hours after the earthquake with initial drawdown of ~ 2 m followed by run up of ~ 5 m. 11 boats were swept away, water surged up and down at 20-minute intervals.
1964	No run-up observed	Tsunami waves, magnitude 9 earthquake, Gulf of Alaska, USA	Maximum wave height was 0.9 m.
2010	No run-up observed. Water level rose up to 0.6 m	Tsunami waves, magnitude 8.8 earthquake, Chile	The sea level was fluctuated, experiencing amplification up to 3 days since the first tsunami wave arrived on 28 February 2010.
2011	No run-up observed	Tsunami waves, magnitude 8.9 earthquake, Japan	The tide was lifted 80 cm (Davidson, 2011). Fluctuation in water level up to 5 days since the first tsunami wave arrived on 12 March 2011.

Tsunamis event that recently take place and recorded in the tidal gauge at Whitianga Wharf are the 2010 Chilean and 2011 Tohoku events. Both of these events have generated destructive tsunamis at the coastal areas in respective countries. In New Zealand, particularly Mercury Bay, the tsunami waves arrived after more than 12 hours travel time and did not cause any significant damages. However, high frequency oscillations as response of tsunami waves arrived from both tsunami waves were well recorded in the tidal gauges at Whitianga Wharf until several days (Figure 2-8).

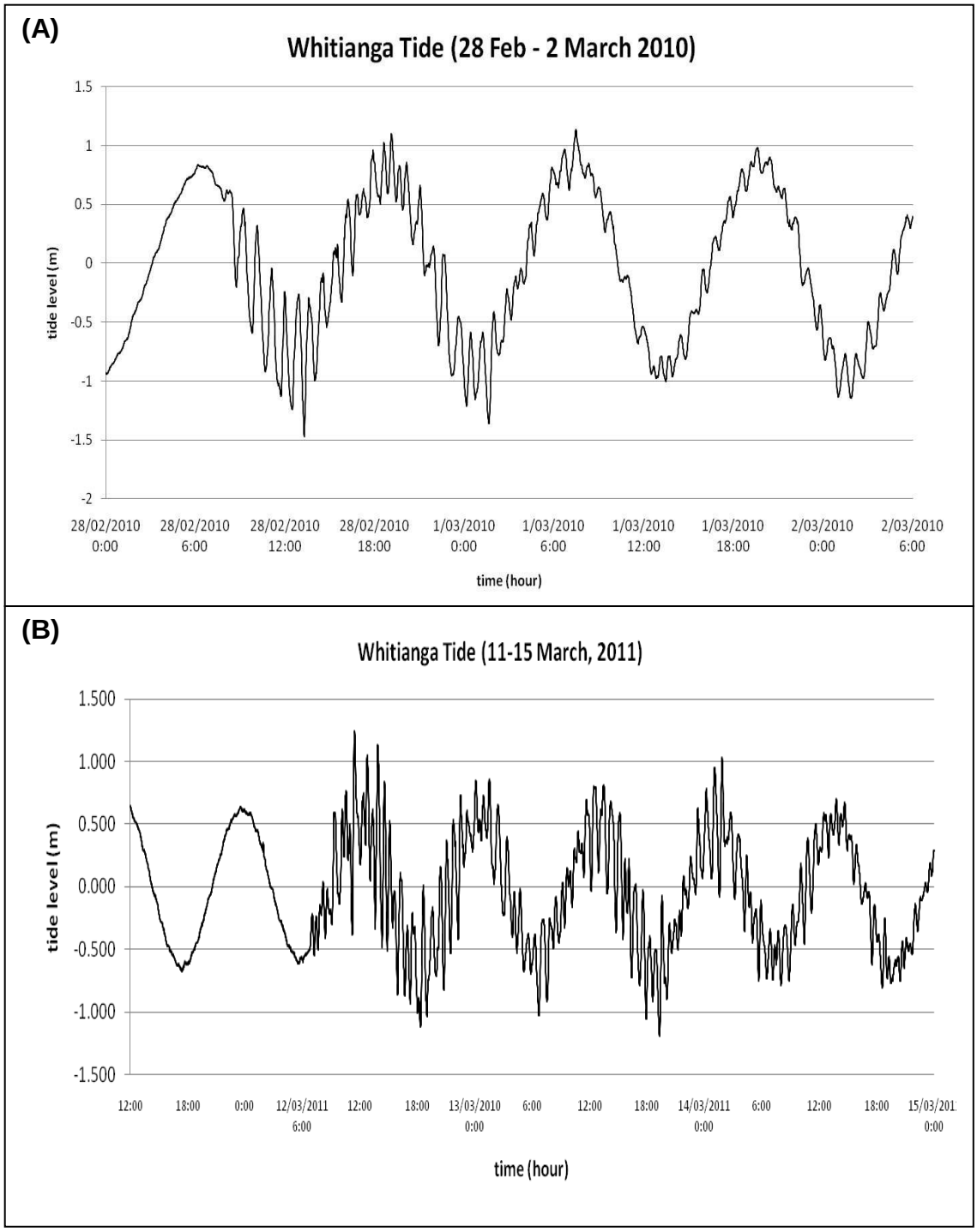

Figure 2-8. High frequency oscillation following the initial tsunami waves were recorded in the tidal gauges installed at Whitianga Wharf represent the response of the Mercury Bay to the 2010 Chilean (A) and (B) 2011 Tohoku earthquakes generated tsunamis. Tide level data are taken from Waikato Regional Council.

During the arrival of 2010 Chilean tsunami waves, Whitianga experienced wave height of up to 1.05 m (BELL, 2010), and 1.53 m for the 2011 Tohoku tsunami waves.

The most recent earthquake of magnitude 7.6 was the Kermadec Trench earthquake on the 6th July, 2011. The earthquake generated tsunami waves that propagated to the east and west of its quake epicenter (Figure 2-9), with very little energy sent south towards New Zealand (POWER, 2011).

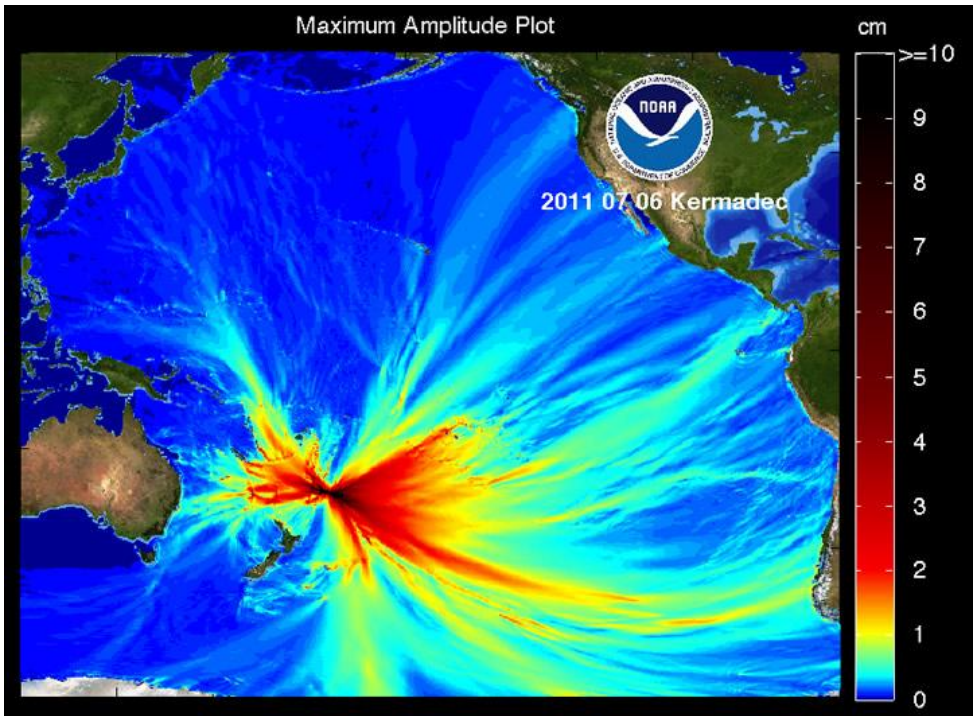

Figure 2-9. The orientation of fault rupture that generated the 6 July 2011 Kermadec Trench quake was north-south and most of the tsunami energy was radiated perpendicular (east and west) to the fault plane (POWER, 2011).

Since most of the energy propagates east towards Americas (de LANGE, 2011), it did not significantly raise the sea-water level in Mercury Bay. In fact, only minor oscillations (resonance) were identified visually from the tidal gauge record of Whitianga Wharf within the Mercury Bay (Figure 2-10).

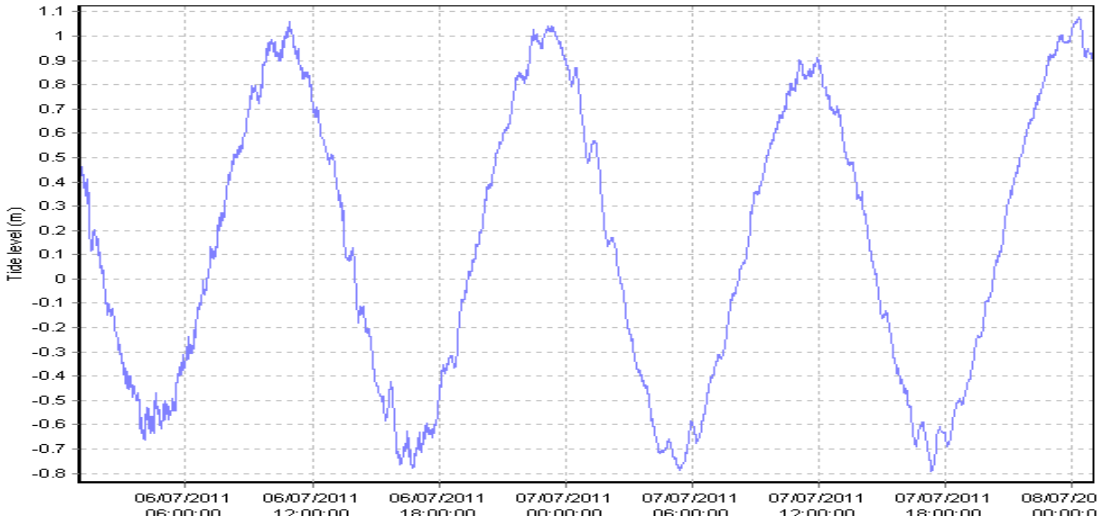

Figure 2-10. Tide record of the gauge installed at Whitianga Wharf during the arrival time of 6 July 2011 Kermadec quake (taken from Waikato Regional Council).

BORRERO (2011-unpublished) conducted numerical modelling using COMMIT software for the 6 July 2011 Kermadec quake. From this simulation it is observed that the earthquake generated waves with maximum height of 10 cm and particularly in Mercury Bay the maximum wave height was about 4 to 5 cm (Figure 2-11).

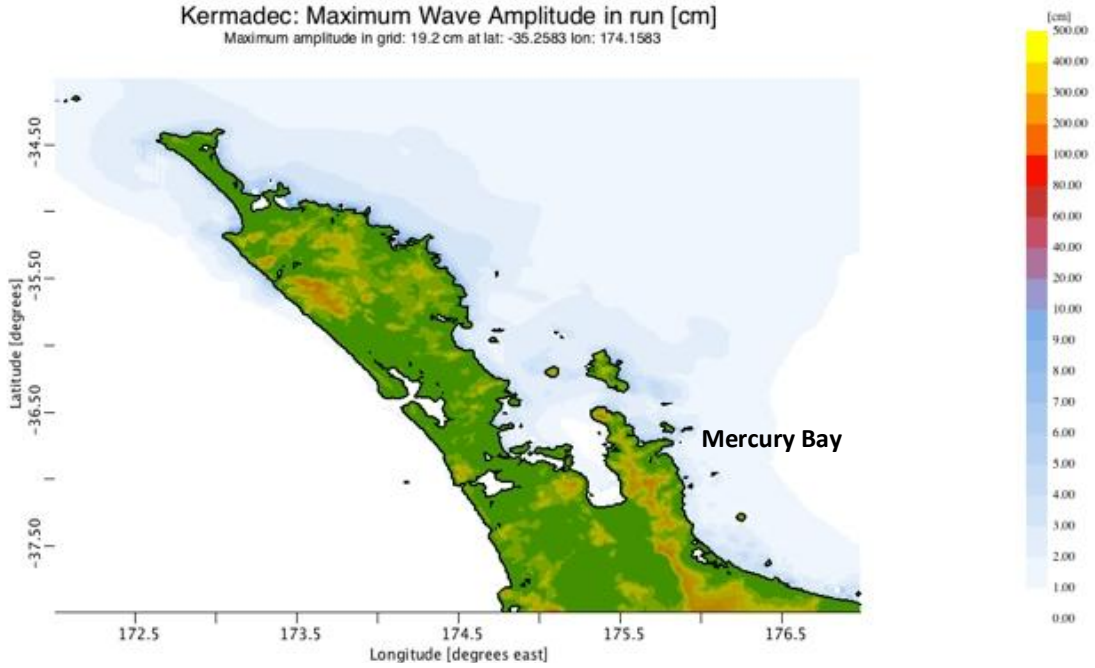

Figure 2-11. The maximum wave amplitude that arrived around the north island of New Zealand. The maximum wave amplitude of 19.2 cm was around the northern tip of north island (Bay of Island) and around Mercury Bay the wave amplitude was about 4 to 5 cm. Numerical model was conducted by BORRERO (2011).

Chapter 3 - THE KERMADEC SUBDUCTION ZONE

3.1 Introduction

The historical record of seismicity on Kermadec Trench is limited (POWER *et al*., 2011); however, this zone has been identified as a potential regional and local tsunami sources that may pose a threat to northern New Zealand (GOFF *et al*., 2006; PRASETYA *et al*., 2008). A study by de LANGE and HEALY (2001) mentioned that the orientation of tsunami propagation which generated in the Tonga-Kermadec Trench is east-west, and not southwards towards New Zealand. However, on the basis of 2004 Boxing Day tsunami in Banda Aceh, Sumatra, where the rupture length of nearly 1200 km which had been never expected to take place, suggests that the Kermadec subduction zone could produce an earthquake of magnitude 9.4 capable of rupturing the entire subduction zone (POWER *et al*., 2011). This uncertainty should be taken into account in assessing the tsunami hazard that pose to New Zealand.

3.2 Tectonic Setting of The Kermadec Subduction Zone

The Kermadec Subduction Zone is located between 38^0S and 25 - 26^0S (Figure 3-1); extending along 1400 km (POWER *et al*., 2011). The trench links the Tonga Trench on the north to the Hikurangi Trench on the south, and marks the site of subduction of the southwestern edge of Pacific plate beneath the northeastern edge of the Australian plate (Von HERZEN *et al*., 2001). Its depths are mainly known from swath-based bathymetry in the south and broad-scale bathymetry in the centre and north, where the trench is deeper than 9000 m in the north, the maximum depth of 10,000 m is at latitude 32^0S and shallows southward (BALLANCE *et al*., 1999). The rates of southward movement of Pacific plates relative to Australian plate which cover the Kermadec Subduction Zone region are 7 cm/year at 27^0S and 5.5 cm/year at 35^0S (PRASETYA & WANG, 2011).

POWER *et al*., (2011) demonstrated that GPS data from a site on Raoul Island (in the Kermadec Islands) suggests that the Kermadec Trench is undergoing strong interseismic coupling, possibly down to depths of about 30 km (figure 3-1). This suggests that the Kermadec Subduction Zone may be capable of producing M_w > 8.0 events. However, the historical events have been up to M_w 8.5.

The short coverage of seismicity record on the Kermadec Trench; less than 100 years, requires us to review the paleotsunami deposits as studied by GOFF et al. (2010) and the archaeological record (McFADGEN & GOFF, 2007). However, in this study we will assess the potential of the Kermadec Trench as tsunamigenic sources to Mercury Bay based on the study of POWER *et al,*. (2011).

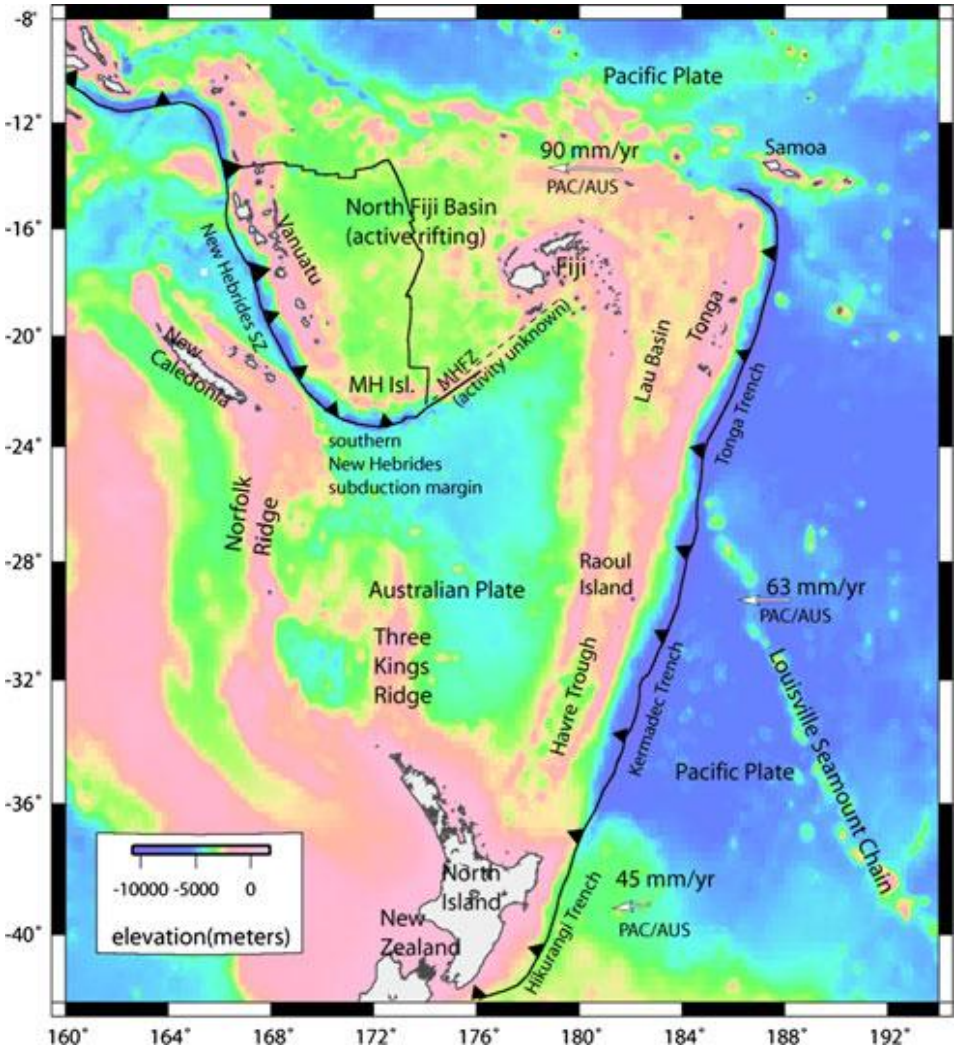

Figure 3-1. Location and tectonic setting of Kermadec Subduction Zone (Kermadec Trench) that links the Tonga Trench in the north and Hikurangi Trench in the south. Black triangles signify the over-riding plate at the regions subduction margins (POWER *et al*., 2011).

3.2.1 Geometry and Seismicity of The Kermadec Subduction Zone

POWER *et al*., (2011) assessed tsunami sources that threaten the northern part of New Zealand by simulating a set of scenarios of large earthquakes that may take place in the Kermadec Subduction Zone (Kermadec Trench). The selection of the scenarios were developed on the basis of large historical earthquakes analysis, moment tensor solutions since 1976, considerations of the tectonic setting and interpretation of regional GPS velocities to estimate long-term convergences rates at the trench and interseismic coupling on the subduction interfaces, and other kinematic data. In this assessment, POWER *et al*., (2011) divided the Kermadec Trench into three segments A, B and C, and this method will be adopted in this study. Each segment consists of patches each with a length of 100 km and width 50 km respectively. These patches along the Kermadec subduction interface are intended to account for the down-dip and along-strike variation of the interpolate as well as to keep a simple representation of the interface geometry for tsunami modelling (POWER *et al*., 2011).

The segment “A” is located on the southern part of the trench that bounded by latitudes of 38.18^0 and 35.8^0 S. Segment “B” extends from 35.8^0 to 30.7^0 S and segment “C” which adjacent with the Tonga Trench, is located between 30.7^0 and 26.35^0 S. The figure that illustrates the segmentation along the Kermadec subduction interface was shown in chapter two (Figure 2-8). Most of the Kermadec Trench is over 8 km deep; however the water depths are getting shallower at the both ends of the trench (POWER *et al*., 2011).

The estimated seismicity along the Kermadec Trench was derived from The International Tsunami Data Base (ITDB/PAC2004) incorporated with the NOAA/NESDIS/NGDC data set (PRASETYA & WANG, 2011) and it is shown that during the period 1900 - 2004; there were 24 earthquakes generated along the Kermadec Trench at depths less than 35 km with magnitudes greater than Ms 7.0. This gives the average number of 1 earthquake event every 5 years (PRASETYA & WANG, 2011). The earthquake data base of USGS (2011) mentioned that the region of the Tonga-Kermadec subduction zone experiences reasonably high levels of

seismic activity, with nearly 50 events of Magnitude 6.5 and above over the past 38 years, and 4 greater than Magnitude 7.5.

The recent earthquake event in Kermadec Trench on 6th July, 2011 of M_w = 7.6 , according to the segmentation of POWER *et al*., (2011), its epicenter was located in middle of segment C (northern part) of the trench (29.312^{0}S latitude, 176.204^{0}W). Figure 3-2 shows (A) M_w = 7 and greater earthquakes density map since year 1900 and (B) seismicity in year 2011 around the Kermadec Islands region between latitudes of 25^0 and 31^0 S (USGS, 2011). In this figure, the Kermadec subduction zone and the epicentre of the 6th July 2011 earthquake is also shown.

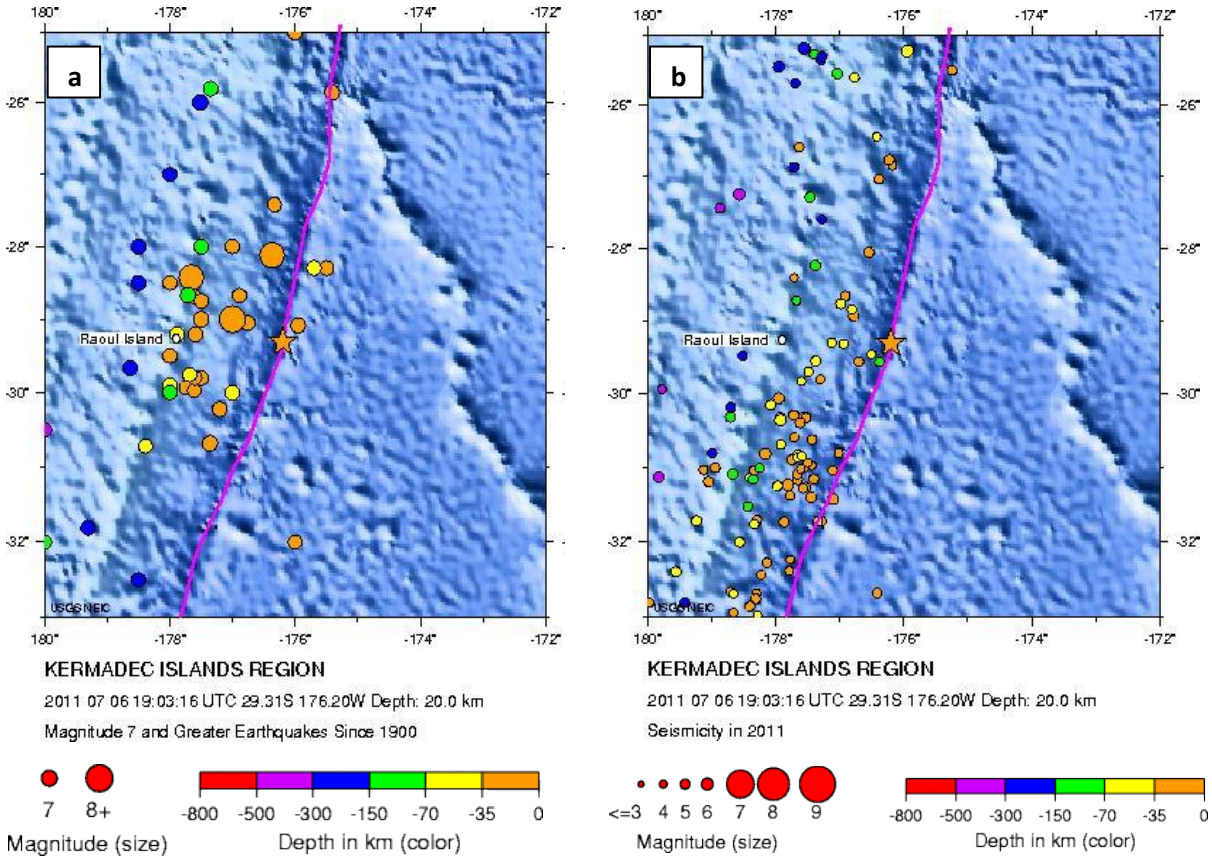

Figure 3-2. Earthquake density map of Kermadec Island region; (a) magnitude 7 and greater since 1900 and (b) seismicity in 2011. The purple line defines the Kermadec subduction zone and star symbol points the epicenter of the July, 6, 2011 earthquake (USGS, 2011).

.

Chapter 4 - HARBOR OSCILLATION AND SEICHES

4.1 Introduction

A basin, whether it is fully or partially enclosed, it will always experience water level oscillations (seiche). These oscillations or standing waves are the result of interaction between the water and many driving forces. In an enclosed basin, a seiche can be generated by wind or atmospheric pressure variations and rarely by earthquake ground motion (MILES, 1974). Whereas, in a partially enclosed basin, a seiche can also be caused by the oscillation of adjacent connected water bodies whose periodicity is close to that of a seiche or one of its harmonics (WŪEST & FARMER, 2003; MASSIE, 1976). The forcing oscillation can be due to tidal influences, storm surges and tsunamis.

Each basin has its *natural* resonant periods (so-called "*eigen periods*"). The eigen periods are determined by basin geometry and depth, and in natural basins, their periods may range from tens of seconds to several hours (RABINOVICH, 2009). These eigen periods are independent of the external mechanism forcing the oscillations, but their amplitudes are strongly depend on the energy source that generated them. The oscillations are known as natural (or *eigen*) *modes*. The mode with the lowest frequency (and thus, the longest period) is referred to as the *fundamental mode.*

Resonance occurs when the dominant frequencies of the external forcing match the eigen frequencies of the basin. The basin as a system will respond to an external forcing by developing a restoring force that re-establishes equilibrium in the system (RABINOVICH, 2009).

Harbour oscillations (*coastal seiches* as a specific type of seiche motion that occur in partially enclosed basins, such as gulfs, bays, fjords, inlets, ports,

and harbours) that are connected through one or more openings to the sea. Harbour oscillations differ from seiches in closed water bodies (for example, in lakes) in three principal ways (RABINOVICH, 2009):

(1) In contrast to seiche generated by external forcing (e.g., atmospheric pressure, wind, and seismic activity), harbour oscillations are mainly generated by long waves entering through the open boundary (harbour entrance) from the open sea.
(2) Energy losses of seiches in closed basins are mostly associated with dissipation while the decay of harbour oscillations is mainly due to radiation through the mouth of the harbour.
(3) Harbour oscillations have a specific fundamental mode, the *Helmholtz mode*, similar to the fundamental tone of an acoustic resonator. This modes is absent in closed basins.

The most important characteristic of a *seiche* is its mode. The mode of a *seiche* is the number of nodes it has within the system (Figure 4-1). The period of a *seiche* with n nodes is given by Merian's formula for closed and open mouth basins:

Closed basin $$T_n = \frac{2L}{n(gh)^{1/2}} \quad \ldots (4.1)$$

Open-mouth basin $$T_n = \frac{4L}{n(gh)^{1/2}} \quad \ldots (4.2)$$

RABINOVICH (2009) proposed a modification on *Merian*'s formula to calculate the fundamental period of a semi-circular shaped basin:

$$T_0 = 2.220\left[\frac{2L}{(gh_1)^{\frac{1}{2}}}\right] \quad \ldots (4.3)$$

where T_n is the period of an nth mode *seiche*,

L is the wavelength of the *seiche* (the length of the basin),

n is the number of nodes/mode of the *seiche*,

g is acceleration due to gravity, 9.81 m/s^2, and

h is average water depth.

Formula (4.1) is for closed and open-mouth rectangular basin of uniform depth. For open systems the formula (4.2) is applied (GIESE *et al*., 1990 as cited in MOLLOY, 2001).

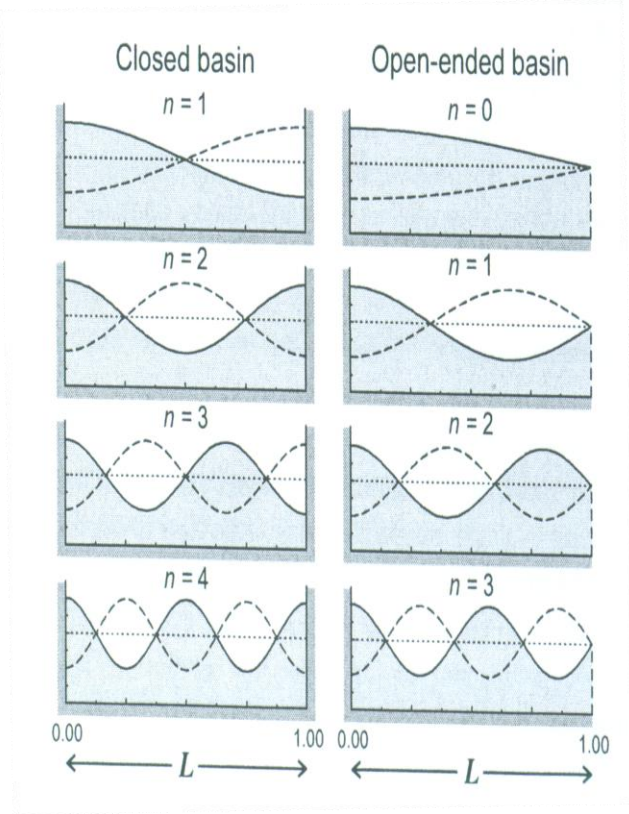

Figure 4-1. Surface profiles for the first four seiche modes in closed and open-ended rectangular basins of uniform depth.

One of the essential properties of oscillations in harbours is that even relatively small vertical motions (sea level oscillations) can be accompanied by large horizontal water motions (harbour currents); when the period of these motions coincides with the natural period of sway, or yaw of a moored ship, further resonance occurs, which can result in considerable motion and possible damage of a moored ship (RABINOVICH, 2009).

4.2 Generation

Because they are natural resonant oscillations, seiches are generated by a wide variety of mechanisms (Figure 3-2), including tsunamis, meteorological tsunamis (RABINOVICH and MONSERRAT, 1998), earthquake ground waves (MILES, 1974), internal ocean waves and jet-like currents (RABINOVICH, 2009).

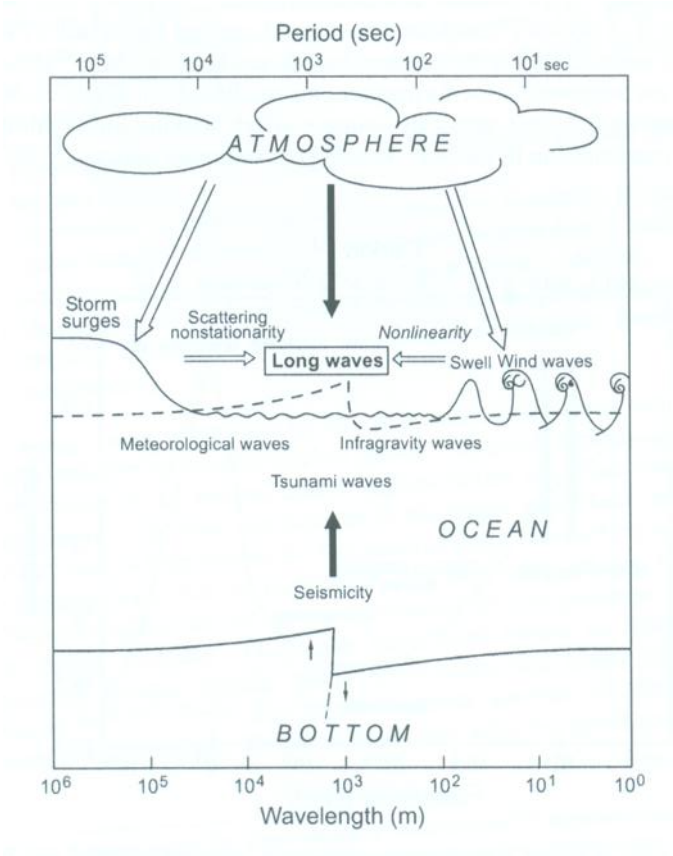

Figure 4-2. Sketch of the main forcing mechanisms generating long ocean waves (RABINOVICH, 2009)

Seiche oscillations produced by external periodic forcing can be both free and forced. The free oscillations are true seiches (i.e., eigen oscillations of the corresponds basin). However, if the external frequency (σ) differs from the eigen frequencies of the basin ($\sigma \neq \omega$), the oscillations can be considered *forced seiches* (WILSON, 1972). Open-ocean waves arriving at the entrance of a specific open-mouth water body (such as a bay, gulf, inlet, fjord, or harbour) normally consist of a broad frequency spectrum that spans the response characteristic of the water body from resonantly generated eigen-free modes to

nonresonantly forced oscillations at other frequencies. Following cessation of the external forcing, forced seiches normally decay rapidly, while free modes can persist for a considerable time (RABINOVICH, 2009).

WILSON (1972) concluded that long-period ocean waves are one of the causes of coastal seiches. RABINOVICH (2009) suggested these waves can be generated by many factors, with tsunami as one of the generation factor which is later explained in this study. Long waves are responsible for the formation and modification of the coastal zone and shore morphology (BOWEN & HUNTLEY, 1984; RABINOVICH, 1993); they also can strongly affect docking and loading/unloading of ships and construction in harbours, causing considerable damage.

4.2.1 Tsunami

Tsunami waves are the main factor creating destructive seiche oscillations in bays, inlets and harbours (HONDA *et al*., 1908; MEI, 1992; MUNK, 1962; MURTY, 1977; WILSON, 1972). Tsunamis can produce "seiche energies" of 10^3 – 10^5 cm^2 throughout the spectrum of frequencies although such events are relatively rare. For comparison, swell/wind waves and tides can produce energy of order 10^4 cm^2 (RABINOVICH, 2009)

The magnitude M_w = 9.3 earthquake that occurred offshore of Sumatra in the Indian Ocean on 26 December 2004 generated the most destructive tsunami in recorded history. Waves from this event were recorded by tide gauges around the world, including near-source areas of the Indian Ocean, and remote regions of the North Pacific and North Atlantic, revealing the unmatched global reach of the 2004 tsunami (MERRIFIELD *et al*., 2005; RABINOVICH *et al*., 2006; TITOV *et al*., 2005; THOMSON *et al*., 2007). In general, the duration of tsunami "ringing" increased with increasing off-source distance and lasted from 1.5 to 4 days (RABINOVICH *et al.*, 2006; RABINOVICH & THOMSON, 2007). The recorded oscillations were clearly polychromatic, with different periods for different sites, but with clear dominance of 40 - 50 min waves at

most sites. The analysis of various geophysical data from this event indicates that the initial tsunami source had a broad frequency spectrum, but most of the energy within the 40 – 50 min band. Therefore, although tsunami waves at different sites induced local eigen modes with a variety of periods, the most intense oscillations were observed at sites having fundamental periods close to 40 – 50 min (RABINOVICH, 2009).

4.3 Sea Level Oscillation in Mercury Bay

According to the shape and geometry of Mercury Bay, it can experience the process of oscillation as open-mouth basin. In open-mouth basin, the oscillation mainly generated by long waves entering through the open boundary from the open sea, and the wave energy decays mainly due to radiation out from the entrance (RABINOVICH, 2009). This condition is applied to Mercury Bay, where its opening is located directly facing the open sea of Pacific Ocean. The oscillation inside the bay may result from the *tides*, *atmospheric pressure*, *wind* and standing oscillations (seiche). Seiches resulting from *seismic activity* of 2010 Chilean and 2011 Tohoku earthquakes generated tsunamis are apparently seen in the tidal records installed in Whitianga Wharf. Locations of tidal gauges around New Zealand are given in Table 4-1.

The observations to identify the oscillation period of Mercury Bay was done by four methods; manually read from the tidal gauge record, calculation of semi-enclosed circular basin shape proposed by RABINOVICH (2009) as described in equation 4-3, by numerical model, and spectral density analysis.

The first method in determining the resonance periods of oscillation in Mercury Bay was by manually reading the periods of incident peaks during neap and spring tide for summer (December 2010) and winter (July 2011) times (Figure 4-3). During December 2010 or a month in summer time, within Mercury Bay, it is recorded that the oscillation period for a neap tide was between 22 to 45 minutes. Spring tide generates longer periods of oscillation, ranges between 33 to 63 minutes. The oscillation periods that generated during winter time range between 30 to 44 minutes (spring) and 22 to 47 minutes

(neap). The ranges of tidal level are about 1.62 m and 1.28 m for spring tide and neap tide respectively (Waikato Regional Council, 2006).

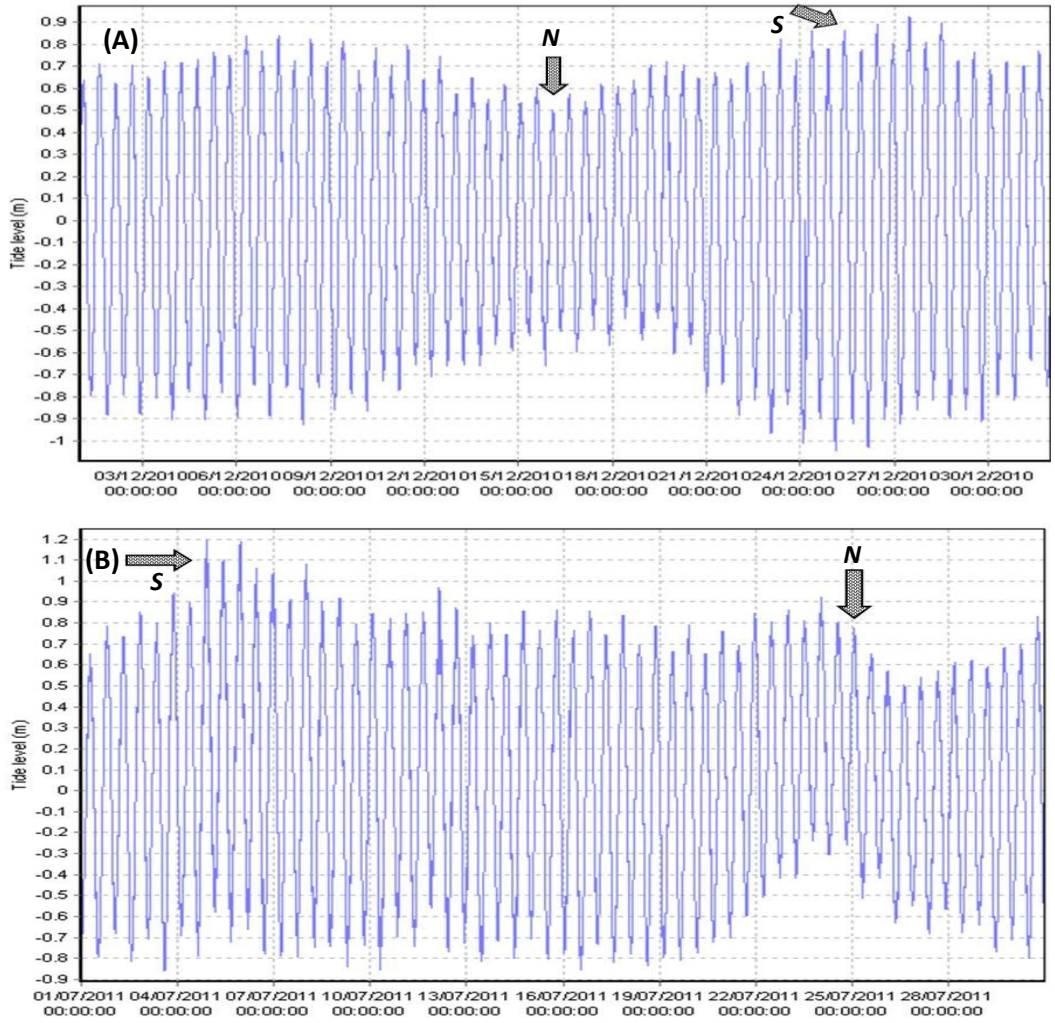

Figure 4-3. The tidal gauge records of Whitianga Wharf for December 2010 (A) and July 2011 (B). Spring and neap tide occurred are used to determine the oscillation period empirically. Note that the arrows with letter *N* and *S* indicates neap and spring tide respectively. Charts are taken from Waikato Regional Council website.

The second method is using the calculation of semi-enclosed circular basin shape (equation 4-3) given by Rabinovich (2009). Here, the bay is considered to shape as circular basin with an opening at one end and closed at the other end. The water depth at the opening is about 12.66 m and length to the other end is 5,303 m, then we can assume that Whitianga Wharf has resonant period of 35 minutes.

Numerical model simulations were performed by COMCOT version 1.7 (WANG, 2009) and from this simulation, sea level oscillation data was produced and used in spectral density analysis. The methods that have been employed in this study are explained in the following chapter.

Chapter 5 - METHODS

5.1 Introduction

In order to achieve the aim of this research, several procedures had to be taken that all are included as methods. The sequence of method is as follow:

1) Scenarios of earthquake events and hydrodynamic model.
2) Data processing
3) Comparing the results of modelled and measured data.

5.2 Scenarios of Earthquake Events and Hydrodynamic Model

5.2.1 Scenarios of Earthquake Events

The setting up of the scenarios was done by applying several fault plane models which were based on the previous study of POWER *et al*., historical tsunamis, and by any plausible scenarios of earthquake events in the Kermadec-Tonga Subduction Zone. Overall, 17 scenarios were developed:

a. Three scenarios based on the logic trees for the magnitude-frequency parameters of large earthquakes generated in the Kermadec Subduction Zone (Power et al., 2011);
    1. $M_{w=}$ 8.5 earthquake for southern segment.
    2. $M_{w=}$ 8.9 earthquake for middle segment.
    3. $M_{w=}$ 8.8 earthquake for northern segment.
b. Eleven scenarios of magnitude $M_{w=}$ 8.5 to $M_{w=}$ 9.5 that rupture the entire area of the Kermadec Subduction Zone.
c. Two scenarios of earthquakes that rupture composite segments of the Kermadec Subduction Zone; $M_{w=}$ 9.2 earthquake scenario for middle and southern segments, and $M_{w=}$ 9.3 earthquake scenario for middle and northern segments.
d. The 6th July 2011 M_w = 7.6 earthquake.

Table 5-1. Set of scenarios along the Kermadec Subduction Zone. The 'A" denotes southern part, B = middle part, C = northern part and the entire segments is ABC.

Scenario	Segment	Length (km)	Width (km)	Slip (m)	Magnitude (M_w)
1	ABC	1400	100	1	8.5
2	ABC	1400	100	1.5	8.6
3	ABC	1400	100	2	8.7
4	ABC	1400	100	2.8	8.8
5	ABC	1400	100	4	8.9
6	ABC	1400	100	5.6	9.0
7	ABC	1400	100	8	9.1
8	ABC	1400	100	10	9.2
9	ABC	1400	100	15	9.3
10	ABC	1400	100	22	9.4
11	ABC	1400	100	30	9.5
12	BC	1100	100	22	9.3
13	AB	900	100	22	9.2
14	C	500	100	8	8.8
15	B	600	100	10	8.9
16	A	300	100	5	8.5
17	6 July 2011	118	22	1.4	7.6

5.2.2 Hydrodynamic Model

5.2.2.1 Numerical Model

The tsunami scenarios that have been set up earlier in this chapter were then simulated using numerical model COMCOT (Cornell Multi-grid Coupled Tsunami model) version 1.7 by WANG (2009). The model COMCOT has been extensively used to investigate tsunami events, such as the 2003 Algeria tsunami (WANG and LIU, 2005), and the 2004 Indian Ocean tsunami (WANG and LIU, 2006; WIJETUNGE, 2009).

COMCOT adopts an explicit staggered leap-frog finite difference scheme to solve Shallow Water Equations in both Spherical and Cartesian Coordinates. A nested grid system, dynamically coupled up to 12 levels (which will be also referred to as layers) with different grid resolution, can be implemented in the model to fulfill the need for tsunami simulations in different scales. Spherical or Cartesian coordinate system, as well as either linear or nonlinear version of governing

equations can be chosen for each region. The nested grid system can provide simulations in both deep-water and near-shore coastal regions. The COMCOT model also provides a moving boundary algorithm to simulate tsunami inundation (WANG and LIU, 2006).

In the COMCOT model, water surface displacement is assumed to be the same as the deformation of the sea floor as long as the uplift motion is much faster than the wave propagation; otherwise, a submarine landslide model should be used to include transient effects. For a given earthquake, the displacement of seafloor is determined from linear elastic dislocation theory (MANSINHA & SMYLE, 1971; OKADA, 1985 in WANG, 2009). More details of COMCOT is given in WANG (2009).

5.2.2.2 General Parameters for Numerical Simulation

In COMCOT, the first set up that must be done is to define the general parameters for the numerical simulation. These include the total run time (seconds), time interval (second), initial and boundary conditions. For more detail, please refer to WANG (2009). In this study, the general parameters for all tsunami scenarios were the same and they can be seen in Figure 5-1.

```
####################################################
# Control file for COMCOT program (v1.7)
####################################################
#--+-----1----+----2----+----3----+----4----+----5----+----6----+----7----+----8
#=============================================:============================
# General Parameters for Simulation          : Value Field
#=============================================:============================
#Job Description: Kermadec Trench Simulation
 Total run time (Wall clock, seconds)          : 28800.000
 Time interval to Write Data   ( unit: sec )   :    1800.0
 Output Zmax & TS (0-Max Z;1-Timeseries;2-Both) :     2
 Start Type (0-Cold start; 1-Hot start)        :     0
 Resuming Time If hot start (Seconds)          :     0.00
 Specify Min WaterDepth offshore  (meter)      :     0.00
 Initial Cond. (0:FLT,1:File,2:WM,3:LS,4:FLT+LS):    0
 Specify BC  (0-Open;1-Sponge;2-Wall;3-FACTS)  :     0
 Specify Input Z filename (for BC=3, FACTS)    : 23926h.asc
 Specify Input U filename (for BC=3, FACTS)    : 23926u.asc
 Specify Input V filename (for BC=3, FACTS)    : 23926v.asc
#=============================================:============================
```

Figure 5-1. General parameters section in COMCOT.CTL for all tsunami scenarios applied in the numerical simulation.

5.2.2.3 Model Grids

Four dynamically coupled systems of nested grids were employed to simulate the tsunami propagation from Kermadec Trench towards Mercury Bay. Those grids were derived from GEBCO and high resolution of shallow multibeam data from University of Waikato, and digital terrain data (LIDAR data sets 2004) provided by Environment Waikato.

The first grid area contains the whole bathymetric data from the location where the earthquake generated tsunami to the research area. The first grid as the largest grid spans from 170 to 190 degrees east Longitude and 40 to 26 degrees south Latitude (Figure 5-2A). The second grid is embedded in grid 1, and covers the area from 175.2 to 176.6 degrees east Longitude and 38 to 26 degrees south Latitude (Figure 5-2B). Bathymetry data for the first and the second grids employed in the simulations were obtained from GEBCO, the grid sizes were 1.852 m and 400 m respectively. In the COMCOT model, the bathymetry data of respective grids should be in ASCII format and written in 3 columns (latitude, longitude, depth).

The grid 3, which is nested in grid 2 has a finer resolution of 10 m. Grid 4 which covers the area of Mercury Bay to Whitianga Township has grid spacing of 5 m. Both of these nested model grids (Figure 5-2C and 5-2D) were derived from highly accurate digital terrain data (LIDAR data set) provided by Environment Waikato.

A description of the spatial extent and the resolution of each grid as well as the type of shallow-water equations (SWE) used are given in Table 5-2.

Table 5-2. The spatial extent of grid areas employed in COMCOT numerical simulation of Kermadec Trench tsunami propagation to Whitianga Wharf (grid-4) of New Zealand.

Grid	Latitude (^{0}S)		Longitude (^{0}E)	
Area	y _Start	y_End	x _Start	x_End
1	-40	-26	170	189.98
2	-38	-36.0	175.26	176.6067
3	-37.2477	-36.2022	175.3022	176.1844
4	-36.9148	-36.664	175.5452	175.77826

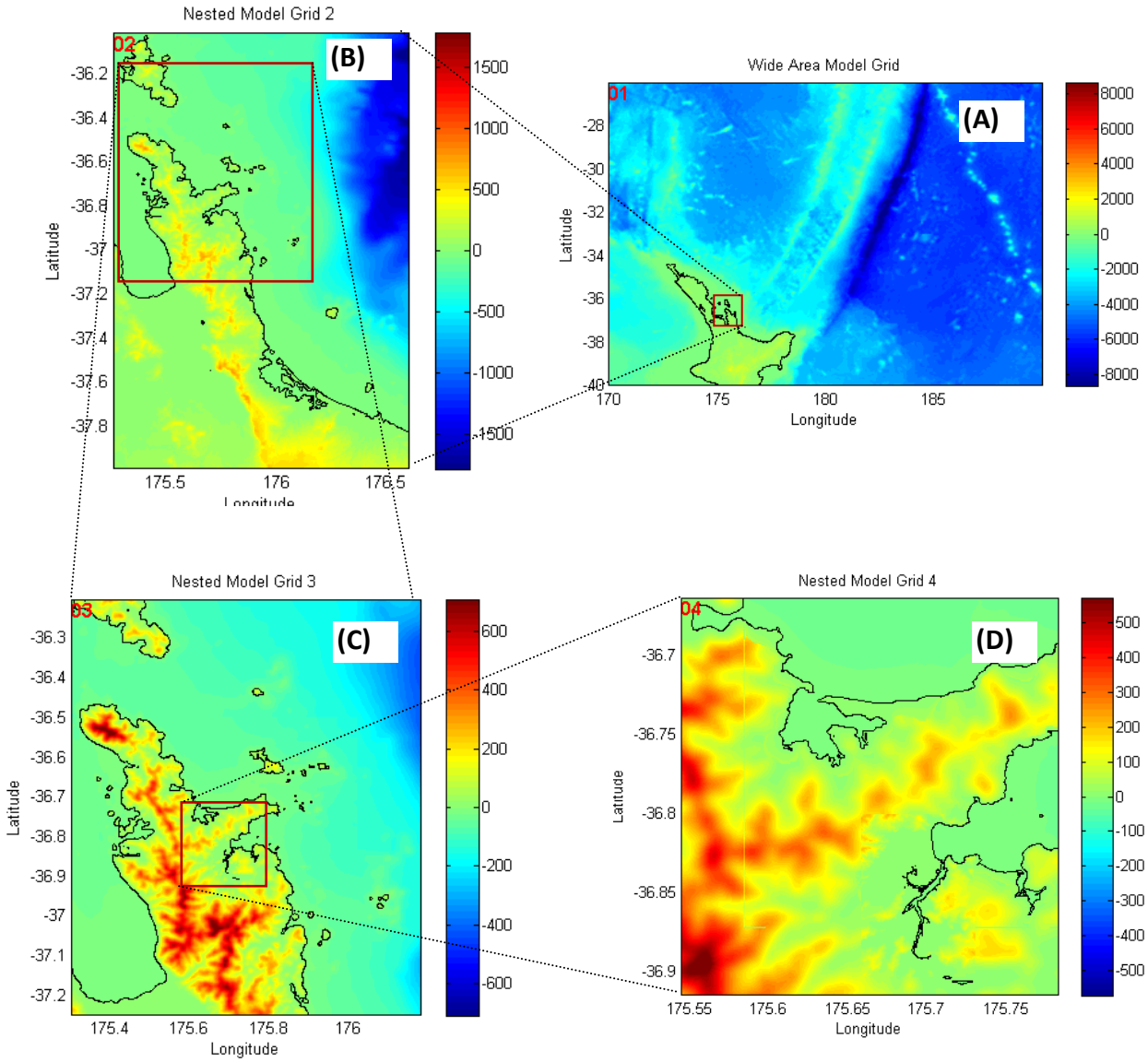

Figure 5-2. Four layer grids applied as computational domain; wide area model as Grid 1(A), nested model grid 2 (B), grid 3 (C) and grid 4 (D) has the finest resolution of 5 m.

5.2.2.4 Virtual Tide Gauge Stations

There were 10 virtual tide gauges employed in the simulation to record the sea level oscillations caused by tsunamis. Those stations were divided into two categories; near tsunami sources and Mercury Bay stations. Their positions are given in the Table 5-3 and they are shown in Figure 5-3 (A and B).

Table 5-3. Location of virtual tide gauge stations employed at near tsunami source and within Mercury Bay. Note in the remarks, the KSZ stands for Kermadec Subduction Zone. Segment A = southern segment, segment B = middle segment, and segment C = northern segment of the Kermadec Subduction Zone.

Tide Gauge (TS)	Coordinates		Remarks
	Longitude	Latitude	
01	175.90	-29.18	Near source 6 July 2011 event
04	175.759	-36.8067	At the entrance of Mercury Bay
07	175.7298	-36.8161	At the entrance of Buffalo Bay
09	175.7065	-36.8183	In the vicinity of Whitianga Township
12	175.7094	-36.8358	At Whitianga Wharf
13	180.0	-32.3015	At the middle of the KSZ
14	179.5163	-37.1886	At the southern end of the KSZ
15	179.761	-36.82805	At the middle of segment A
16	181.65285	-33.1434	At the middle of segment B
17	183.4556	-28.48635	At the middle of segment C

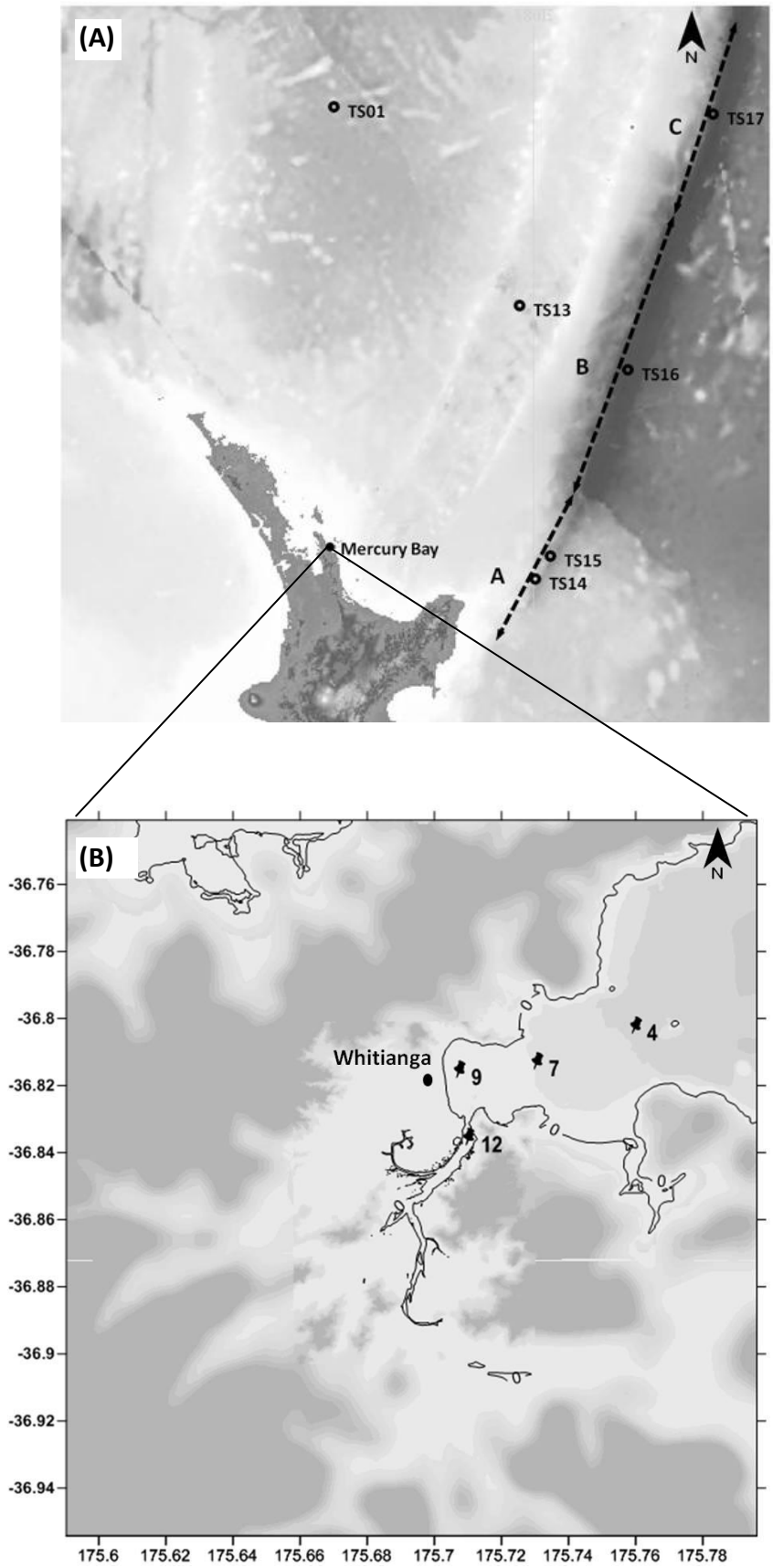

Figure 5-3. The location of virtual tide gauges employed to record the tsunami waves; (A) at the tsunami sources, and (B) within the Mercury Bay. Figure (A) was edited from Gebco_08 (2007).

5.2.2.5 Elastic Fault Plane Parameters

COMCOT simulates the seafloor displacement caused by an earthquake event by applying elastic finite fault plane theory (MANSINHA & SMYLE, 1971; OKADA, 1985 in WANG, 2009). The theory assumes a rectangular fault plane being buried in a semi-infinite elastic half plane. This plane is an idealized representation of the interface between two colliding tectonic plates where violent relative motion (i.e. dislocation) occurs during an earthquake event. The dislocation (or slip motion) occurring on the fault plane will then deform the surface of the semi-infinite medium, which is considered as the seafloor displacement during the earthquake event (WANG, 2009.). In COMCOT, the deformation will be computed if all the fault parameters required have been filled in the COMCOT.ctl file. For multiple fault planes, an additional file of deformation data written in ASCII format is needed.

The description of strike, dip and slip as fault parameters are shown in Figure 5-4 below.

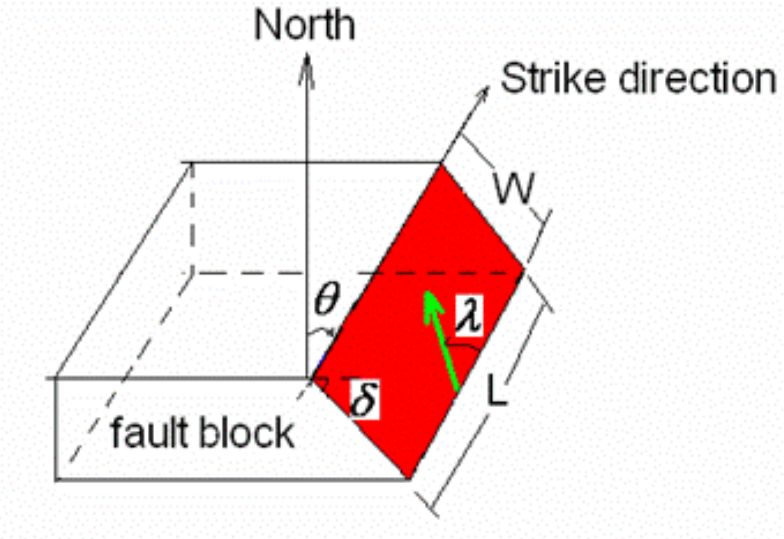

Figure 5-4. Description of Strike (θ), Dip (δ) and Slip/Rake angle (λ) as fault plane parameters (from *Cornell edu.*)

Where Shearer (2009) defined:

- Strike (θ) direction is the azimuth of the fault from north where it intersects a horizontal surface.

- Dip (δ) is the angle from the horizontal.
- Rake angle (λ) is the angle between the slip vector and the strike.

For the July 6th 2011 Kermadec earthquake, we adopted the fault plane parameters (strike, dip, slip and moment magnitude) from the Global CMT Moment Tensor Solution. The length and width of the fault plane were calculated using the empirical equation of Wells and Coppersmith (1994) for an earthquake with moment magnitude ranging from M_w4.8 – M_w8.1. Table 5-4 gives the fault plane parameters of July 6th 2011 Kermadec earthquake.

Table 5-4.Fault plane parameters for the July, 6th 2011 Kermadec earthquake.

Epicenter (Lon,Lat)	Focal depth (km)	Length (km)	Width (km)	Strike (N..^{0}E)	Dip (^{0})	Slip (^{0})
175.76, -29.18	20	118	22	171.00	33	-105

Table 5-5 summarizes the hypothetical fault plane parameters which were used for various Kermadec Trench tsunamis scenarios applied in this study.

Table 5-5. Geometric description of unit patches for the Kermadec subduction interface (adopted from POWER *et al*., 2011). The southern segment consist of unit patches 01a-01b to 03a-03b, middle segment consist of unit patches 04a-04b to 09a-09b, and the northern segment consist of unit patches 10a-10b to 10a-10b.

KT unit patch	Epicenters (Lon; Lan)	Focal depth (km)	Length (km)	Width (km)	Strike (N..^{0}E)	Dip (^{0})	Slip (^{0})
01a	179.6930, -37.8079	3.97	100	50	212.40	4	90
02a	180.2999, -37.0525	4.90	100	50	212.30	4.60	90
03a	180.8188, -36.2624	5.82	100	50	202.90	5.21	90
04a	181.2725, -35.4410	6.69	100	50	205.00	5.79	90
05a	181.6950, -34.6118	7.31	100	50	200.00	6.00	90
06a	182.0470, -33.7591	7.73	100	50	197.50	6.00	90
07a	182.3678, -32.8986	8.00	100	50	196.90	6.58	90
08a	182.6807, -32.0381	8.00	100	50	197.00	8.12	90
09a	183.0170, -31.1854	8.00	100	50	199.90	9.67	90
10a	183.4003, -30.3483	8.00	100	50	202.80	11.22	90
11a	183.7524, -29.5035	8.00	100	50	196.70	9.55	90
12a	184.0184, -28.6351	7.54	100	50	193.20	11.07	90
13a	184.2452, -27.7589	7.03	100	50	192.40	13.37	90
14a	184.4564, -26.8828	6.52	100	50	191.70	15.67	90
01b	179.2142, -37.5678	7.46	100	50	212.40	6.00	90
02b	179.8257, -36.8133	8.92	100	50	212.30	8.71	90
03b	180.3078, -36.0883	10.36	100	50	202.90	11.45	90
04b	180.7754, -35.2521	11.74	100	50	205.00	14.07	90
05b	181.1850, -34.4590	12.54	100	50	200.00	14.69	90
06b	181.5346, -33.6248	12.96	100	50	197.50	14.27	90
07b	181.8593, -32.7689	13.73	100	50	196.90	14.39	90
08b	182.1791, -31.9081	15.06	100	50	197.00	15.41	90
09b	182.5303, -31.0347	16.40	100	50	199.90	16.44	90
10b	182.9296, -30.1776	17.73	100	50	202.80	17.48	90
11b	183.2649, -29.3762	16.30	100	50	196.70	15.55	90
12b	183.5294, -28.5344	17.14	100	50	193.20	15.96	90
13b	183.7629, -27.6651	18.59	100	50	192.40	16.46	90
14b	183.9816, -26.7951	20.02	100	50	191.70	17.22	90

5.3 Data Processing

5.3.1 Modelled Tsunami

From the numerical simulation, time series of sea level at the virtual tide gauges will be generated. The time step will be recorded in unit second and the sea level is in metres. Based on KARLING (2009), we can determine the first leading wave, the wave heights, the amplitudes and the wave periods directly from a graph that plots the time versus sea level (Figure 5-5). The arrival time was determined based on the study of RABINOVICH & THOMSON (2007), where when the sea level change is gradual, then the first increase or decrease data point is marked as the arrival time. One of the simulation result that have been plotted as graph of time series (in minute) and the recorded sea level at a virtual tide gauge station inside the Buffalo Bay is described in Figure 5-6.

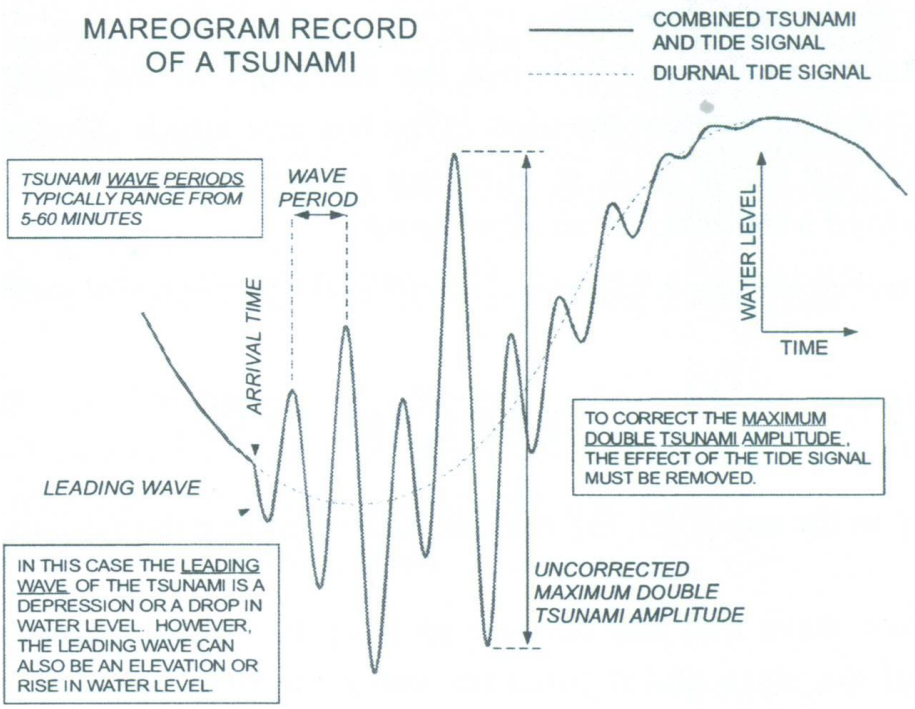

Figure 5-5. Plots or mareogram of tsunami wave trains and methods on how to read the tsunami signal by KARLING (2009).

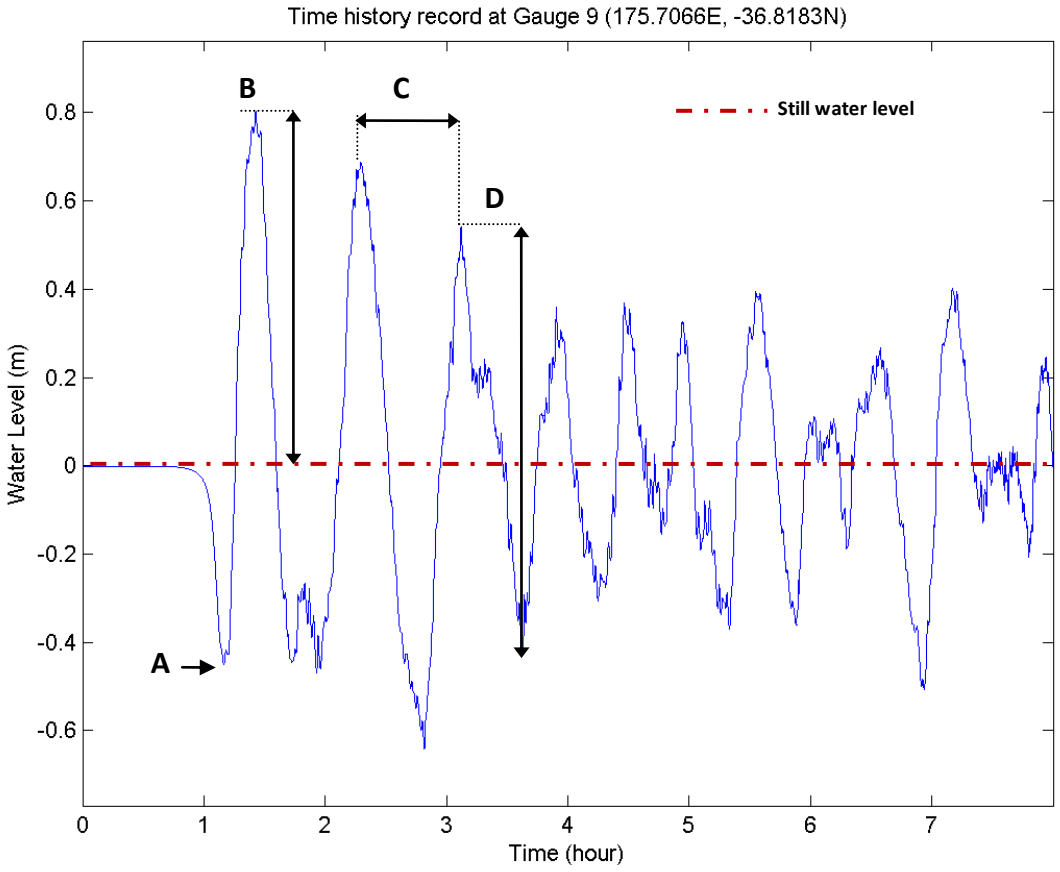

Figure 5-6. Plot of data generated from numerical simulation. The letter (A) marks the tsunami arrival time, (B) is the wave amplitude, (C) is the wave period, and (D) is the peak to trough (wave height).

The sea level elevations that resulted from the modeled tsunamis will be accounted as the amplification level of each respective tsunami scenario.

5.3.2 Power Spectral Density Analysis

To examine spectral properties of long wave oscillation (tsunami waves) that enters the bay, the power spectral density analysis was conducted in this study. Spectra density for each location is mainly controlled by the natural response of the bay or inlet as the function of basin geometry and depth (Rabinovich, 2009), thus, this procedure is expected to identify the response of the Mercury Bay of any tsunami events.

The spectral density estimate via Welch's method (Welch, 1967) was applied to obtain the spectral properties of both modeled and measured tide record data. From

the modeled data, we took 8 hours post earthquake sea level elevation data which means 12,448 points with a time step of 2.32 seconds, divided into 3 Hamming windows (Hamming, 1977) with half-window overlaps. The signal processing toolbox in Matlab R2010a was utilized for this purpose.

In order to determine the spectral properties of the tsunami events at Whitianga Wharf and to compare these properties with those of the background oscillations at the same site, we used the 1-minute interval tide record data provided by Waikato Regional Council. Those are:

a. 47 hours measured tide records data representing spring tide during summer in December 2010 and winter days in July 2011. These data were used for background oscillation.
b. Tide records data from 7.50 am on February, 28th to 7.50 am on Mach 1st 2010 for the Chilean tsunami event.
c. Tide records date March, 12nd (6.23 am) to 14th (5.48 am) for the 2011 Tohoku-Japan tsunami event.

The spectral analysis for measured data was done using the same method with the modeled one, except the number of Hamming's windows was 6.

Chapter 6 - RESULTS AND DISCUSSION

6. 1 Introduction

In the first part of this chapter, the simulated tsunami results will be presented and discussed. The next part will present an analysis of the measured tide record at Whitianga Wharf for 2 recent tsunami events. The final part will present a comparison of spectra properties of both modelled and measured tsunami events.

6.2 The modelled tsunamis

6.2.1 Scenario 1: M_w = 8.5 earthquake for southern segment of Kermadec Trench

In this scenario, I simulated an earthquake that ruptures the southern segment of the Tonga-Kermadec subduction zone (segment A in POWER et al., 2011). The rupture zone extends for 300 km in length and 100 km in width, and the strike direction varied from 202.9° to 212.4° northwards along the rupture, while the dip increased from 4° to 5.21°. The slip angles were uniform at 90° and fault dislocation was 5 m. The simulation was run for 8 hours with data for the whole grid being written every 1800 s. (30 minutes). The snapshot of sea water level will be produced for every 30 minutes, and maximum water surface elevation will be produced for every hour and at the end of a simulation. More frequent snapshots were not possible given the available computing resources. Further, several virtual tide gauges were used, TS04, TS07, TS09 and TS12 (Figure 6-1), where data was stored every time step (2.3 s.).

After tsunami generation, most of the energy propagated as a positive wave to southeast (South America), while a negative wave or depression headed to northwest (see Figure 6-2 (A)). The initial water displacement that reached North

Island of New Zealand was a negative wave. From the virtual tide gauge sea oscillations of simulated tsunami (Figure 6-2), the arrival time of tsunami after the earthquake can be estimated by the first leading increase/ decrease data point (RABINOVICH and THOMPSON, 2007). Hence, the arrival time of tsunami from this scenario is at 56 minutes at the entrance of Mercury Bay (TS04), 62 minutes at the entrance of Buffalo Bay (TS07), 73 minutes in front of Whitianga Township within Buffalo Bay (TS09) and 75 minutes at Whitianga Wharf (TS12). The distance between virtual tide gauge sites at Mercury Bay entrance (TS04) to the entrance of Buffalo Bay (TS07) is about 2.8 km, and from here to the one at the vicinity of Whitianga Township (TS09) is about 4.9 km, and the distance from the latest site to the Whitianga Wharf (TS12) is about 1.9 km (Figure 6-3).

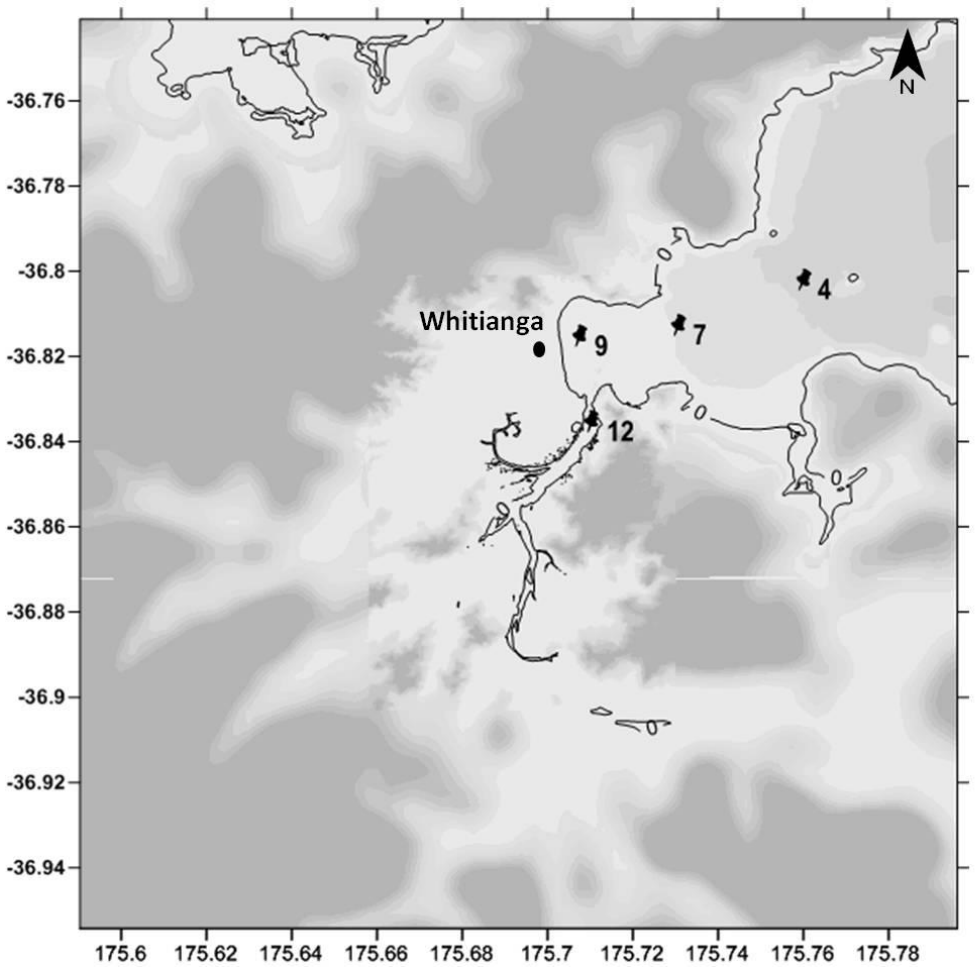

Figure 6-1. The location of virtual tide gauges within Mercury Bay.

Figure 6-2 (B) is a half hour snapshot that shows first depression wave of tsunami and figure 6-2 (C and D) show that there were 2 times of maximum water levels in the vicinity of Whitianga Township and Whitianga estuary inlet were achieved after 1.5 and 3 hours of the earthquake (also see Figure 6-5).

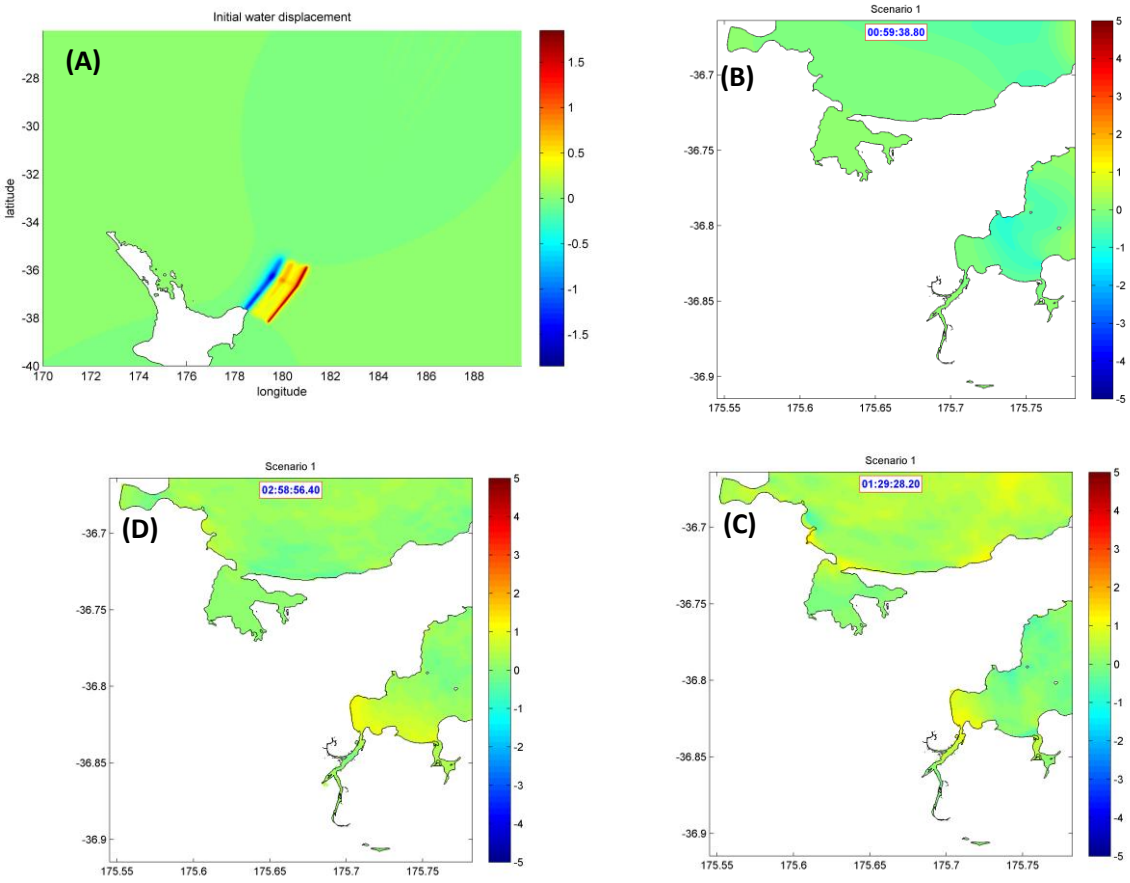

Figure 6-2 The initial water displacement generated by southern segment scenario with M_w= 8.5 propagated the energy mostly towards the southeast and propagated a depression wave to the northwest (A), (B) the first depression wave marks the tsunami arrival at the entrance of Mercury Bay about 1 hours after the earthquake, (C) and (D) shows the maximum water level within Mercury Bay 1.5 and 3 hours after the earthquake. Note that the scale bar unit is in metres.

In the figure 6-2 above, it is seen that the initial water displacement at the tsunami source that propagated to the north-west was down to -1.5 m and the trough was reduced into about 50% as it arrived at the entrance of Mercury Bay (Figure 6-2B and 6-3). It only took about 28 minutes after the first trough arrived at TS04 (entrance of MB) for the first highest peak of tsunami to arrive in the vicinity of Whitianga Township (Figure 6-2C and 6-3).

Figure 6-3 illustrates the distance between virtual tide gauges and arrival time versus the tsunami amplitudes for respective sites. The left hand side of this graph shows the first troughs as the tsunami arrival time which followed by first peaks that are showed on the right hand side of the graph. It is seen that the tsunami amplitudes increase landward but then the narrowing channel and shallower water as the wave propagated into the Whitianga Wharf attenuated the amplitudes.

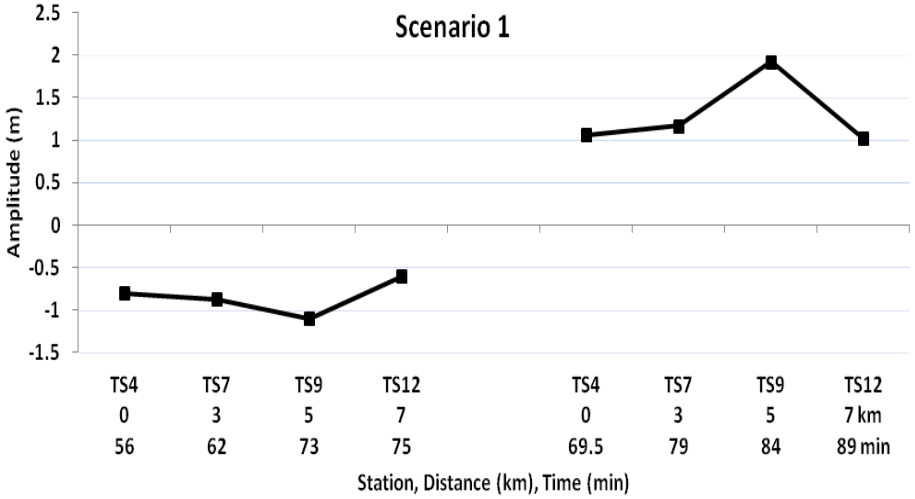

Figure 6-3. Distance and arrival time of first troughs and peaks at each virtual tide gauge plotted with the tsunami amplitudes resulting from scenario 1.

As the tsunami propagated landward, its celerity was reduced by the friction with the seabed but the wave height increased. It took 6 minutes for about 3 km distance from the entrance of Mercury Bay (TS04) to the entrance of Buffalo Bay (TS07), but then the tsunami were significantly slowed down to 11 minutes for 2 km distance from TS07 to TS09 (see Figure 6-1 and 6-3).

Table 6-1 summarises the tsunami arrival times, maximum and minimum amplitudes, and the maximum peak to trough distance resulting from this scenario. At all sites, the highest amplitude was recorded as the first positive wave after the negative leading wave. At sites TS04 and TS12, the water dropped sharply after the first high wave down to the deepest trough. At TS07 that located at the entrance of Buffalo Bay and at TS09, in front of Whitianga Township (Buffalo Bay), the deepest troughs were recorded after the second high wave (see Figure 6-5). The maximum sea level oscillation occurred at site TS09; which the tsunami amplitude reached up to 1.92 m above the mean sea water level. At site TS07, the highest amplitude was

22 cm higher than both sites of TS04 and TS12, where the tsunami amplitudes were up to 1 m.

Table 6-1. Result of simulated tsunami generated in southern segment of the Kermadec Trench. The magnitude was M_w = 8.5.

Tide gauge	Arrival time (min)	Amplitudes (m)		Maximum peak to trough (m)
		Maximum	Minimum	
TS04	56	1.06	- 0.79	1.85
TS07	62	1.22	-1.3	1.52
TS09	73	1.92	-1.55	3.44
TS12	75	1.04	-0.59	1.63

An M_w = 5.1 earthquake event occurred in the Kermadec Subduction Zone on 22 November 2011 at 8:38 am New Zealand time. The focal depth was 12 km and according to its location which was centred at 37.53°S and 179.73°E (Figure 6-4 (A)), it lies within the southern segment (segment A). Based on scenario 1, any tsunami generated from this segment will arrive at Whitianga Wharf 75 minutes after the earthquake, which means in the real time, a tsunami wave would arrive at 9.53 am (NZT). Figure 6-4(B) shows the measured tide level at Whitianga Wharf at corresponding time and it is seen that there was an obvious peak. The tsunami may have been experiencing amplification that produced the 20-25 cm spike (de Lange, personal communication, 2011).

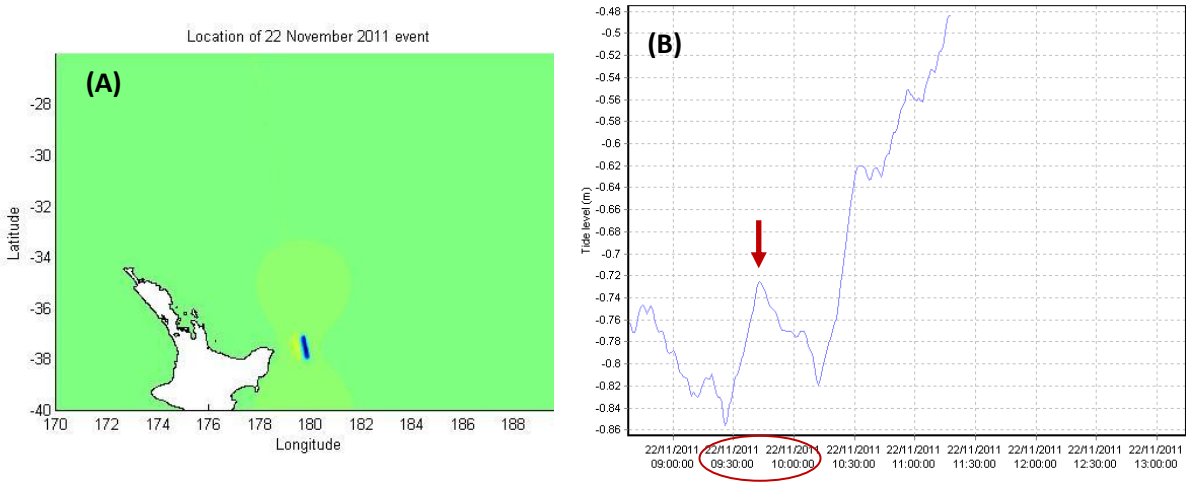

Figure 6-4. (A) Location of M_w = 5.1 earthquake on 22 November 2011 (8:38 am NZT) posited at the southern segment of the Kermadec Subduction Zone. (B) Measured tide level of tide gauge installed at Whitianga Wharf shows a significant peak (red arrow) at about the same tsunami arrival time with modelled tsunami from this segment (75 minutes after the earthquake).

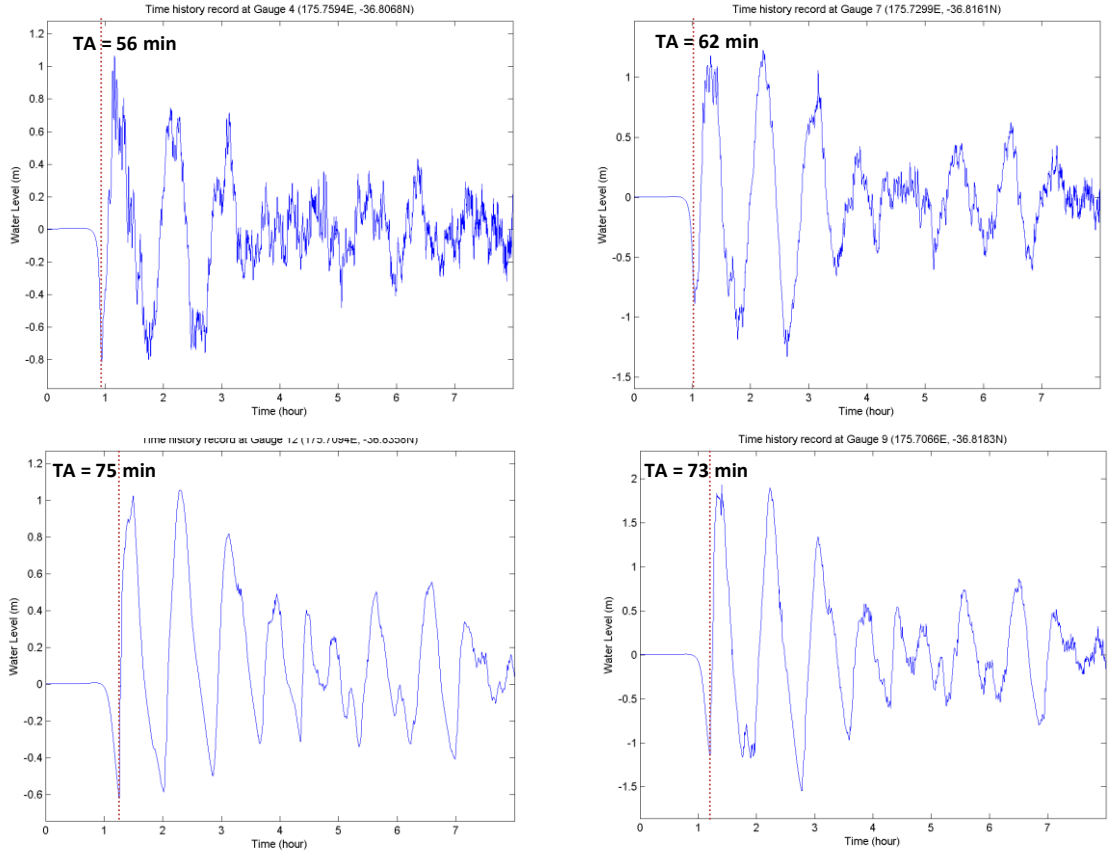

Figure 6-5. The tsunami wave train recorded by virtual tide gauges sited at the entrance of Mercury Bay (TS04), in the vicinity of Whitianga Township within Buffalo Bay (TS09) and at the Whitianga Wharf (TS12). The tsunami was amplified at TS09, the peaks up to 1.9 m, and at TS12, where amplification mostly affected the later waves. The sea water level oscillations started to calmed down after 7 hours of the earthquake.

The periods between successive peaks for the first three highest waves ranged from 47 to 60 minutes. For subsequent waves the periods became shorter (20 to 40 minutes) and the amplitudes declined. The fundamental periods of Mercury Bay is at around 35 minutes (Chapter 4) and tsunami periods seemed to coincide with the periods of Mercury Bay after about 3 hour's elapsed time of the earthquake. A significant difference can be seen in the tsunami record at gauge TS04 compared to the other records (Figure 6-5). At this site, the recorded oscillations were polychromatic with denser oscillations than the other two sites located inside the bay. This indicates that Mercury Bay filters the tsunami wave, enhancing lower frequencies, and attenuating the higher frequencies.

6.2.2 Scenario 2: M_w = 8.9 earthquake for middle segment of Kermadec Trench

An earthquake of magnitude M_w = 8.9 was simulated for the middle segment (segment B in POWER et al., 2011) of the Tonga Kermadec Subduction Zone. This segment extends from 181° to 183°W and -35.8° to -30.7°S. The length and width of the rupture zone are 600 km and 100 km respectively. The strike direction varied from 196.9° to 205° from south to north. The dips increased from from 5.79° to 16.44° towards the north. The slip angles were uniform at 90° and fault dislocation was 10-m. The simulation was run using the same time step and data storage settings as Scenario 1.

As can be seen in Figure 6-6(A), the tsunami waves from the source area propagated mostly to the northwest and southeast. At Mercury Bay, the first tsunami wave was characterized by a gradually decreasing water level. The tsunami arrival times for this scenario were slightly later than those from the southern segment; being 68 minutes at the entrance (TS04), 74 minutes at the entrance of Buffalo Bay (TS07), 81 minutes within Buffalo Bay (TS09), and 84 minutes at the Whitianga Wharf (Figure 6-7). It took 6 minutes for the tsunami waves to propagate from the entrance of Mercury Bay to arrive at the entrance of Buffalo Bay (TS07), then from this point 7 minutes to reach the vicinity of Whitianga Township, and another 3 minutes to Whitianga Wharf. These times are similar to those for Scenario 1, but not the same.

The maximum sea level of up to 1.5 m was reached at about 1.5 hours after the earthquake (Figure 6-7) with the highest occurring at the northern end of Buffalo Bay and off Cooks Beach in the south eastern corner of Mercury Bay (Figure 6-6B). Here, the arrival of first trough cannot be presented due to the arrival time lag and the 30 minutes snapshot, however, it is clearly seen that the arrival of peaks and trough were alternate with each other every 30 minutes (Figure 6-6B, C, and D).

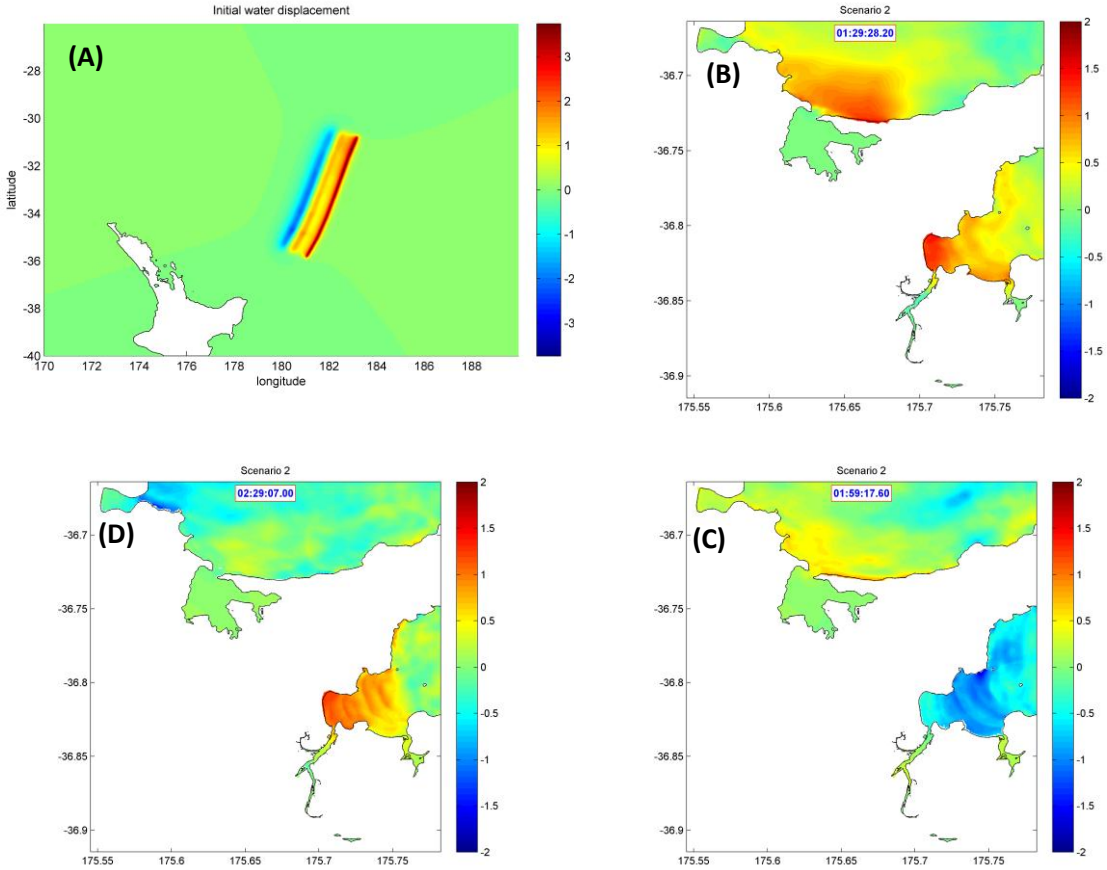

Figure 6-6. (A) The initial water displacement generated from middle segment scenario with M_w = 8.9. The tsunami energy propagated mostly to southeast and a depression wave propagated to the northwest. (B) Contoured water elevation around Mercury Bay 1.5 hours after the earthquake showing the first highest peaks which then followed by deepest trough in about 30 minutes later (C). (D) shows the second peaks that arrive around Mercury Bay. The scale bar unit is in metres.

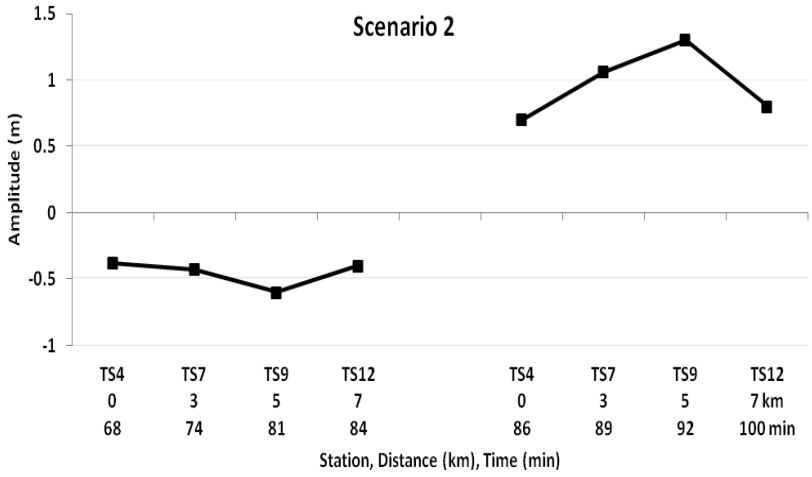

Figure 6-7. Distance and arrival time of first troughs and peaks at each virtual tide gauge plotted with the tsunami amplitudes resulting from scenario 2.

Table 6- 2 shows the tsunami arrival time, maximum and minimum amplitudes, and the maximum peak to trough distance resulting from this scenario. The tide gauge in front of Whitianga Township (Buffalo Bay – TS09) recorded the greatest amplification; at this site the sea water level was 1.28 m above the mean water level, 41% and 10% higher than at the entrances to Mercury Bay and Buffalo Bay respectively. Overall the tsunami displacement was 43% larger at site TS09. In contrast, the tsunami response was attenuated by 17% at Whitianga Wharf (TS12).

Table 6-2 Result of simulated tsunami generated in middle segment of Kermadec Trench. The magnitude was M_w = 8.9.

Tide gauge	Arrival time (min)	Amplitudes (m)		Maximum peak to trough (m)
		Maximum	Minimum	
TS04	68	0.7	-1.07	1.7
TS04	74	1.0	-1.17	2.17
TS09	81	1.28	-1.25	2.4
TS12	84	0.8	-0.67	1.4

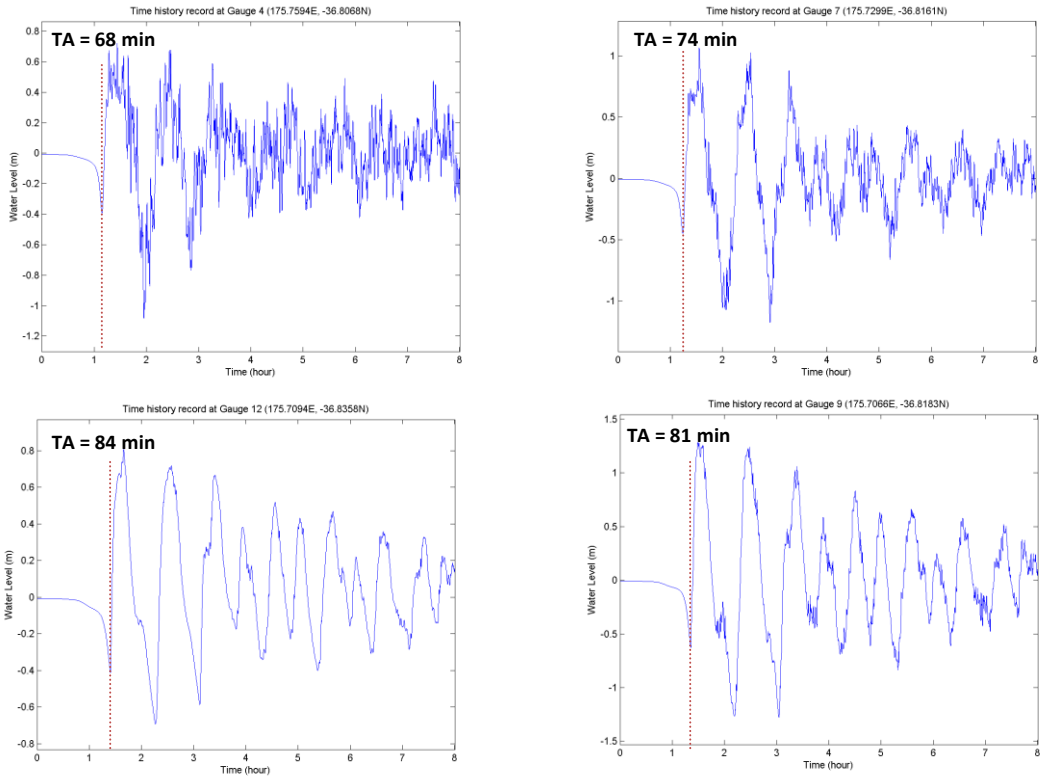

Figure 6-8. Tsunami wave trains recorded at virtual tide gauges sited at the entrance of Mercury Bay (TS04), at the entrance of Buffalo Bay (TS07), in the vicinity of Whitianga Township within Buffalo Bay (TS09), and at the Whitianga Wharf (TS12).

Tsunami wave periods ranged from 49 to 61 minutes for the first few waves, and subsequent periods shortened to the fundamental period of the basin as the amplitudes decreased (Figure 6-8). The decay was started 7 hours after the earthquake. Overall the behaviour observed at the virtual tide gauges was similar to the southern segment scenario.

6.2.3 Scenario 3: M_w = 8.8 earthquake for northern segment of Kermadec Trench

An earthquake induced tsunami scenario was applied for the northern segment of the Tonga-Kermadec Subduction Zone (segment C in POWER et al., 2011). The rupture zone is 500 km long and 100 km wide. The strike direction increased from 191.7° to 202.8° to the north and the dips increased from 9.55° to 17.22°. The slip angles were uniform at 90° and fault dislocation was 8 m. Otherwise, same simulation settings were used as for previous scenarios.

Figure 6-9(A) shows the initial water displacement at the tsunami source, where it is clearly seen that most of tsunami wave energy propagated toward the west and east. The initial direction of tsunami wave propagation and the distance from earthquake epicenter to Mercury Bay significantly reduced the tsunami oscillations and delayed the arrival time recorded at all virtual tide gauges. Unlike the previous scenarios, the tsunami wave arrived at Mercury Bay as a positive leading wave; so the sea level initially rose instead of receded (Figure 6-9A). From the 30 minutes snapshot, the maximum tsunami response occurred at about 3 hours after the earthquake (Figure 6-9D).

The following table 6-3 shows the tsunami arrival time, maximum and minimum amplitudes, and the maximum peak to trough distance resulting from this scenario. The tsunami arrival time is determined by the first increase in water level. The tide gauge in front of Whitianga Township (Buffalo Bay – TS09) recorded the highest amplification; at this site the sea water level was amplified by 60% and 28% relative to TS04 and TS07 respectively.

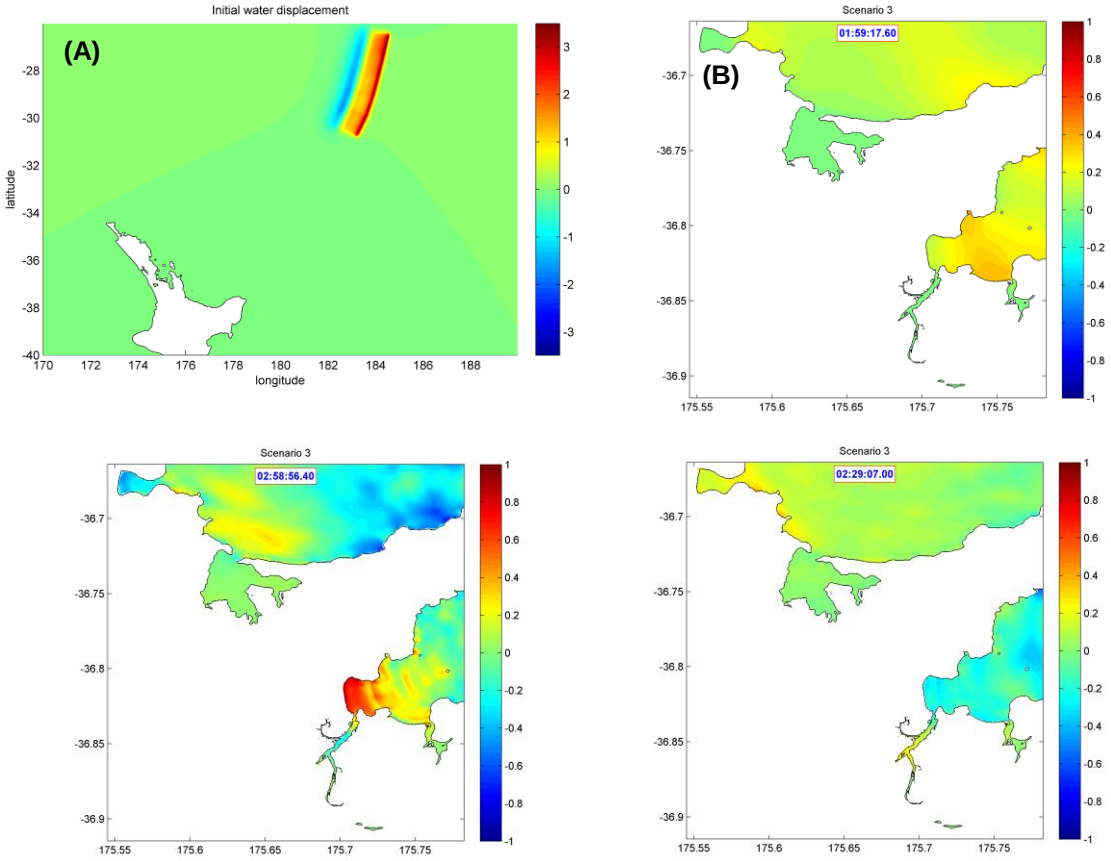

Figure 6-9. (A) The initial water displacement generated by the northern segment earthquake scenario with M_w = 8.8. The tsunami propagated the energy mostly to the east and west. (B) and (C) show the first arrival of tsunami peaks and troughs respectively, and (D) shows the maximum response around Mercury Bay occurred at about 3 hours after the earthquake. Scale bar unit is in metres.

Table 6-3. Result of simulated tsunami generated in northern segment of Kermadec Trench. The magnitude was M_w = 8.8.

Tide gauge	Arrival time (min)	Amplitudes (m)		Maximum peak to trough (m)
		Maximum	Minimum	
TS04	122	0.5	-0.5	1
TS04	126	0.6	-0.55	1.15
TS09	127	0.9	-0.7	1.6
TS12	131	0.4	-0.4	0.8

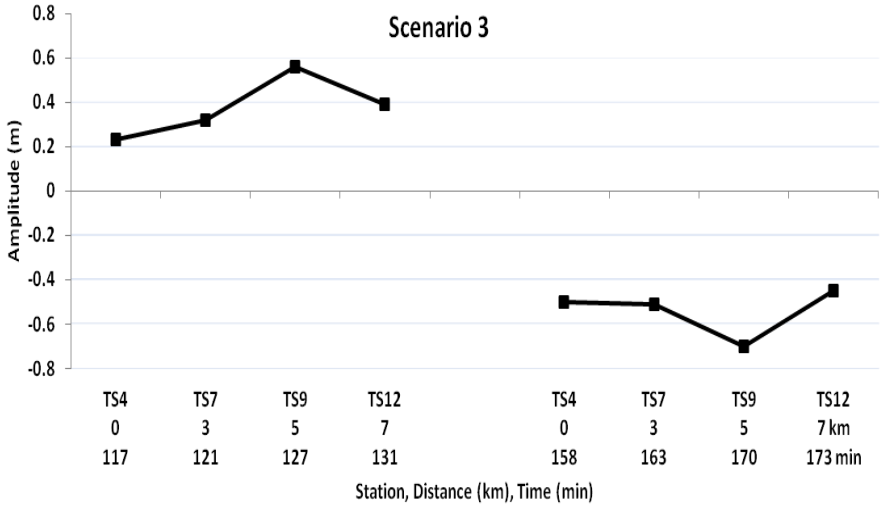

Figure 6-10. Distance and arrival time of first troughs and peaks at each virtual tide gauge plotted with the tsunami amplitudes resulting in scenario 3.

Figure 6-10 describe the distance and time plotted versus the amplitudes of first peaks and troughs that arrived in Mercury Bay. The first tsunami peak propagated from the entrance of Mercury Bay to vicinity of Whitianga Township within 10 minutes over a 5 km distance.

The periods of the first three tsunami waves ranged from 49 to 71 minutes at all sites. The periods started to shorten as the amplitudes decreased after 6.5 hours had elapsed since the time of the earthquake (Figure 6-11). Here, it is also seen that the bay's topography filtered the 'noise' of tsunami as it propagated further landward.

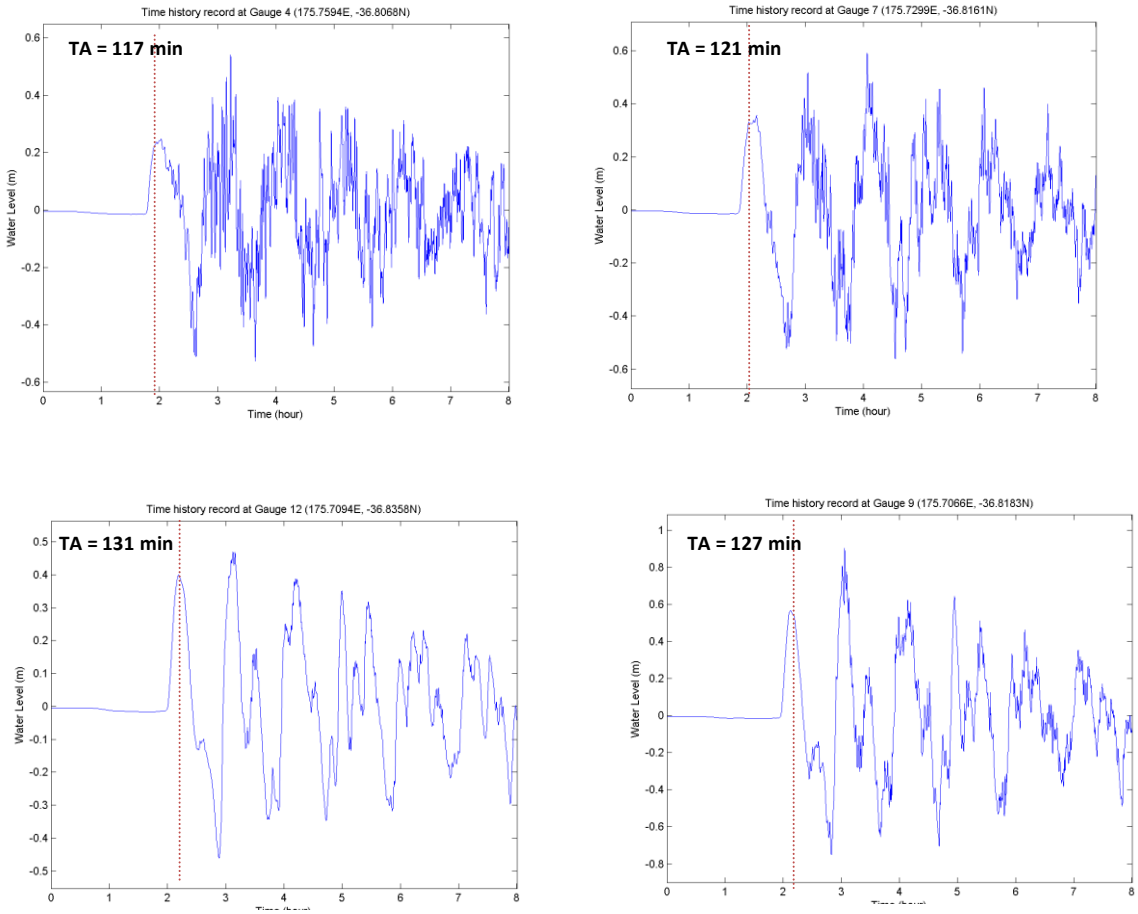

Figure 6-11. Tsunami wave trains recorded at virtual tide gauges sited at the entrance of Mercury Bay (TS04), at the entrance of Buffalo Bay(TS07), within Buffalo bay (TS09), and at the Whitianga Wharf (TS12).

6.2.4 Scenario 4: M_w = 9.2 earthquake for middle-southern segments of Kermadec Trench

A set of fault model parameters were created to simulate an earthquake of magnitude M_w = 9.2 that ruptures the middle and southern segments (segment B-A in POWER et al., 2011) of the Tonga-Kermadec Subduction Zone. This region extends from 178.9° to 183.19°E and -37.94° to -30.76°S. The rupture zone length and width are 900 km and 100 km respectively. The strike direction varied from 196.90° to 205° from south to north, and the dips increased from 4° to 16.44°. The slip angles were uniform at 90° and fault dislocation was 22 m. Otherwise the same simulation settings were used as for previous scenarios.

Figure 6-12(A) shows the initial water displacements indicated that the tsunami energy mostly propagated normal to the strike direction. Negative waves propagated to the northwest and positive waves with an initial height up to 8 m propagated in the southeast direction. At Mercury Bay, the arrival of tsunami waves was indicated by receding water (Figure 6-12B), followed by a crest up to 4 m in height (Figure 6-14). From the 30 minutes snapshot, the largest tsunami wave was about 1.5 hours after the earthquake (Figure.6-12C).

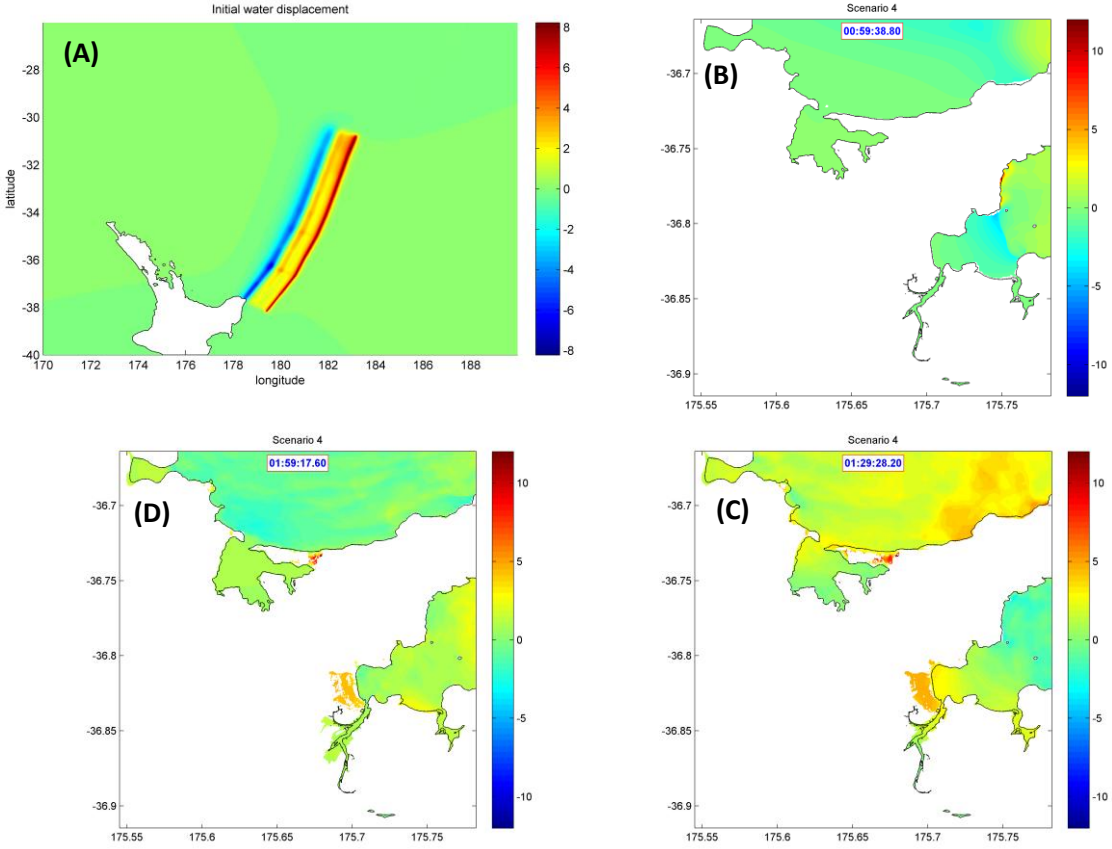

Figure 6-12. (A) The initial water displacements generated by the middle and southern segments scenario with M_w = 9.2. Tsunami energy mostly propagated towards the southeast, with a smaller depression wave propagating to the northwest, (B) Snapshot of water elevations Mercury Bay 2 hours after the earthquake. At this point, the tsunami has already inundated Whitianga Township.

The highest wave that arrived in Mercury Bay after about 1.5 hours of earthquake inundated the Whitianga Township up to 5 m depth and the flood remained even when the water was drawn back to the sea (Figure 6-12D).

The tsunami arrival time was indicated by receding water. The depth of the initial trough decreased with distance increased into the embayment; however, due to the limited water depth and drying, it is not possible to determine the depth of trough at TS09. Tsunami wave trough of -3.45 m was found at the entrance of Mercury Bay (TS04), -3.3 m at the entrance of Buffalo Bay (TS07), and -0.7 m at Whitianga Wharf (Figure 6-13 and Figure 6-14). Table 6-4 summarises the tsunami arrival times, maximum and minimum amplitudes, and the maximum peak to trough distances resulting from this scenario.

Table 6-4 . Result of simulated tsunami generated in the middle and southern segments of the Kermadec Trenchfor a M_w = 9.2 earthquake. Note that the minimum trough at TS09 is not considered due to the truncation trough.

Tide gauge	Arrival time (min)	Amplitudes (m)		Maximum peak to trough (m)
		Maximum	Minimum	
TS04	58	4.2	-3.45	7.65
TS07	65	4.9	-3.3	8.2
TS09	70	6.2	Truncated	-
TS12	73	3.3	-0.7	4.3

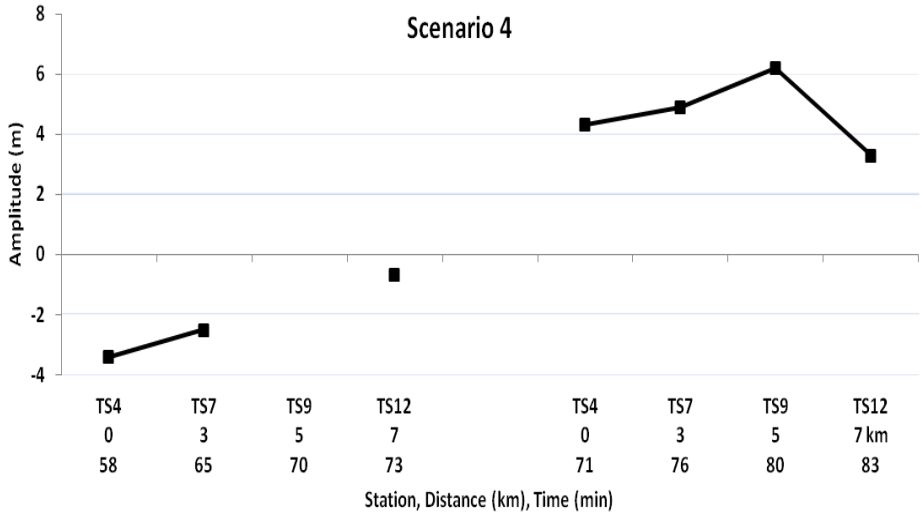

Figure 6-13. Distance and arrival time of first troughs and peaks at each virtual tide gauge plotted with the tsunami amplitudes resulting from scenario 4: earthquake M_w = 9.2 for southern and middle segment of Kermadec Subduction Zone. The gap at TS09 was due to the truncated trough that made impossible to determine the first negative amplitude (trough).

The tsunami amplitudes that resulted from this scenario were large, and at both sites TS07 and TS09 the receding water exposed the seabed so that the recorded sea level oscillations were truncated at some points of their troughs. On the other hand, like other scenarios, the maximum 6.2 m amplitude occurred in the vicinity of Whitianga Township (TS09), which is 47% higher than the amplitude at the entrance of Mercury Bay (TS04).

From the entrance of Mercury Bay to the coastal area of Whitianga Township, the tsunami requires approximately 9 minutes and another 3 minutes to flood the Whitianga Wharf. The celerity of tsunami wave train from this scenario was faster than both scenarios 1 and 2, where the tsunamis were simulated for each single segment. The tsunami arrival for this scenario (scenario 4: middle and southern segment) and scenario 1 (southern segment) were only 2 minutes in difference, but in scenario 4 with larger dislocation distance as its fault parameter that determine the earthquake's magnitude produced larger initial water movement at the source and furthermore, generated earlier peaks after the first leading trough.

All virtual tide gauges showed that the first 4 waves are forced oscillations with periods ranging from 43 to 54 minutes. However, significant higher frequency energy is evident at the entrance of Mercury Bay (Figure 6-14A). This is filtered out at the inner sites.

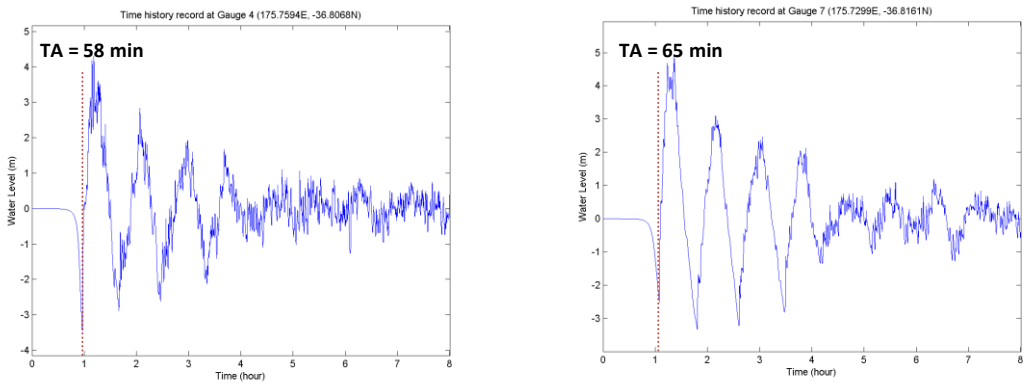

Figure 6-14A. Tsunami wave trains from a M_w = 9.2 earthquake in the middle and southern segments recorded by virtual tide gauges sited at; the entrance of Mercury Bay (TS04) and the entrance of Buffalo Bay (TS07).

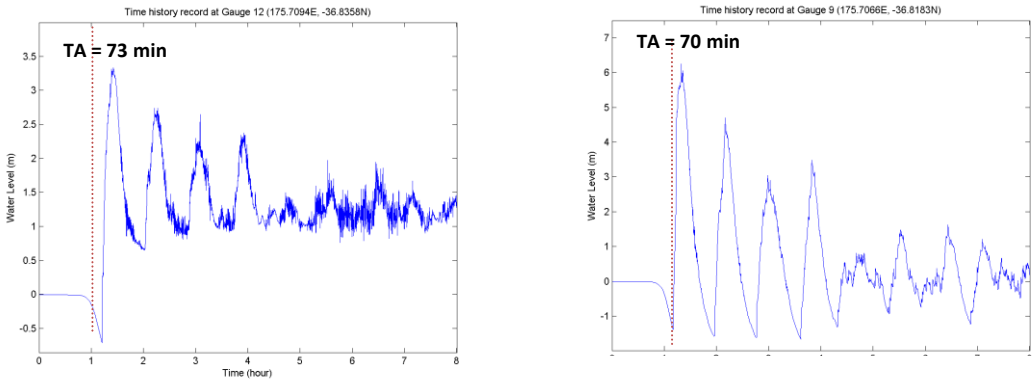

Figure 6-14B. Tsunami wave trains from a M_w = 9.2 earthquake in the middle and southern segments recorded by virtual tide gauges sited in the vicinity of Whitianga Township within Buffalo Bay (TS09), and at the Whitianga Wharf (TS12).

Sea water levels at all sites were amplified and maximum amplitude was recorded at the site TS09. It is clearly seen that the peaks were enhanced more than the troughs; moreover, inside the inlet of Whitianga Wharf, the mean sea water level has elevated from the zero level up to 1.2 m above MSWL (Figure 6-14B).

6.2.5 Scenario 5: M_w = 9.3 earthquake for middle and northern segments of Kermadec Trench

An earthquake of magnitude M_w = 9.3 was simulated to rupture the middle and northern segments (segment BC in POWER et al., 2011) of the Kermadec Subduction Zone. These segments extend from 179.46°W to 175.92°W and -35.65° to -26.35°S. The length and width of the rupture zone are 1100 km and 100 km respectively. The strike direction varied from 191.70° to 205° and the dips increased from 5.79° to 17.48° towards the north. The slip angles were uniform at 90° and fault dislocation was 22 m. Otherwise the same simulation parameters were used as for the previous scenarios.

Figure 6-15(A) shows the initial water displacements after the earthquake. The tsunami waves from the source area propagated mostly to the northwest and southeast. The tsunami waves arrived in Mercury Bay as negative wave with troughs of; -0.8 m at TS04 (entrance of Mercury Bay), -1.0 m at TS09 (Whitianga Township – Buffalo Bay), and -0.6 m at TS12 (Whitianga Wharf). From the 30 minutes snapshot

generated from simulation (Figure 6-15B), around 1.5 hours after the earthquake up to 2.3 m wave heights occurred in the vicinity of Whitianga Township and the tsunami has already flooded northern Whitianga beach. At this point, the water level at Whitianga Wharf was up to 1.3 m above still water level (Figure 6-17).

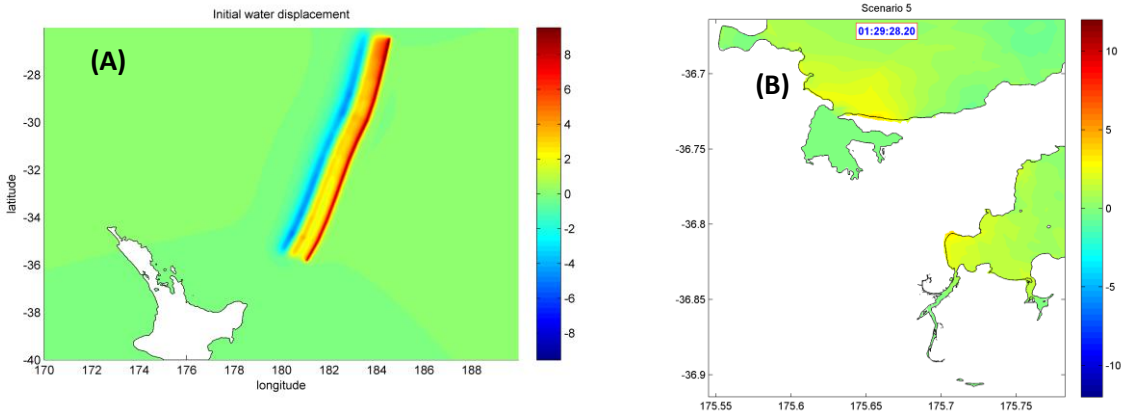

Figure 6-15. (A) The initial water displacements generated by the middle and northern segments scenario with M_w = 9.3. Tsunami energy mostly propagated towards the southeast, with a smaller depression wave propagating to the northwest, (B) Snapshot of water elevations Mercury Bay 1.5 hours after the earthquake. At this point, the tsunami level was maximal at southern corner of Cooks Bay, Simpson Bay and northern corner of Buffalo Bay.

The tsunami arrival times from the combined segments (Table 6-5) matched those generated by the middle segment only (Scenario 2). It took 13 minutes for the tsunami waves to propagate from the entrance of Mercury Bay to reach the vicinity of Whitianga Township, and another 3 minutes to flood Whitianga Wharf (Figure 6-16).

Maximum enhancements of sea water level were recorded as the first peaks at all sites and the deepest troughs were recorded after the first peaks.

Table 6-5. Result of simulated tsunami generated in the middle and northern segments of the Kermadec Trench for an M_w = 9.3 earthquake.

Tide gauge	Arrival time (min)	Amplitudes (m)		Maximum peak to trough (m)
		Maximum	Minimum	
TS04	68	1.4	-1.3	2.7
TS07	75	1.8	-1.4	3
TS09	81	2.3	-1.3	3.6
TS12	84	1.3	-0.6	1.9

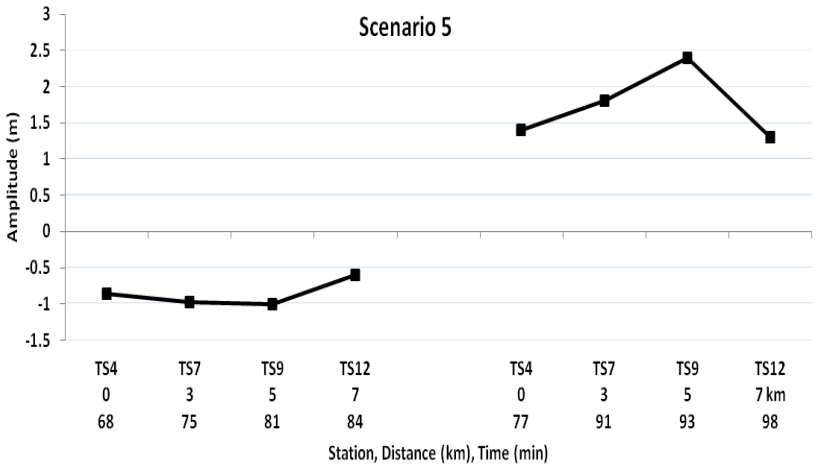

Figure 6-16. Distance and arrival time of first troughs and peaks at each virtual tide gauge plotted with the tsunami amplitudes resulting from scenario 5: earthquake M_w = 9.3 for northern and middle segment of Kermadec Subduction Zone.

Like other scenarios, the highest peak and maximum wave height (peak to trough) occurred in the vicinity of Whitianga Township. However, in this scenario the lowest trough occurred at the entrance of Buffalo Bay (see Table 6-5). As the highest wave arrived in the vicinity of Whitianga Wharf, the sea water displacement was up to 33% relative to TS04 which is located at the entrance of Mercury Bay.

The initial periods of the tsunami waves ranged from 52 to 67 minutes. The fundamental periods of Mercury bay is at around 35 minutes and tsunami periods seemed to coincide with the periods of Mercury Bay after about 3 hour's elapsed time of the earthquake (Figure 6-17).

In Figure 6-17, it is seen that sea level oscillations were denser at the sites close to the open sea (TS04 and TS07) and they were filtered landward. About 25% of the tsunami energy is reflected at the continental shelf, while 100% do so at the arrival to the coast (SOLEVIEV and GO, 1974), which explains the reason that greatest amplification constantly occurred at the site close to Whitianga Township (TS09).

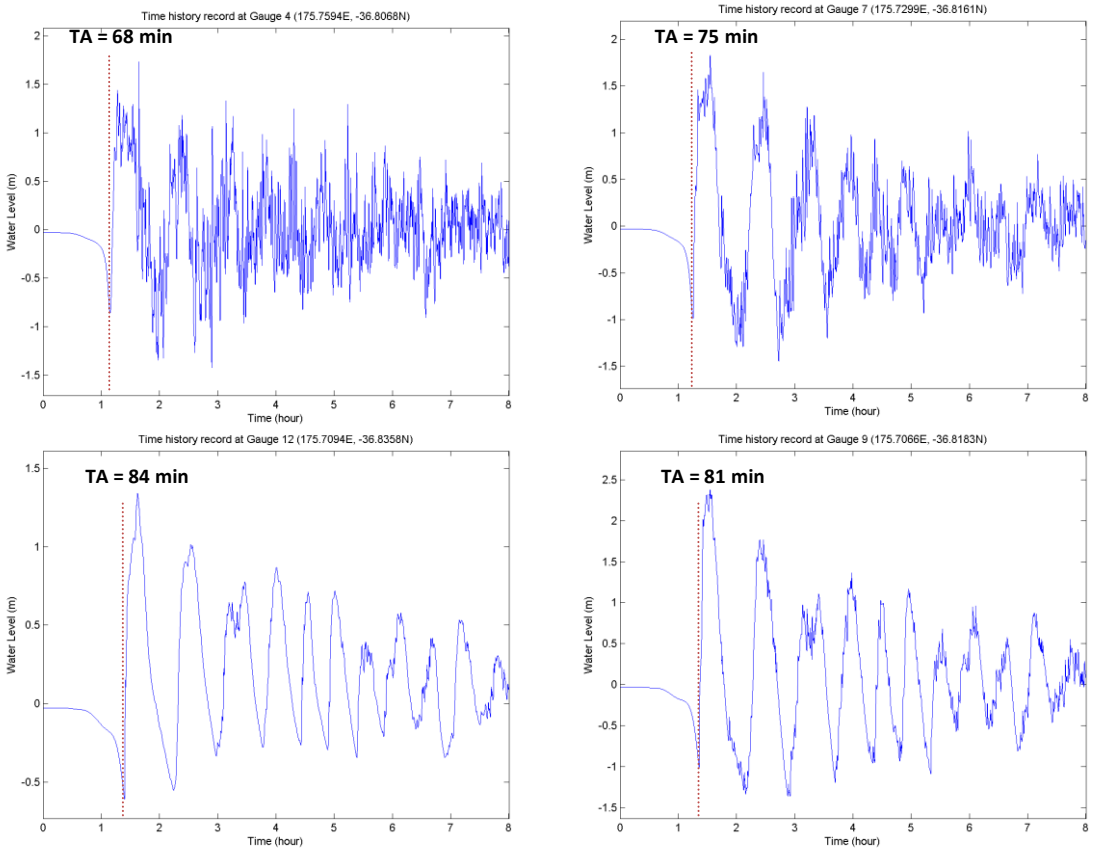

Figure 6-17. The tsunami wave train from M_w 9.2 earthquake in the middle to northern part segments that recorded at virtual tide gauge; sited at the entrance of Mercury Bay (TS04), in the vicinity of Whitianga Township of Buffalo bay (TS09) and at the Whitianga Wharf (TS12).

6.2.6 Scenario 6: M_w8.5 to M_w9.5 earthquakes for all segments of Kermadec Trench

Several earthquakes were generated for this scenario, with magnitudes from $M_{w=}$ 8.5 to $M_{w=}$ 9.5 involving all three segments of the Kermadec Subduction Zone. Each earthquake had a different dislocation corresponding to the different magnitude scales (Table 6-6). However, they had similar rupture zones, with a length of 1,400 km and width 100 km, dips ranging from 4° to 17.48° towards the north, and the slip angles were uniform at 90°. The worst scenario of $M_{w=}$ 9.5 earthquake was based on the recent 2004 Sumatra and 2011 Tohoku tsunami events.

Table 6-6. The dislocation distance for each earthquake involving all three segments of the Kermadec Subduction Zone.

M_w	Dislocation (m)
8.5	1
8.6	1.5
8.7	2
8.8	2.8
8.9	4
9.0	5.6
9.1	8
9.2	10
9.3	15
9.4	22
9.5	30

Table 6-7 gives the tsunami arrival times at the entrance of Mercury Bay (TS04) and their characteristics at the virtual tide gauge site at the entrance of Buffalo Bay (TS07). This site was chosen due to the truncated troughs which were resulted from this scenario in the recorded sea level at TS09, where the highest amplitudes occurred. The highest amplitude is consistently occurred at TS09 (in the vicinity of Whitianga Township). This phenomenon is due to the superposition of reflected and incident waves, as well as the shoaling effect, causing significant amplification of tsunami waves at the coast (ABE, 2011), and one of the tsunami event that shows the response of the study area can be seen on the attached CD (movie of tsunami M_w 9.4).

Furthermore, the tsunami generated in this scenario did not all have the same characteristics. The maximum peak and amplitudes were not always associated with the same wave. So the maximum peak to trough (maximum wave height) may differ from the difference of these two values. For earthquakes ranging from $M_w = 85$ to $M_w = 8.9$, the maximum positive amplitudes (highest peak) occurred as the first peak (after first receding water as indication of tsunami arrival time). While the maximum negative amplitudes (lowest trough) occurred as the third wave. For larger magnitudes the lowest trough followed the highest peak.

Table 6-7.Result of simulated earthquake generated tsunamis. Note that the tide records were taken from tide gauge TS07where the highest wave amplitude occurred and records from TS04 for the tsunami arrival time.

Magnitudes	Arrival Time (min)	Maximum Amplitudes (m)		Maximum Peak to Trough (m)
		Peak	Trough	
8.5	55.8	0.33	-0.34	0.66
8.6	56	0.48	-0.49	0.97
8.7	56	0.61	-0.64	1.25
8.8	56	0.84	-0.82	1.66
8.9	56.1	1.1	-1.13	2.23
9.0	56.5	1.5	-1.5	2.8
9.1	56.7	1.79	-2.04	3.77
9.2	56.9	2.18	-2.4	4.4
9.3	57.3	3.1	-3	6.1
9.4	58	4.65	-3.33	7.98
9.5	58.1	6.3	-3.3	9.43

All the simulated tsunami waves arrived in Mercury Bay as negative waves and their arrival time were varied between 55.8 to 58.1 minutes at TS04 (Figure 6-18). The tsunami arrival time scales shows a rising trend as the magnitudes increase for earthquakes with magnitudes from M_w 8.5 to M_w 9.5; the greater the magnitude, the longer the tsunami arrival time. Nevertheless, this increasing trend is little and was not exceed 3 minutes in difference such a great span of earthquake magnitudes.

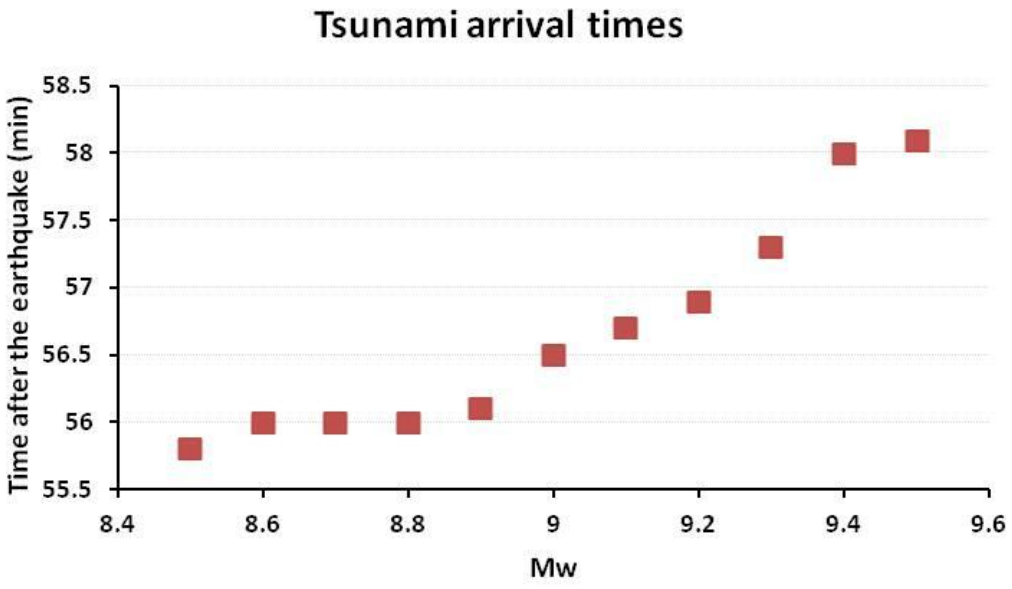

Figure 6-18. The tsunami arrival time for earthquakes generated tsunamis scenarios.

The Figure 6-19 shows the amplitudes for both of the negative and positive values. Here, it is clearly seen that there is a strong correlation between the magnitude scales of the earthquakes and their tsunami characteristics. Both the positive (peaks) and negatives (trough) amplitudes increase as the magnitudes scale increase. The same trend is seen with the maximum wave heights (peak to trough) which were increased as the magnitude scale of the earthquake escalated (Figure 6-20).

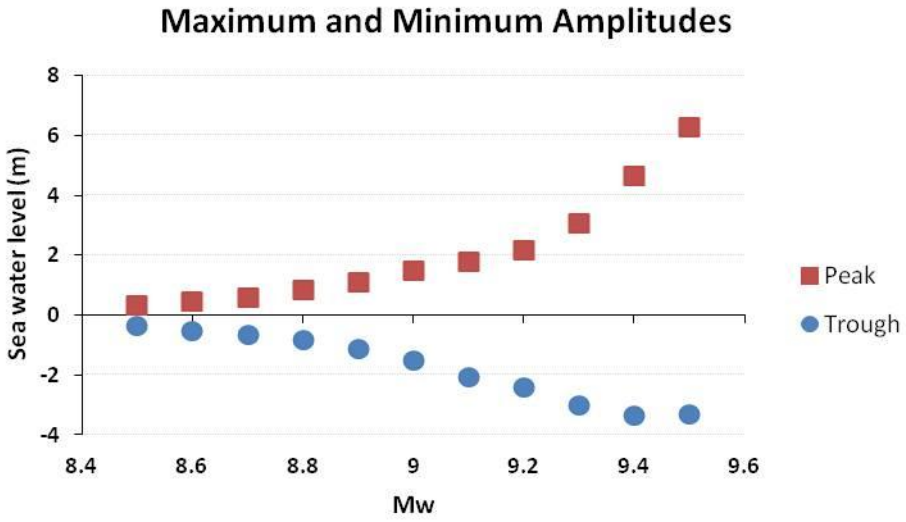

Figure 6-19. Maximum amplitudes resulted from simulated tsunamis. The positive amplitudes are the peaks and negative amplitudes are the troughs.

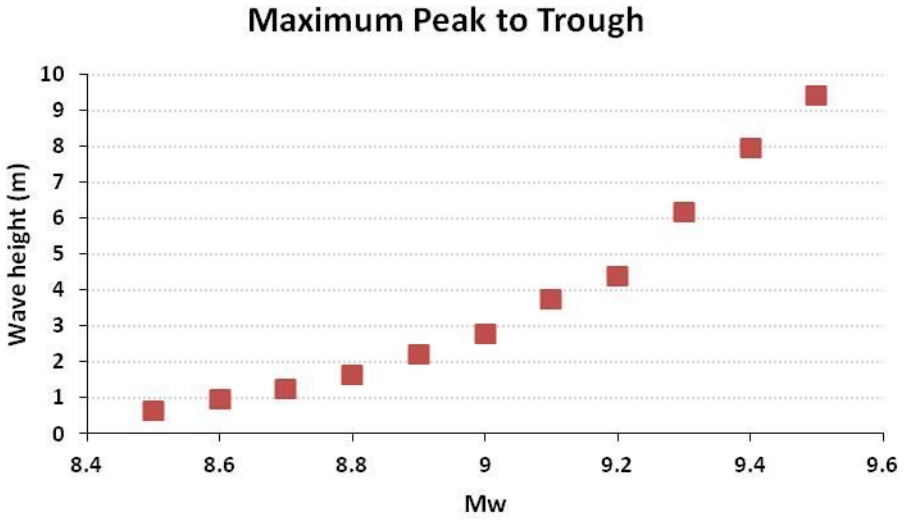

Figure 6-20. Relationship between the moment magnitude Mw and tsunami wave height for the scenario 6. The wave height increases as the earthquake magnitude increased.

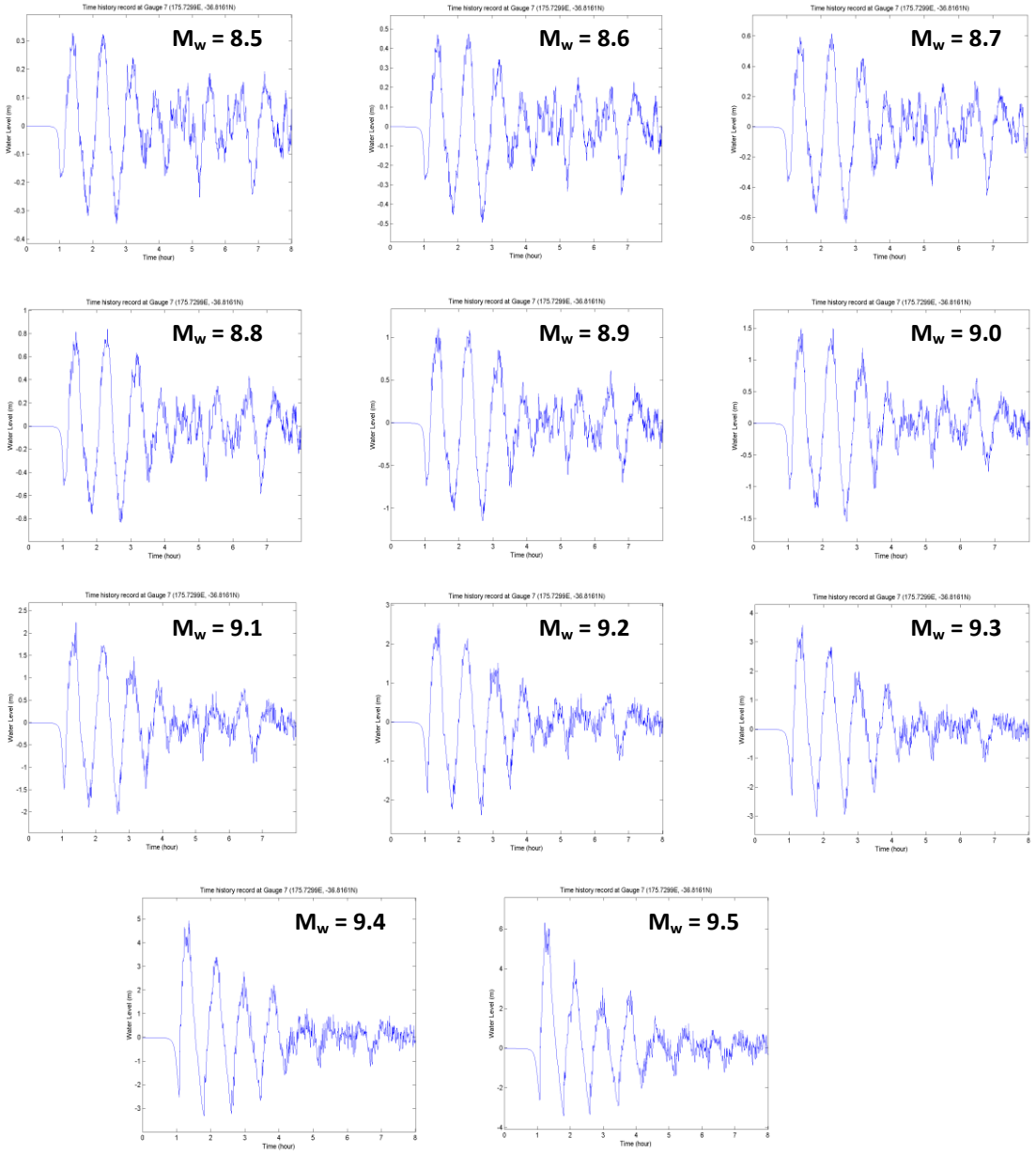

Figure 6-21. Tsunami records at the entrance of Buffalo bay (TS07). The magnitudes of simulated earthquakes were varied from M_w 8.5 to M_w 9.5. Note that all records have in common that the first tsunami wave arrived as negative wave which then formed a wave with the highest amplitude.

6.2.7 Scenario 7: 6 July 2011 M_w = 7.6 earthquake

A M_w = 7.6 tsunamigenic earthquake event occurred on 6 July 2011 UTC time (on 7 July 2011 at 7.03 am local time) about 210 km east of Raoul Island in the Kermadec Islands (segment three). The resulting tsunami was about 1.9 m high at

Raoul Island, and was recorded on gauges around the New Zealand coast, including at Whitianga Wharf. This scenario was set up to simulate this event. The fault plane parameters for this model were adapted from Global CMT Moment Tensor Solution posted on USGS website. The length and width of rupture area were calculated using the empirical equation of Wells and Coppersmith (1994), giving a rupture area 118 km in length and 22 km in width. The strike direction was 171° and its dip was 33°. The slip angle was at -105° and the maximum fault dislocation was 1.43 m. The epicenter of the earthquake was at 175.76°W and -29.18°, which is located to west of the northern segment of Kermadec Trench. The other simulation parameters were kept the same as previous simulations.

In Figure 6-22(A), it is seen that most of the tsunami energy propagated westwards towards Raoul Island, while the negative wave or depression headed towards the east (South America). The initial water displacements were small, hardly exceeding 0.4 m in both negative and positive wave. As New Zealand and Mercury Bay lie almost 90° to the principal axis of the tsunami, the expected impact is minor. The first tsunami wave in Mercury Bay was a negative wave (Figure 6-23), about 110 minutes after the earthquake, at the entrance of Mercury bay (TS04). An additional 13 minutes were required to reach Whitianga Township within Buffalo Bay (TS09), and 4 more minutes to reach Whitianga Wharf (TS12). Table 6-8 gives the results of simulated M_w = 7.6 earthquake in Kermadec Trench.

Table 6-8**.** Result of simulated earthquake event of 6 July 2011, magnitude M_w = 7.6 in the Kermadec Trench.

Tide gauge	Arrival time (min)	Amplitudes (m)		Maximum peak to trough (m)
		Maximum	Minimum	
TS04	110	0.03	-0.03	0.06
TS07	115	0.05	-0.05	0.08
TS09	123	0.09	-0.09	0.18
TS12	127	0.07	-0.07	0.14

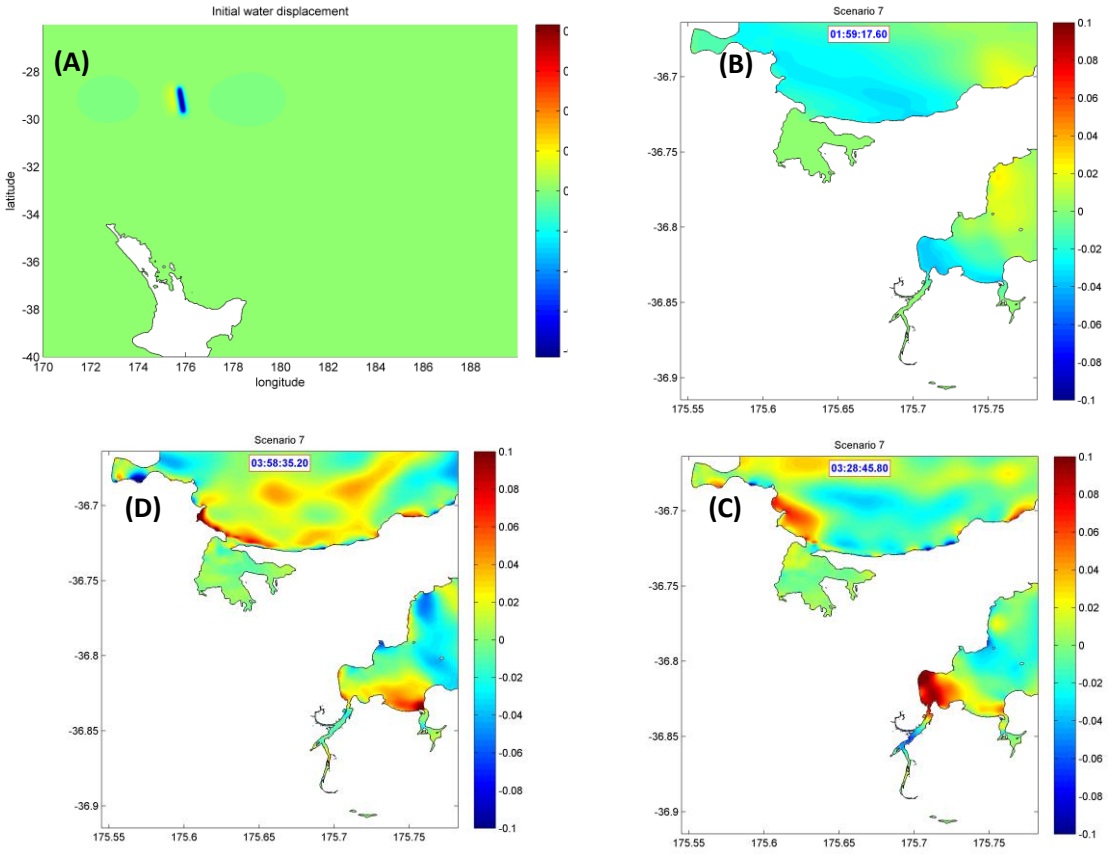

Figure 6-22. (A) The initial water displacement generated by the 6 July 2011 Kermadec earthquake scenario with M_w = 7.6. The tsunami propagated the energy mostly to east and west, (B) tsunami arrival after 2 hours of the earthquake, (C) maximum response within Mercury Bay occurred 3.5 hours after the earthquake, and (D) at about 4 hours after the earthquake, the maximum response occurred at southern corner of Cooks Bay. Scale bar unit is in meter.

Figure 6-22(B) shows the arrival of tsunami as negative wave in the vicinity of Whitianga Township at about 2 hours after the earthquake. However, the maximum response of Buffalo Bay was obtained after several peaks, about 3.5 hours after the earthquake. At this point, the maximum amplitude of about 10 cm occurred in the vicinity of Whitianga Township (Figure 6-22C) and the maximum response of Cooks Bay occurred 30 minutes later (Figure 6-22D).

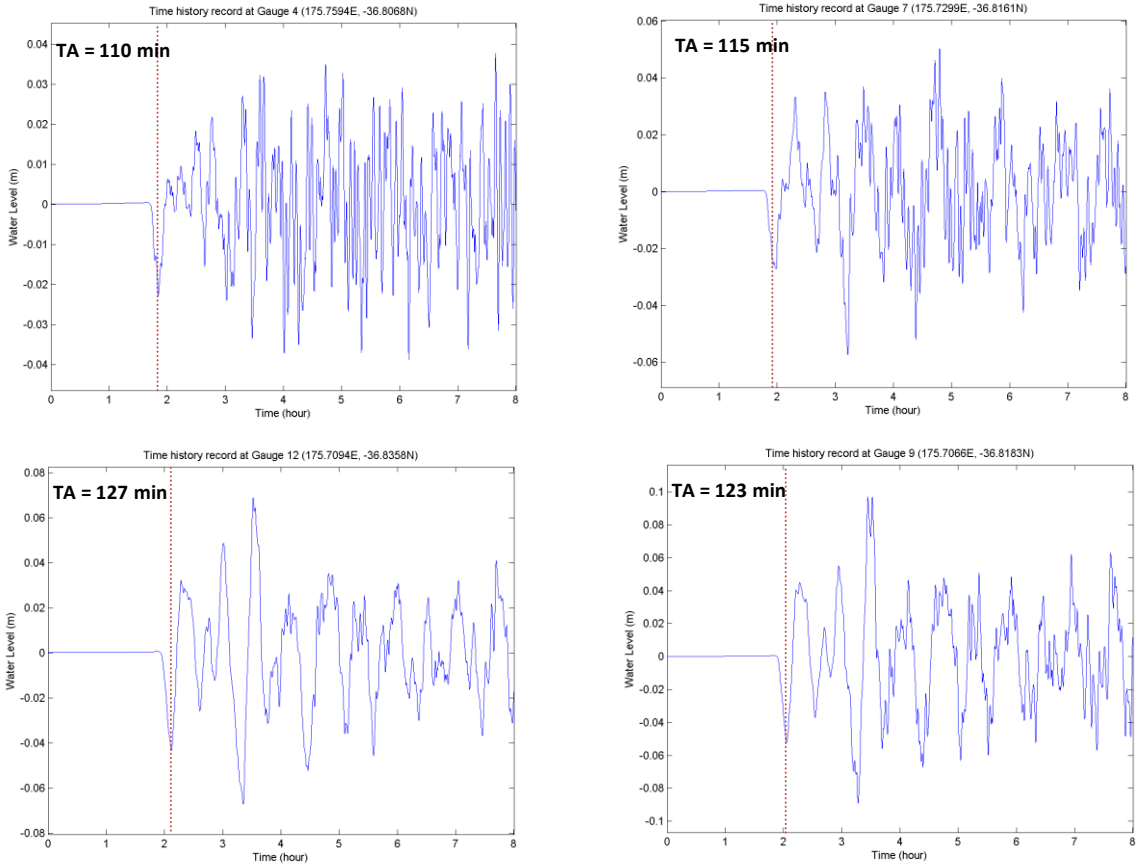

Figure 6-23. Tsunami waves generated by the simulated earthquake M_w = 7.6 6 July 2011earthquake near the Kermadec Islands. The highest wave was less than 10 cm.

A measured tide record was taken from Whitianga Wharf in order to compare between the modelled and measured tsunami of this event. According to New Zealand time, the 6 July 2011 event occurred on 7 July 2011 at 7.03 am (NZT). Thus, based on the tsunami arrival time recorded in the virtual gauge sited at Whitianga Wharf, the tsunami will arrive within 127 minutes after the earthquake (Figure 6-23), the tsunami should arrive at Whitianga Wharf at 9.10 am (Figure 6-24).

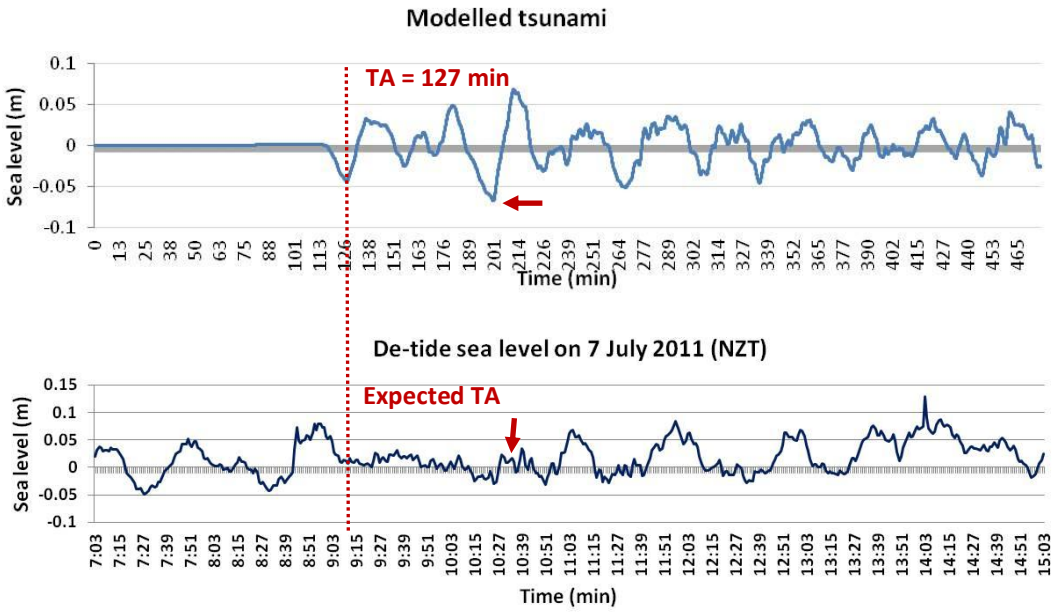

Figure 6-24. Modelled and measured tsunami of 7 July 2011 (NZT) event. It is seen that the tsunami arrival time of the measured one did not agree with the modelled one. Red arrows in the first graph points the deepest trough which was followed by the highest peak as the response of Mercury Bay and at the second graph (de-tide sea level) points the corresponding time.

In the figure 16-24 it is not evident whether a tsunami matching the predicted characteristics (upper panel) arrived at Whitianga. Although the measured data were filtered, there are still marked oscillations at the expected tsunami frequencies present before the expected tsunami arrival time, and these continue throughout the record. This complicates the identification of the tsunami event. However, the filtered record does show a change in behaviour between the expected times of tsunami arrival (9:09 am) and the maximum response (10:34 am), which may be due to interactions between the tsunami and the existing oscillations. Comparing peaks and troughs in this section of the record with the predicted wave shows a reasonable match, although the amplitude is smaller than predicted. It is also possible that the modelled tsunami is incorrect, particularly as different fault parameters will result different tsunami characteristics (GEIST, 1998; GEIST & YOSHIOKA, 1996), and the modelled one was based on USGS data. Therefore, further analysis with different source parameters is still needed.

In the following part of this chapter, I will present the spectral properties of the tsunami for both modelled and measured events. The spectral properties for modelled tsunamis taken at the near sources will be also presented.

6.3 Spectral Analysis of Modelled and Measured Tsunami Events

I have used spectral analysis to identify more precisely the dominant periods for both modelled and measured tsunami waves. It is expected that one of the dominant periods will have good agreement with the calculated *eigen* period of Mercury Bay (35 minutes).

The peak of each tsunami spectra as the wave travelled further landward in the Bay were getting less prominent, however this modification did not alter the dominant period's value (Figure 6-25). Further, within the bay geometry started to modify the spectra of tsunami. The tsunami spectra for all modelled tsunamis showed similarity in their dominant periods at around 52 minutes (Figure 6-26). This figure does not show all the results from the numerical model scenarios, because all had the same dominant period. Thus, from this result, we assume that the uniformity indicates a consistent response for the interaction between the forcing tsunami wave and the Mercury Bay natural resonance response. In the other hand, different tsunamis events recorded at the same place usually present similar spectra contents, because the energy related to the tsunami source is mostly shaded by the usually more energetic topographic contribution (VICH and MONSERRAT, 2009; ABE, 2011).

Table 6-9 gives the coordinates of each virtual tide gauge and Figure 6-27 shows the location of respective sites. Figure 6-28, 6-29 and 6-30 show the tsunami spectra at each single segment of the Kermadec Subduction Zone, and for the entire subduction zone, tsunami spectra of earthquake M_w = 9.4 are shown in Figure 6-31. The other figures of tsunami spectra taken at the near source are given in appendix 2.

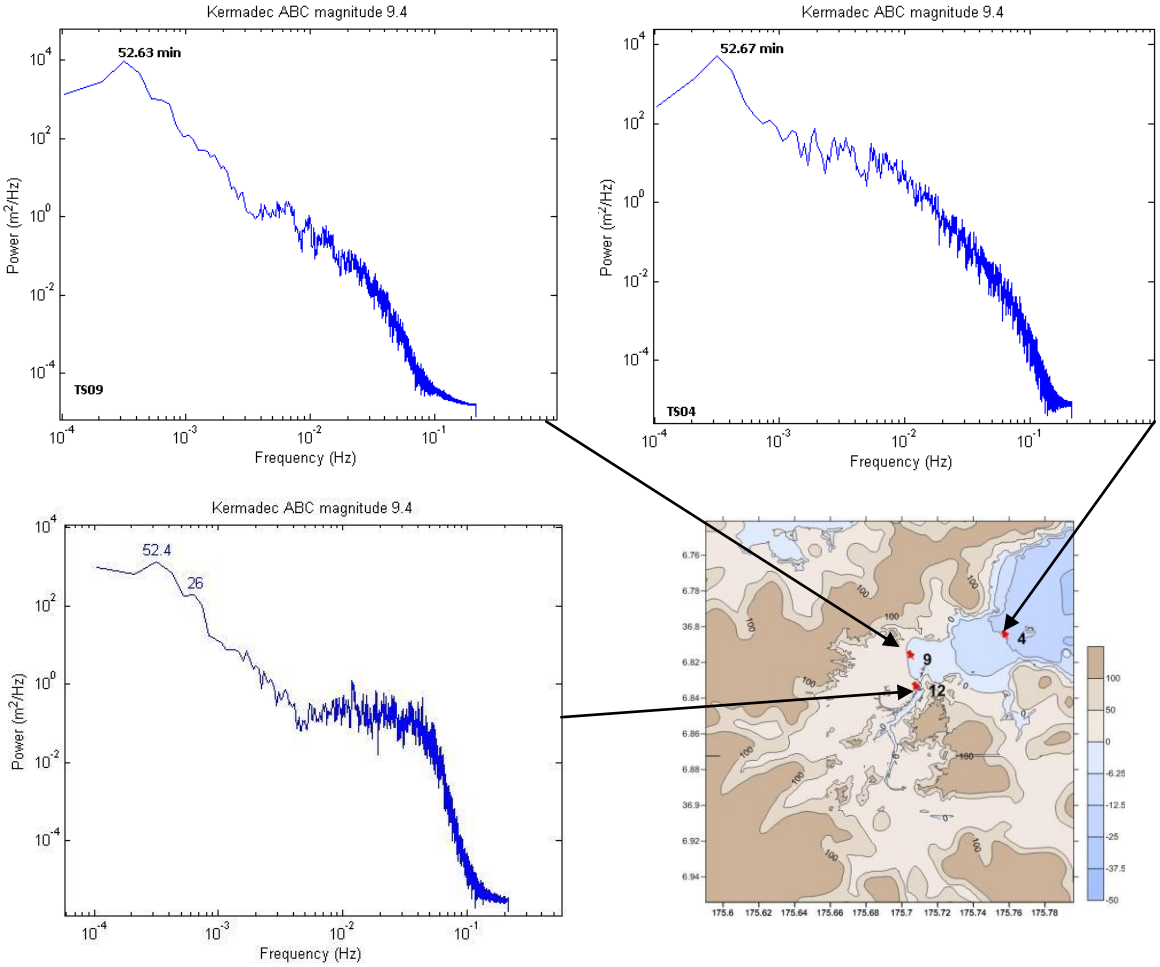

Figure 6-25. Spectra of modelled tsunamis from the entrance of Mercury Bay to Whitianga Wharf were being less prominent as the distance increase and the bathymetry shallower.

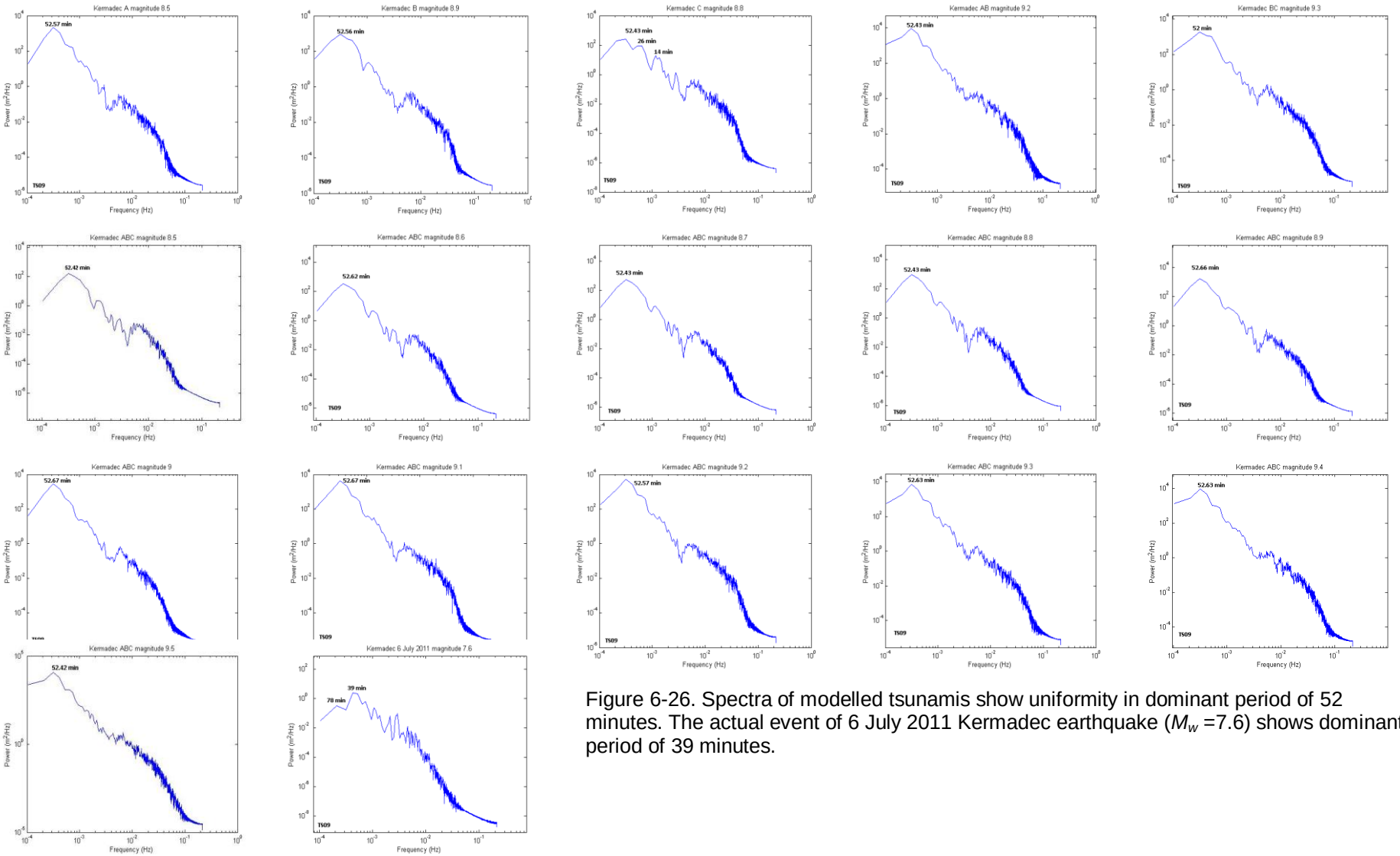

Figure 6-26. Spectra of modelled tsunamis show uniformity in dominant period of 52 minutes. The actual event of 6 July 2011 Kermadec earthquake (M_w =7.6) shows dominant period of 39 minutes.

Table 6-9. The location of virtual tide gauges that posited near to the tsunami sources.

Tide gauge stations	Coordinates		Position
	Latitude	Longitude	
TS01	-29.18	175.90	Near the epicenter of 6 july 2011 Kermadec earthquake
TS13	-32.3015	180.0	Middle of ABC segments
TS14	-37.1886	179.5163	Southern end of segment A
TS15	-36.82805	179.761	Middle of segment A
TS16	-33.1434	181.65285	Middle of segment B
TS17	-28.48635	183.4556	Middle of segment C

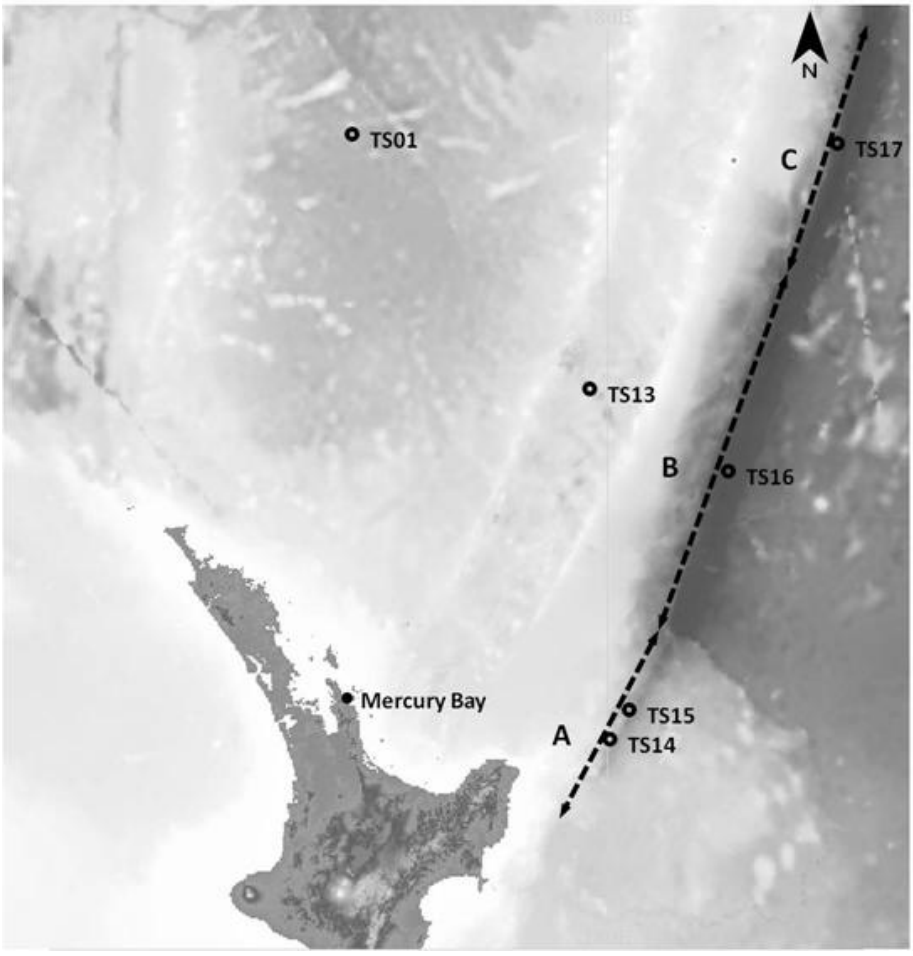

Figure 6-27. Several virtual tide gauges are posited along the Kermadec Subduction Zone and at the epicenter of 6 July 2011 Kermadec earthquake (TS01) in order to identify the dominant period of each tsunami source (initial tsunami spectra).

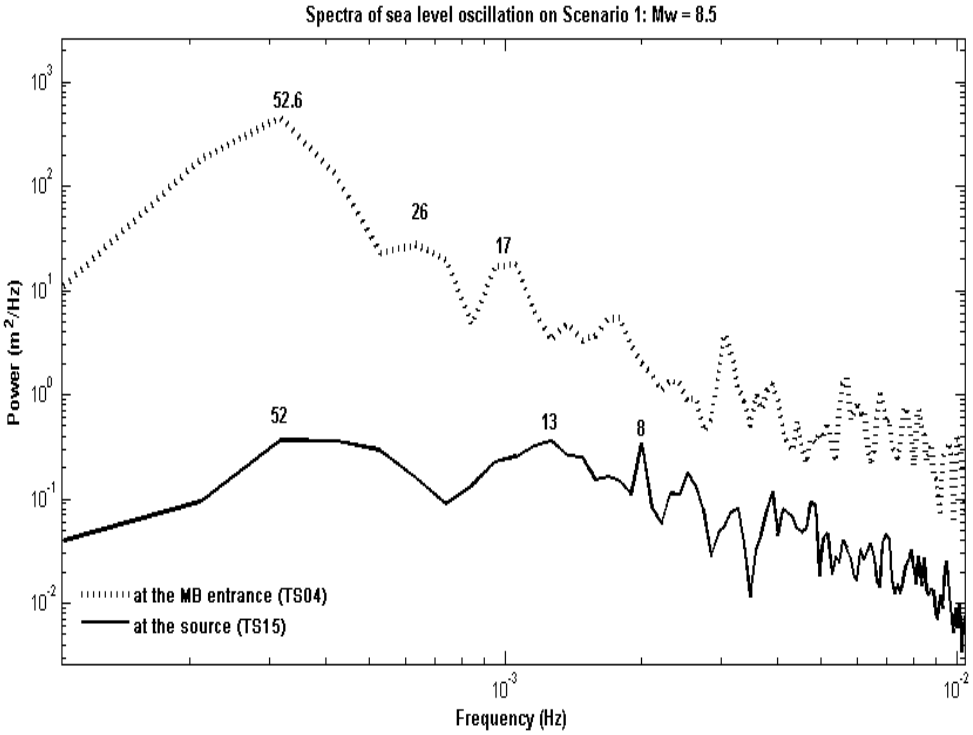

Figure 6-28. The initial tsunami spectra generated from southern segment of the Kermadec Subduction Zone (scenario 1), M_w = 8.5; at the source (TS15) and at the entrance of Mercury Bay (TS04) both shows similarity in their dominant period of at about 52 minutes.

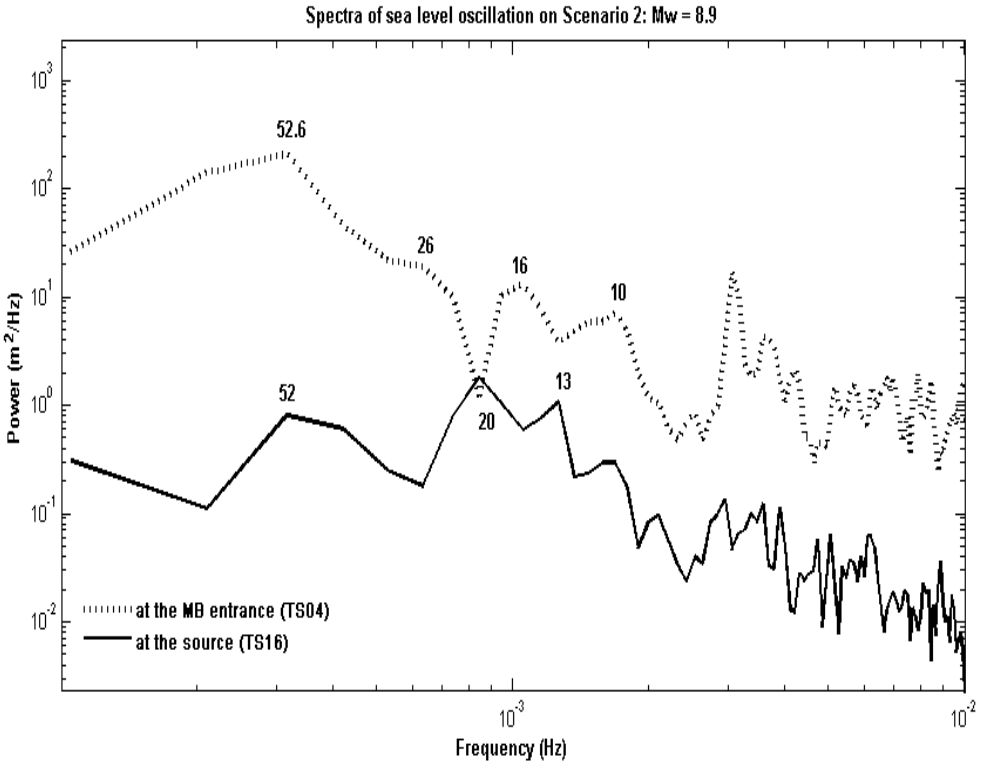

Figure 6-29. The initial tsunami spectra generated from middle segment of the Kermadec Subduction Zone (scenario 2), M_w = 8.9; at the source (TS15) and at the entrance of Mercury Bay (TS04) both shows similarity in their dominant period of at about 52 minutes.

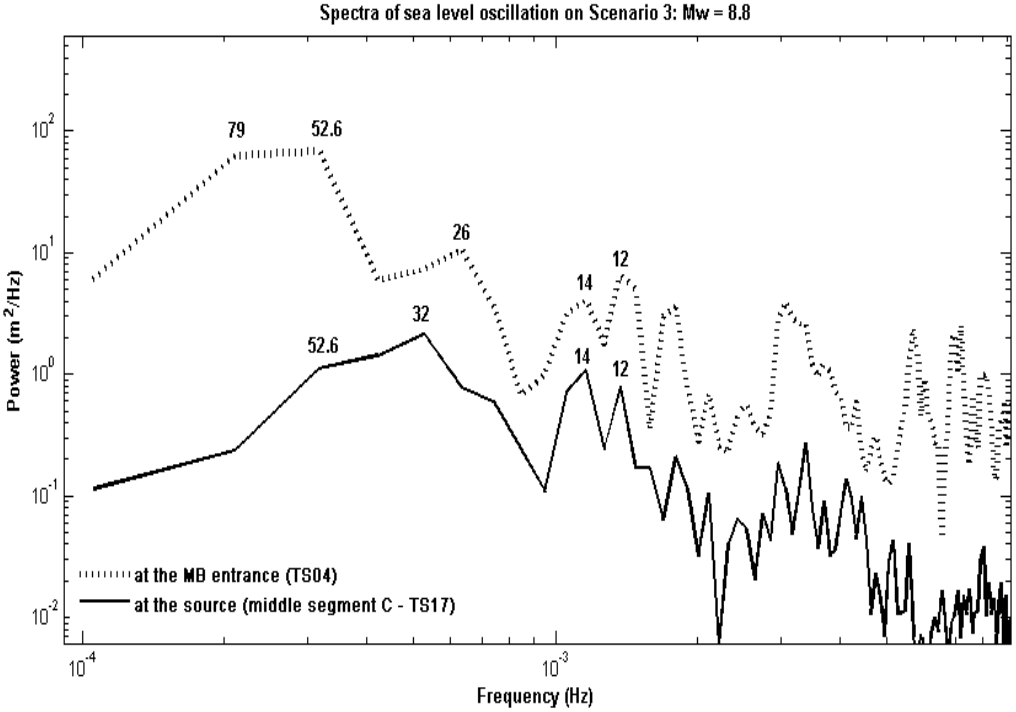

Figure 6-30. The initial tsunami spectra generated at northern segment of the Kermadec Subduction Zone (scenario 3), M_w = 8.8; at the source (TS17) and at the entrance of Mercury Bay (TS04). The periods of 52 minutes were not the prominent period at the source, but it was altered as tsunami wave enters the Mercury Bay.

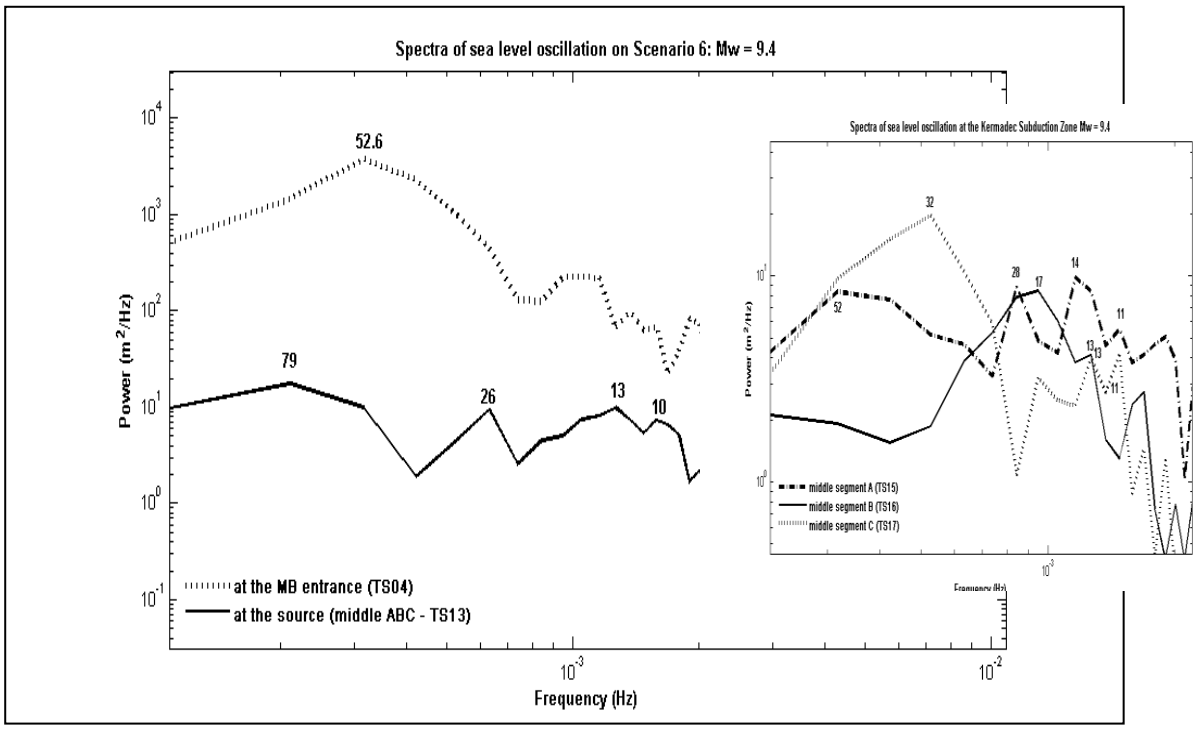

Figure 6-31. The initial tsunami spectra generated by entire segment of the Kermadec Subduction Zone (scenario 6), M_w = 9.4. TS13 posited in the middle of the subduction zone and TS04 posited at the entrance of Mercury Bay. Figure index shows the spectra of each segment, only the southern segment that has the same tsunami dominant period as at the entrance of Mercury Bay (52 minutes).

From the initial tsunami spectra generated by each segment, the 52 minute dominant period constantly appeared and it seems that the continental shelf of New Zealand amplified it up to twice from the original spectra. These 52 minutes of dominant period may also the characteristic response of New Zealand continental shelf, which is close to the nationwide 60 minutes resonance captured by WALTERS (2003). However, the initial tsunami spectra produced by composite segments of Kermadec Subduction Zone alters the dominant periods of each segment and generates peaks with 78, 26 and 13 minutes period. A closer look to the dominant periods for each segment (for entire zone earthquake), shows that only the southern segment, which is closest to Mercury Bay, had a 52 minute dominant period (see index Figure 6-31).

A background spectrum of the typical oscillations in Mercury Bay was prepared using 47 hours of one minute interval measured tide record taken on December 2010 and July 2011 (Figure 6-32). These spectra then we use them in comparison with the measured tsunami events of the 2010 Chilean, 2011 Tohoku Japan and 2011 Kermadec Islands events (Table 6-10). The results are shown in figures 6-33A and 6-33B respectively. The spectra of the residual data (de-tided) shows (Figure 6-34A and B) that the prominent peaks (dominant period) of Chilean event were 51, 36, 28 and 22 minutes and the Tohoku event were 47, 37, 27 minutes. The background oscillation taken from the tide record in December 2010 shows the dominant periods of 73, 47, 37 and 30 minutes and July 2011 shows the prominent peaks of 51, 37, 30 and 26 minutes. Here it is seen that the dominant periods of each event match the periods of Whitianga Wharf. The period of 36 minutes (Chilean event), 37 minutes (Tohoku event) and 37 minutes (measured spring tide) were close to the calculated eigen period of Mercury Bay, which is 35 minutes. Near identical peaks of corresponding tsunami spectrum with the locality spectrum indicates that the local topography has a major effect on the longwave oscillations (RABINOVICH and THOMSON, 2007)

The spectra of the observed tsunami wave with tide and without tide of both distant tsunami events yield a result of the same dominant periods. The spectra of tsunami events with tide which are shown in Figure 6-33 have essentially the same dominant periods with the de-tided ones (Figure 6-32). The Chilean event has dominant periods of 51, 37, 28 and 22 minutes, and the Tohoku event with dominant

periods of 47, 37, and 27 minutes. The period 51 (Chilean) and 47 (Tohoku) have good agreement with 51 and 47 minutes of dominant period during spring tides and the 52 minutes period for simulated tsunamis from the Kermadec Subdution Zone. The latter 37 minutes have a good agreement with the 40 minute resonance mentioned by WALTERS (2003) for Mercury Bay, 35 minutes and 20 minutes oscillation by SMITH (1980), and oscillation in every 40 minutes for 1960 Chilean event (FRASER data base, 1998) which are close to the calculated 35 minutes of Mercury Bay's eigen period. This similarity in periods of both external tsunami energy and the Mercury Bay's period provide clues to the significant amplification that appear in this site.

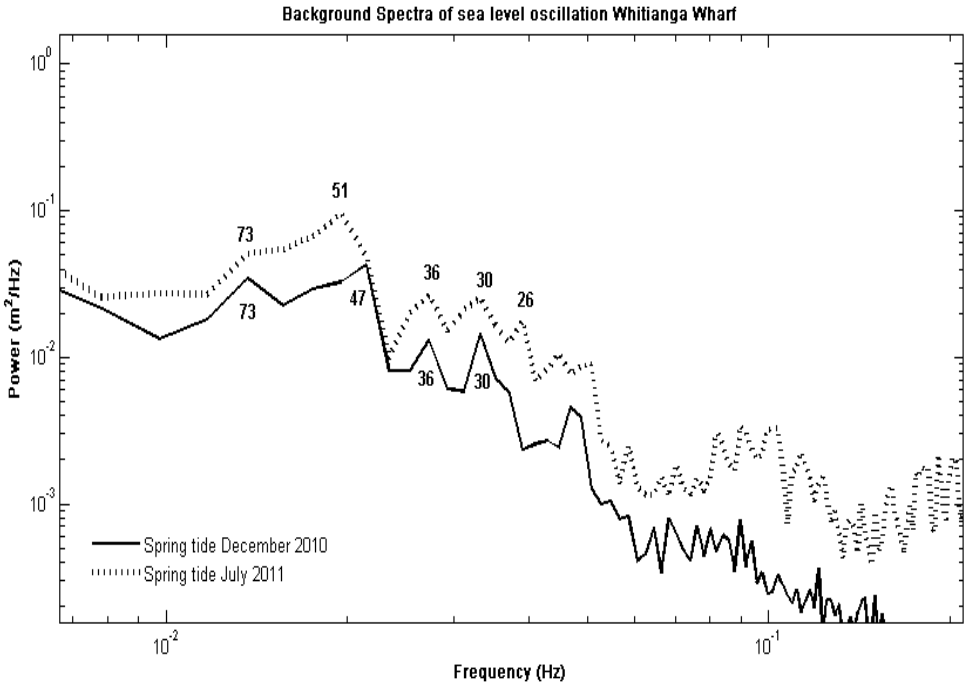

Figure 6-32. Background Spectra taken from measured tide level at Whitianga Wharf. Note that the tide has been filtered.

Table 6-10. Spectra of measured tsunami events and spectra of the time when the tsunami is absent at Whitianga Wharf.

Events	Dominant Periods
Spring tide December	73, 47, 36, 30, 26
Spring tide July	73, 51, 36, 30
Chilean 2010	51, 36, 28, 22
Tohoku 2011	73, 47, 37, 27
6 July 2011	78, 39
Model	52, 26

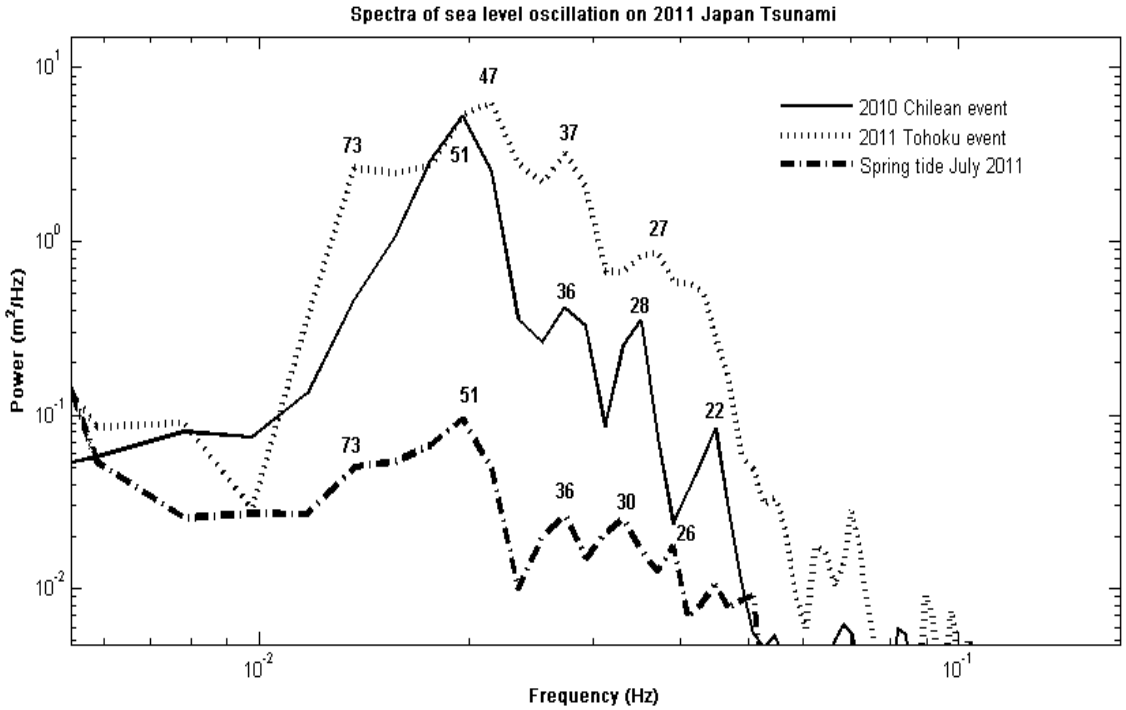

Figure 6-33. Spectra of two recent distant tsunami events recorded in tide gauge at WHitianga Wharf and the background spectra of winter spring tide; it is clearly seen that both of the tsunami events amplified the sea level twice from its original level.

CHAPTER 7 - SUMMARY AND CONCLUSIONS

Tsunami hazards are one of the most disastrous, resulting in losses in the cities located on the coast, both in human lives and infrastructure. Whitianga Township, within Mercury Bay, has been the fastest growing population in the Coromandel area, and should be concerned about tsunami hazards.

There are 3 types of tsunami sources that pose a threat to Whitianga Township and they are classified according to their tsunami wave arrival time; distant, regional and local sources. Kermadec Subduction Zone (KSZ) is known as an active and hazardous seismic zone in the southern Pacific. Seismic activity in this region is associated with the boundary between southern Pacific and Australian plates. On the basis of tsunami arrival time generated from this region, this zone is classified as regional and local tsunami source for New Zealand, particularly for Whitianga Township. The arriving tsunami can be significantly being amplified if their periods match with the resonant period of Mercury Bay.

I simulated 17 different earthquake scenarios and analysed 2 recent distant tsunami events in order to assess the respond of Mercury Bay to any earthquake induced tsunami event. To record the sea level oscillations produced by tsunami, I set 10 virtual tide gauges; 4 sites within the Mercury Bay to Whitianga Wharf and 6 sites near the tsunami sources. The local sites are at the entrance of Mercury bay (TS04), at the entrance of Buffalo Bay (TS07), in front of Whitianga Township (Buffalo Bay – TS09), and at Whitianga Wharf (TS12). Near source sites are TS01 (by the 6 July 2011 epicenter), TS13 the middle of KSZ, TS14 at the southern end of KSZ, and TS15. TS16 and TS17 in the middle of southern, middle and northern segments of KSZ respectively.

Spectral analysis was conducted to obtain the dominant period of each tsunami scenario. For the spectra analysis of the actual tsunami events (2010 Chilean and 2011 Tohoku) I have used the measured tide level taken from the tide gauge installed at Whitianga Wharf for both corresponding events. The background spectra

of ordinary sea level oscillation during spring and neap tides were taken from the same site and then compared with the spectra of tsunami events.

The results of simulated and measured tsunamis are summarised as follows:

(1) The tsunami waves that have been recorded at the virtual tide gauges show main features that:

- Most of the tsunami waves arrived as negative wave, except the one that was generated in the northern segment of the Kermadec Subduction Zone; the tsunami wave arrived as a positive wave. I marked the first increase or decrease of the water level as the tsunami arrival time. The tsunami arrival times at the entrance of Mercury Bay ranged from 56 to 158 minutes, another 10 to 17 minutes to reach the vicinity of Whitianga Township within Buffalo Bay, and 3 to 4 minutes to arrive at Whitianga Wharf.
- The tsunami waves at the entrance of Mercury Bay were irregular, and showed high frequency sea level oscillations for each scenario. This high frequency oscillation was then filtered by the bay bathymetry as the tsunamis propagated further landward.
- Maximum amplitude (positive) occurred as the first peak for almost all scenarios, except for the magnitude M_w8.8 earthquake in the northern segment (segment C) when the maximum amplitude occurred as the second peak (3 hours after the earthquake), and the third peak was the maximum amplitude for magnitude M_w = 7.6 earthquake (the 6 July 2011 event). In other words, the greater the distance of earthquake's epicenter, the latter the maximum amplitude would occur.
- It seems that the maximum wave height for all scenarios occurred in the vicinity of Whitianga Township (TS09), however, due to the truncated troughs in the observed tide records for several events, it is not possible to determine their maximum peak to trough. For this reason, I have used the tide data from the entrance of Buffalo Bay (TS07).The least distance between peak to trough occurred at Whitianga Wharf.
- In general, the first four waves have periods ranging from 43 to 71 minutes. The later waves have shorter periods ranging from 20 to 40 minutes.
- The tsunami ringing started to be calmed down after 5.5 to 6 hours of the arrival of tsunami.

(2) The 6 July 2011 event did not generate tsunami in Mercury Bay, whereas from the simulation we obtained a highest amplitude less than 10 cm.

(3) Scenario M_w8.5 earthquake in southern part of Kermadec Trench generated tsunami waves that arrived in Mercury bay within 56 to 75 minutes after the earthquake. The highest amplitude reached 1.92 m, the minimum amplitude was -1.55 m.

(4) Scenario M_w8.9 earthquake in middle part of Kermadec Trench generated tsunami waves that arrived in Mercury Bay within 68 to 84 minutes after the earthquake. The highest amplitude was 1.28 m, the lowest water drop was -1.25 m and the maximum wave height was 2.4 m.

(5) It took more than 2 hours (122 to 131 minutes) after the earthquake for the tsunami wave generated by M_w = 8.9 earthquake in northern segment of Kermadec Trench to arrive in Mercury Bay. The highest amplitude was 0.9 m, the lowest water drop was -0.7 m and the maximum wave height was 1.6 m.

(6) Scenario M_w = 9.2 earthquake in middle and southern segments of the Kermadec Subduction Zone generated tsunami waves that arrived in Mercury Bay within 58 to 73 minutes after the earthquake. The highest amplitude was 6.2 m (at the vicinity of Whitianga Township), and due to the truncated trough in the tide record, the lowest water drop was -3.45 m and the maximum wave height was 7.65 m measured at the entrance of Mercury Bay.

(7) Scenario M_w9.3 earthquake in middle-northern part of Kermadec Trench generated tsunami waves that arrived in Mercury bay within 68 to 84 minutes after the earthquake. The highest amplitude was 2.3 m, the lowest water drop was -1.3 m and the maximum wave height was 3.6 m.

(8) Eleven different scenarios of M_w8.5 to M_w9.5 earthquakes that ruptured the entire Kermadec Trench show that the tsunami wave arrive at the entrance of Mercury Bay in 55 to 58 minutes after the earthquakes.

(9) Modelled M_w7.6 earthquake shows that sea level started to oscillate at 110 to 127 minutes after the earthquake. The highest amplitude was 0.09 m, the lowest water drop was -0.09 m and the maximum wave height was 0.18 m. There is a mismatch in tsunami arrival recorded from the modelled to the measured one, this probably due to inaccurate fault parameters that have been used in the model.

(10) The 52 minutes dominant period that constantly occurred for each different earthquake scenario shows the response of Mercury Bay to any forced period resulted from tsunami events. This period is close to the 60 minutes response of New Zealand continental shelf (WALTERS, 2003).

(11) The spectra of modelled tsunami taken from the near sources show that the spectra of each single segment (source) and at the local sites were similar, but the spectra will be significantly different when it is taken from the middle of entire KSZ.

(12) The background spectra from spring tide where tsunami is absence at Whitianga Wharf shows the prominent peak with period of 51 minutes and the other three weaker peaks of 37, 30 and 26 minutes. From calculation of eigen period of semi-circular shaped basin proposed by RABINOVICH (2009), the zeroth mode of Mercury Bay is 35 minutes.

(13) The spectra of initial tsunami at the source for earthquake that rupture only a single segment will have dominant period that similar with the one that arrive in Mercury Bay. From the spring tide oscillation, the 51 minutes period is identified which is close to 52 minutes period of tsunami generated in the Kermadec Subduction Zone. In the bay, the tsunami's period match the bay's resonant period and the tsunami were being about 2 times amplified.

(14) The spectra of measured distant tsunamis events in Mercury Bay show dominant periods at about 47 and 51 minutes, and the latter periods were about 36 and 37 minutes which approach to the value calculated for the 35 minutes "eigen" period of Mercury bay. Similarity in the period of tsunami with the resonant period of Mercury Bay explains the reason for significant amplification of tsunami in this site. The 35 minutes calculated eigen period has a good agreement with the study of SMITH (1980) which showed periodicity of sea level oscillation in Mercury Bay at about 35 and 20 minutes, and 40 minutes resonance by WALTER, 2003. For the 6 July 2011 event, its spectra show a dominant period of 39 minutes.

Further research could be undertaken is to reconstruct the historical distant tsunami source spectra based on the tide gauge records by separate the source and topography effects method proposed by RABINOVICH (1997) which recently has

been applied by VICH and MONSERRAT (2009), and ABE (2011). The modelling undertaken also did not consider the effects of tides.

REFERENCES

ABE, K. (1994). Estimate of Tsunami Run-up Heights from Earthquake Magnitudes. TSUCHIYA, Y. and SHUTO, N. (eds), Tsunami: Progress in Prediction, Disaster Prevention and Warning. Kluwer Academic Publishers. (pp. 21-35).

ABE, K. (2011). Syntesis of a Tsunami Spectrum in a Semi-enclosed Basin Using Its Background Spectrum. Pure Applied Geophysics vol. 168. DOI: 10.1007/s00024-010-0222-x.

BABEROPOULOU, A., QAMAR, A., PRATT, T. L. and STEELE, W. P. (2006). Long-period effects of the Denali Earthquake on water bodies in the Puget Lowland: Observations and modelling, Bull. *Seism. Soc. Amer*. 96(2) (pp 519 – 535).

BALLANCE, P. F., ABLAEV, A. G., PUSCHCHIN, I. K., PLETNEV, S. P., BIRYLINA, M. G., ITAYA, T., FOLLAS, H. A., and GIBSON, G. W. (1999). Morphology and history of the Kermadec trench-arc-backarc basin-remnant arc system at 30 to 32^0S: geophysical profile, microfossil and K-Ar data. *Marine Geology* 159.

BELL, R. G., GOFF. J., DOWNES, G., BERRYMAN, K., WALTERS, R. A., CHAGUĖ-GOFF, C., BARNES, P., WRIGHT, I. (2004). Tsunami Hazard for the Bay of Plenty and Eastern Coromandel Peninsula: Stage 2, Environment Waikato Technical Report 2004/32. ISSN 1172-4005.

BELL, R. G. (2010). New Zealand Gauges: Chile Tsunami 2010. NIWA, Hamilton.

BELL, R. G., (2010). Did sea-level gauges in New Zealand detect the 2010 Chile Tsunami?, NIWA, Hamilton.

BERRYMAN, K. (2005). Review of tsunami hazard and risk in New Zealand. Lower Hutt: GNS Science.

BORRERO, J. C. (2011). Personal communication through e-mail: Kermadec-maximum wave height plots.

BRYANT, E., (2008). *Tsunami The Underrated Hazard*, Second Edition. Praxis Publishing Ltd, Chichester, UK, 27 – 47 p.

CHAPMAN, D. C. and GIESE, G. S. (2001). Seiches, Encyclopedia of Ocean Sciences, eds Steele, J. H., Turekian, K. K. and Thorpe, S. A., Vol. 5 (Academic Press, London) (pp. 2724 – 2731).

DAVIDSON, I., 2011. Every inch of NZ coast touched by far-reaching tsunami**,** http://www.nzherald.co.nz/nz/news/article.cfm?c_id=1&objectid=10712971

DJUMAGALIEV, V. A., RABINOVICH, A. B., FINE, I. V. (1994). Theoretical and experimental estimation of transfer pecularities of the Malokurilsk Bay coast, the Island of Shikotan, *Atmosph. Oceanic Phys*. 30 (pp. 680 – 686).

DOWNES, G., WEBB, T., MCSAVENEY, M., DARBY, D., DOSER, D., CHAGUE´ - GOFF, C. and BARNETT, A., The 26 March and 17 May 1947 Gisborne earthquakes and tsunami: implications for tsunami hazard for the east coast, North Island, New Zealand, In Tsunami Risk Assessment Beyond 2000: Theory, Practice and Plans, (GUSIAKOV, V.K., LEVIN, B.W. and YAKOVENKO, O.I., 2001). (pp 55–67).

de LANGE, W. P. (1983). Tsunami Hazard; An Investigation Into the Potential Tsunami Hazards of the Bay of Plenty Region Using Numerical Models. Master Thesis. pp 6-24.

de LANGE, W. P., and HEALY, T. R (1986a). Tsunami hazards in the Bay of Plenty, New Zealand: an example of hazard analysis using numerical models. *Journal of Shoreline Management 2*: 177-197, in Tsunami Hazard for the Bay of Plenty and Eastern Coromandel Peninsula: Stage 2, Environment Waikato Technical Report 2004/32, by BELL et al (2004).

de LANGE, W. P, in press. Tsunami and storm surge hazard in New Zealand, in Rouse, H.L., Goff, J.R. and Nichol, S. (eds.) The coast of New Zealand: Te Tai O Aotearoa. Lincoln University Press, New Zealand.

de LANGE, W. P., and HEALY, T. R. (1999). Tsunami & Tsunami Hazard. Tephra Oct. 99. http://www.civildefence.govt.nz

de LANGE, W. P., and HEALY, T. R. (2001). Tsunami Hazard for the Auckland Region and Hauraki Gulf, New Zealand. *Natural Hazards* 24.

de LANGE, W. P and MOON, V. G. (2007). Tsunami wash over deposits, Tawharanui, New Zealand. *Sedimentary Geology*, Elsevier B. V. DOI:10.1016/j.sedgeo.2007.01.006.

de LANGE, W. P. and McSAVENEY, E. (2009). Tsunamis - New Zealand's tsunami history, Te Ara - the Encyclopedia of New Zealand.
URL: http://www.TeAra.govt.nz/en/tsunamis/2

de LANGE, W. P (2011). Personal communication through e-mail: Kermadec-maximum wave height plots.

DONN, W. L. (1994). Alaskan Earthquake of 27 March 1964: Remote seiche simulation, *Science* 145 (pp. 261 – 262).

ENVIRONMENT WAIKATO. (2010). *Chilean 2010 tsunami recorded at Whitianga Wharf.*

GIESE, G. S. and HOLLANDER, R. B. (1987). The relation between coastal seiche at Palawan Island and tide-generated internal waves in the Sulu Sea, J. Geophys. 92 (pp 5151 – 5156).

GIESE, G. S. and CHAPMAN, D. C. (1993). Coastal seiches, Oceanus 36, (pp. 38-46).

GOFF, J., WALTERS, R., LAMARCHE, G., and CHAGUE-GOFF, C. (2005). Tsunami Overview Study. Auckland Regional Council.

GOFF, J., WALTERS, R., CALLAGHAN, F. (2006). Tsunami Source Study, *Environment Waikato Technical Report* 2006/49.

GOFF. J, NICHOL, S., and KENNEDY, D. (2010). Development of a palaeotsunami database for New Zealand. *Natural Hazards 54*. DOI 10.1007/s1 1069-009-9461-5.

GOFF, J., PEARCE, S., NICHOL, S. L., CHAGUE-GOFF, C., HORROCKS, M., and STROTZ, L. (2010). Multy-proxy records of regionally-sourced tsunamis, New Zealand. Geomorphology 118. DOI: 10.1016/j.geomorph.2010.02.005.

GRAPES, R. and DOWNES, G. (1997). The 1855 Wairarapa, New Zealand, earthquake: analysis of historical data, *Bulletin of the New Zealand National Society for Earthquake Engineering* 20(4), In Tsunami Forecasting and Monitoring in New Zealand, Pure Appl. Geophys. 168 (2011), 1125-1136. (POWER, W. and GALE, N. , 2010). DOI 10.1007/s00024-010-0223-9.

GNS. (2010). Chilean 2010 tsunami recorded by the New Zealand Tsunami Gauge Network.

HAMMING, R.W. (1977). Digital Filters (3rd ed.). Courier Dover Publications. ISBN 0-486-65088-X. (pp 281).

HEINZEL, G., RÜDIGER, A., and SCHILLING, R. (2002). Spectrum and spectral density estimation by the Discrete Fourier transform (DFT), including a comprehensive list of window functions and some new flat-top windows. Max-Planck-Institute für Gravitationsphysik, Hannover. (pp. 1 - 32)
http://www.rssd.esa.int/SP/LISAPATHFINDER/docs/Data_Analysis/GH_FFT.pdf

HENRY, R. F. and MURTY, T. S. (1995). Tsunami amplification due to resonance in Alberni Inlet: Normal modes, in Tsunami: Progress in Prediction, Disaster Prevention and Warning, eds. Tsuchiya, Y. and Shuto, N. (Kluwer Acad. Publ., Dordrecht, The Netherlands) (pp. 117-128).

HOLGATE, S. J., P. L. WOODWORTH, P. R. FODEN, J. PUGH, 2008: A Study of Delays in Making Tide Gauge Data Available to Tsunami Warning Centers. *J. Atmos. Oceanic Technol.*, 25, 475–481.

HONDA, K., TERADA, T., YOSHIDA, Y. and ISITANI, D.(1908). An investigation on the secondary undulations of oceanic tides, J. College Sci. Imper. Univ. Tokyo. (pp. 108).

HOUGH, S. E., (2004). Earthshaking Science, *What We Know (and Don't Know) about Earthquakes*. Princenton Univ. Press. pp 21-32.

HUTCHINSON, G. E. (1957). A Treatise on Limnology. *Volume 1. Geography, Physics and Chemistry* (Wiley, J., New York, 1957). (pp. 1015).

ITIC-International Tsunami Information Centre; About Tsunamis. http://ioc3.unesco.org/itic/contents.php/id=19

KARLING, H. M., (Ed). (2005). Tsunamis: The Great Wave. Tsunami Classification. Nova Science Publisher, Inc. pp 111.

KORGEN, B. J. (1995). Seiches, *Amer. Sci*. 83. (pp. 330-341).

LAND INFORMATION NEW ZEALAND, (1999), Chart 531 - Great Barrier Islands to Mercury Bay.

MASSIE, P. E. (1976). Coastal Engineering, Volume I – Introduction. Coastal Engineering Group, Department of Civil Engineering. Delft University of Technology, Netherlands. (pp. 88-89).

McFADGEN, B. G. and GOFF, J. R. (2007). Tsunamis in the New Zealand archaeological record. *Sedimentary Geology* 200.

McGARR, A. (1965). Excitation of seiches in channels by seismic waves, J. Geophys. Res. 70. (pp. 847 – 854)

McIVER, R. D. (1982). Role of naturally occurring gas hydrates in sediment transport, in de LANGE, W. P. (1983). Tsunami Hazard; An Investigation Into the Potential Tsunami Hazards of the Bay of Plenty Region Using Numerical Models. Master Thesis. pp 6-24.

MEI, C. C. (1992). The Applied Dynamics of Ocean Surface Waves. World Scientific, London. (740 pp).

MERRIFIELD, M. A. et al. (2005). Tide gauge observations of the Indian Ocean tsunami, December 26, 2004, Geophys. Res. Lett. 32, L09603, doi:10.1029/2005GL022610.

MILES, J. W. (1974). Harbor Seiching, Annual Rev. Fluid Mechanic. 1974.6:17-33. (pp. 17-35).

MOLLOY, E. (2001). Seiching in Cockburn Sound. Dept. of Environmental Engineering, University of Western Australia.(pp. 1 – 12).

MUNK, W. H. (1962). Long waves, *The Sea* (J. Wiley, New York, 1962). (pp. 647-663).

MURTY, T. S. (1977). *Seismic Sea Waves – Tsunamis* (Bull. Fish. Res. Board Canada 198, Ottawa, 1977). (pp. 337).

NAKANO, M. (1932). Secondary undulations in bays forming a coupled system, Proc. Phys. Math. Soc. Japan **3**. (pp. 372-380).

NAKANO, M. (1933). Possibility of excitation of secondary undulations in bays by tidal or oceanic currents, *Proc. Imp. Acad. Japan* **9**. (pp. 152-155).

OKIHIRO, M., GUZA, R. T. and SEYMOUR, R. J. (1993). Excitation of seiche observed in a small harbour, *J. Phys. Res*. **98**. (pp. 18201-18211).

POWER, W. and GALE, N. (2010). Tsunami Forecasting and Monitoring in New Zealand. Pure Applied Geophysic. 168(2011), 1125-1136. DOI 10.1007/s00024-010-0223-9.

POWER, W. (2011). Pacific quake sent most of its energy north on NZ scientist say-07/07/2011. GNS Media Releases. http://www.gns.cri.nz/Home/News-and-Events/Media-Releases/Quake-sent-energy-north.

POWER, W., WALLACE, L., WANG, X., and REYNERS, M. (2011). Tsunami Hazard Posed to New Zealand by the Kermadec and Southern New Hebrides Subduction Margins: An Assessment Based on Plate Boundary Kinematics, Interseismic Coupling, and Historical Seismicity. *Pure Applied Geophysic*. DOI 10.1007/s00024-011-0299-x.

PRASETYA, G., HEALY, T. R., de LANGE, W. P. (2008, revised version 2011). Hydrodynamic Modelling of Tsunami Overwash of Whitianga Township and Harbour. Coastal Marine Group, Department of Earth and Ocean Sciences, University of Waikato.

PRASETYA, G. & WANG, X. (2011). Tsunami frequency analysis for Eastern Coromandel and Waikato Region from Kermadec Trench and local sources within the Bay of Plenty. GNS Science Consultancy Report 2011/135.

PRESS, F., and HARKRIDER, D. (1966). Air-sea waves from the explosion of Krakatoa. Science 154(3574), in Tsunami Hazard; An Investigation Into the Potential Tsunami Hazards of the Bay of Plenty Region Using Numerical Models. Master Thesis by de LANGE, W. P. (1983).

RABINOVICH, A. B. (1993). Long Ocean Gravity Waves: Trapping, Resonance, and Leaking (Gidrometeoizdat, St. Petersburg, 1993). (pp. 325).

RABINOVICH, A. B. (1997). Spectral analysis of tsunami waves: Separation of source and topography effects, *J. Geophys. Res*. **102**. (pp. 12663-12676).

RABINOVICH, A. B., Thomson, R. E. (2007). The Sumatra tsunami of 26 December 2006 as observed in the North Pacific and North Atlantic oceans, *Surveys Geophys*. **27**. (pp. 647-677).

RABINOVICH, A. B., and THOMSON, R. E. (2007). The 26 December 2004 Sumatra Tsunami: Analysis of Tide Gauge Data from the World Ocean Part 1. Indian Ocean and South Africa. *Pure and Applied Geophysics*. DOI: 10.1007/s00024-006-0164-5.

RABINOVICH, A. B. (2009). Seiches and Harbor Oscillations, Handbook of Coastal and Ocean Eng. (edited by Kim, Y. C.), World Scientific Publ., Singapore. (pp. 193-236).

RAICHLEN, F. (1966). Harbor resonance, *Estuary and Coastline Hydrodynamics*, ed. A. T. Ippen (McGraw Hill Book Co., New York, 1966). (pp. 281-340).

RAICHLEN, F. (2002). The effect of ship-harbor interactions on port operations, *Maritime Technol*. (pp. 11-20).

SATAKE, K. & KANAMORI, H. (1991). Use of Tsunami Waveforms for Earthquake Source Study. Kluwer Academic Publisher, Netherlands. *Natural Hazards* **4**. pp 193-208.

SATAKE, K. & TANIOKA, Y. (1999). Sources of tsunamis and tsunamigenic earthquakes in subduction zones. Pure applied geophysics vol. 154. (pp. 467 – 583).

SAUNDERS, W. S. A., PRASETYA, G., and LEONARD, G. S. (2011). New Zealand's Next Top Model: Integrating tsunami inundation modelling into land use planning. GNS Science Miscellaneous Series 34. Lower Hutt, Wellington. 2-7p.

SAWARAGI, T. and KUBO, M. (1982). Long-period motions of a moored ship induced by harbour oscillations, *Coast. Eng. Japan* **25**. (pp. 261-275).

RISHWORTH, S., 2011. Small surge arrive here. www.gisborneherald.co.nz/article/?id=21812

SHEARER, P. M. (2009). Introduction to SEISMOLOGY, second edition. Cambridge University Press. (pp. 271).

SMITH, D. B., (1980), Sea Level Oscillations, Hydrology & Sedimentology in Mercury Bay. MSc Thesis., University of Waikato, Hamilton, New Zealand., 6 p.

SOLEVIEV, and GO, 1974 in Farreras. S., and Reyes, J. (2002). Tsunami Response Simulation at Guadalupe Island (Mexico). http://nsgl.gso.uri.edu/hawau/hawauw92002/hawauw92002_part3.pdf.

STEEGHS, L. and HEALY, T. (2007). Tidal inlet configuration and bathymetric changes resulting from active sedimentation, Buffalo Bay, New Zealand. Journal of Coastal Research, Special Issue 50, 2007. ISSN 0749.0208.

TANGUY, J.C. and RIBIERI, C.H. and SCARTH, A. and TJETJEP, W.S. 1998. Victims from volcanic eruptions: a revised database. Bulletin of volcanology. 60, 137-144.

THAMES-COROMANDEL District Council (2011), The Eastern Coromandel Tsunami Strategy; managing tsunami risk in Whitianga. http://www.tcdc.govt.nz/Global/Maps/Tsunami%20Open%20Day%20Reference%20Document%20062011.pdf

THOMSON, R. E., RABINOVICH, A. B. and KRASSOVSKI, M. V. (2007). Double jeopardy: Concurrent arrival of the 2004 Sumatra tsunami and storm-generated waves on the Atlantic coast of the United States and Canada, *Geophys. Res. Lett*. 34, L15607, doi:10.1029/2007GL030685.

THOMPSON, J. (2011). Cascadia's Fault: The Earthquake and Tsunami That Could Devastate North America. Berkeley, CA: Counterpoint: Distributed by Publishers Group West, c2011.

TITOV, V. V., RABINOVICH, A. B., MOFJELD, H., THOMSON, R. E. and GONZALEZ, F. I. (2005). The Global reach of the 26 Desember 2004 Sumatra tsunami, *Science* 309. (pp. 2045-2048).

USGS. (2011). Historic seismicity. Magnitude 7.6 Kermadec Islands Region, Wednesday, July 06, 2011 at 19:03:16 UTC. http://neic.usgs.gov/neis/eq_depot/2011/eq_110706_c0004pbm/neic_c0004pbm_h.html

VICH, M. M., and MONSERRAT, S. (2009). Source spectrum for the Algerian tsunami of 21 May 2003 estimated from coastal tide gauge data. Geophysical Research Letters, Vol. 36. DOI:10.1029/2009GL039970.

VON HERZEN, R., RUPPEL, C., MOLNAR, P., NETTLES, M., NAGIHARA, S., and EKSTRŐM, G., (2001). A constraint on the shear stress at the Pacific-Australian plate boundary from heat flow and seismicity at the Kermadec forearc. *American Geophysical Union*. Paper # 2000JB900469.

WAIKATO REGIONAL COUNCIL. (2011). Tide level at Whitianga tide. http://www.waikatoregion.govt.nz

WANG, X. and LIU, P. L. F. (2005). A Numerical investigation of Boumerdes_Zemmouri (Algeria) Eartquake and Tsunami. Computer Modelling in Engineering and Sciences, 10(2): pp 171-184.

WANG, X. and LIU, P. L. F. (2006). An analysis of 2004 Sumatra earthquake fault plane mechanisms and Indian Ocean tsunami. Journal Hydraulics Res., (pp 147 – 154).

WANG, X. (2009). User Manual For COMCOT Version 1.7 (First Draft). Institute of Geological & Nuclear Science, New Zealand.

WARD, S. N. (2000). Landslide Tsunami. *Journal of Geophysical Research*. pp 1-27.

WELCH, P. D. (1967). The use of fast Fourier transforms for the estimation of power spectra: A method based on time averaging over short modified periodograms. IEEE Transactions on Audio and Electroacoustics, vol. 15. (pp. 70-73).

WELLS, D. L. and COPPERSMITH, K. J. (1994). New Empirical Relationship among Magnitude, Rupture Length, Rupture Width, Rupture Area, and Surface Displacement. Bulleting of the Seismological Sociecty of America, Vol. 84.

WIEGEL, R. L. (1964). Tsunamis, storm surges, and harbour oscillations, Oceanographical Engineering (Prentice-Hall, Englewood Cliffs, NJ, 1964). (Ch. 5, pp. 95-127).

WIJETUNGE, J. J. (2009). Field measurements and numerical simulations of the 2004 tsunami impact on the south coast of Sri Lanka. Ocean Engineering 36. DOI:10.1016/j.oceaneng.2009.06.002. (pp. 960 – 973).

WILSON, B. (1972). Seiches, *Advances in Hydrosciences* **8**. (pp. 1-94).

WU, J. K. and LIU, P. L-F. (1990). Harbor excitations by incident wave groups, *J. Fluid Mech*. **217**. (pp. 595-613).

WŪEST, A. and FARMER, D. M. (2003). Seiche. McGraw-Hill Encyclopedia of Science & Technology.

http://library.thinkquest.org/03oct/00046/tsunami/causes.htm

Appendices

Appendix 1. Grid layer information

Properties	Grid 1	Grid 2	Grid 3	Grid 4
Coordinate system	Spherical	Spherical	Spherical	Spherical
Shallow water equation	Linear	Linear	Linear	Non-Linear
Bottom friction	-	-	-	0.013
Surface displacement output	disabled	disabled	disabled	enabled
Parent grid ID	-	1	2	3
Grid size ratio	-	5	3	3
Time step size ratio	-	3	2	1
Grid size positions - x_start (degree) - x_end(degree) - y_start (degree) - y_end(degree)	 170.0 189.9833 -40.0 -26.01667	 175.260 176.6067 -37.990 -36.010	 175.3022 176.1844 -37.24777 -36.20222	 175.5452 175.7826 -36.91481 -36.66407
Grid dimension (NX*NY)	1200*840	405*595	795*942	642*678
Grid size (DX, minute)	1	0.2	6.6666670E-02	2.2222223E-02
Grid size (DY, minute)	1	0.2	6.6666670E-02	2.2222223E-02
Time step size (DT, second)	2.313588	0.7711961	0.3855981	0.3855981
Child grid layer ID	2	3	4	-

Appendix 2: Table of information input for the simulation

a. Kermadec ABC Mw = 8.5 earthquake (Scenario 6)

General Information
Total run time (second) : 86400.00
Time interval for output (second) : 1800.000
Time step size (second) : 2.313588
Total steps to run (steps) : 37345
Step interval for output (steps) : 778
Max. surface displacement output : ENABLED
Time history record output : ENABLED
Shoreline located at depth contour : 0.0000000E+00
Boundary condition : RADIATION (OPEN)

Initial Condition Information. Total number of fault segments : 28

Fault segment	Fault rupture time (second)	Epicenter		Focal depth (km)	Fault length (km)	Fault width (km)	Strike (degree)	Dip (degree)	Slip (degree)	Dislocation (meter)	Domain Origin	
		Lat	Lon								Lat	Lon
1	0.0	179.6930	-37.80790	3.970603	100	50	212.4	4.0	90	1	170.0	-40.0
2	0.0	180.2999	-37.05250	4.903464	100	50	212.3	4.602309	90	1	170.0	-40.0
3	0.0	180.8188	-36.26240	5.815893	100	50	202.9	5.210596	90	1	170.0	-40.0
4	0.0	179.2142	-37.56781	7.458427	100	50	212.4	6.0	90	1	170.0	-40.0
5	0.0	179.8257	-36.81326	8.915419	100	50	212.3	8.710391	90	1	170.0	-40.0
6	0.0	180.3078	-36.08834	10.35673	100	50	202.9	11.44768	90	1	170.0	-40.0
7	0.0	181.2725	-35.44100	6.691522	100	50	205.0	5.794348	90	1	170.0	-40.0
8	0.0	181.6950	-34.61180	7.310587	100	50	200.0	6.0	90	1	170.0	-40.0
9	0.0	182.0470	-33.75910	7.731237	100	50	197.5	6.0	90	1	170.0	-40.0
10	0.0	182.3678	-32.89860	8.0	100	50	196.9	6.582	90	1	170.0	-40.0
11	0.0	182.6807	-32.03810	8.0	100	50	197.0	8.122018	90	1	170.0	-40.0
12	0.0	183.0170	-31.18540	8.0	100	50	199.9	9.666493	90	1	170.0	-40.0
13	0.0	180.7754	-35.25214	11.73943	100	50	205.0	14.07456	90	1	170.0	-40.0
14	0.0	181.1850	-34.45902	12.53701	100	50	200.0	14.68941	90	1	170.0	-40.0
15	0.0	181.5346	-33.62477	12.95766	100	50	197.5	14.26876	90	1	170.0	-40.0
16	0.0	181.859	-32.76889	13.73125	100	50	196.9	14.388	90	1	170.0	-40.0
17	0.0	182.1791	-31.90809	15.06408	100	50	197.0	15.41468	90	1	170.0	-40.0
18	0.0	182.5303	-31.03468	16.39565	100	50	199.9	16.44433	90	1	170.0	-40.0
19	0.0	183.4003	-30.34830	-30.34830	100	50	202.8	11.21627	90	1	170.0	-40.0
20	0.0	183.7524	-29.50350	8.0	100	50	196.7	9.550721	90	1	170.0	-40.0
21	0.0	184.0184	-28.63510	7.541041	100	50	193.2	11.06531	90	1	170.0	-40.0
22	0.0	184.2452	-27.75890	7.029047	100	50	192.4	13.36929	90	1	170.0	-40.0
23	0.0	184.4564	-26.88280	6.518828	100	50	191.7	15.66527	90	1	170.0	-40.0

Fault segment	Fault rupture time	Epicenter		Focal depth (km)	Fault length (km)	Fault width (km)	Strike (degree)	Dip (degree)	Slip (degree)	Dislocation (meter)	Domain Origin	
		Lat	Lon								Lat	Lon
26	0.0	183.5294	-28.53444	17.13743	100	50	193.2	15.68844	90	1	170.0	-40.0
27	0.0	183.7629	-27.66506	18.59037	100	50	192.4	16.45643	90	1	170.0	-40.0
24	0.0	182.9296	-30.17756	17.72565	100	50	202.8	17.47752	90	1	170.0	-40.0
25	0.0	183.2649	-29.37622	16.29603	100	50	196.7	15.55072	90	1	170.0	-40.0
28	0.0	183.9816	-26.79510	20.01967	100	50	191.7	17.22176	90	1	170.0	-40.0

b. **Kermadec ABC Mw = 8.6 earthquake (Scenario 6)**

General Information
Total run time (second) : 86400.00
Time interval for output (second) : 1800.000
Time step size (second) : 2.313588
Total steps to run (steps) : 37345
Step interval for output (steps) : 778
Max. surface displacement output : ENABLED
Time history record output : ENABLED
Shoreline located at depth contour : 0.0000000E+00
Boundary condition : RADIATION (OPEN)

Initial Condition Information. Total number of fault segments : 28

Fault segment	Fault rupture time (second)	Epicenter		Focal depth (km)	Fault length (km)	Fault width (km)	Strike (degree)	Dip (degree)	Slip (degree)	Dislocation (meter)	Domain Origin	
		Lat	Lon								Lat	Lon
1	0.0	179.6930	-37.80790	3.970603	100	50	212.4	4.0	90	1.5	170.0	-40.0
2	0.0	180.2999	-37.05250	4.903464	100	50	212.3	4.602309	90	1.5	170.0	-40.0
3	0.0	180.8188	-36.26240	5.815893	100	50	202.9	5.210596	90	1.5	170.0	-40.0
4	0.0	179.2142	-37.56781	7.458427	100	50	212.4	6.0	90	1.5	170.0	-40.0
5	0.0	179.8257	-36.81326	8.915419	100	50	212.3	8.710391	90	1.5	170.0	-40.0
6	0.0	180.3078	-36.08834	10.35673	100	50	202.9	11.44768	90	1.5	170.0	-40.0
7	0.0	181.2725	-35.44100	6.691522	100	50	205.0	5.794348	90	1.5	170.0	-40.0
8	0.0	181.6950	-34.61180	7.310587	100	50	200.0	6.0	90	1.5	170.0	-40.0
9	0.0	182.0470	-33.75910	7.731237	100	50	197.5	6.0	90	1.5	170.0	-40.0
10	0.0	182.3678	-32.89860	8.0	100	50	196.9	6.582	90	1.5	170.0	-40.0
11	0.0	182.6807	-32.03810	8.0	100	50	197.0	8.122018	90	1.5	170.0	-40.0
12	0.0	183.0170	-31.18540	8.0	100	50	199.9	9.666493	90	1.5	170.0	-40.0
13	0.0	180.7754	-35.25214	11.73943	100	50	205.0	14.07456	90	1.5	170.0	-40.0
14	0.0	181.1850	-34.45902	12.53701	100	50	200.0	14.68941	90	1.5	170.0	-40.0
15	0.0	181.5346	-33.62477	12.95766	100	50	197.5	14.26876	90	1.5	170.0	-40.0
16	0.0	181.859	-32.76889	13.73125	100	50	196.9	14.388	90	1.5	170.0	-40.0
17	0.0	182.1791	-31.90809	15.06408	100	50	197.0	15.41468	90	1.5	170.0	-40.0
18	0.0	182.5303	-31.03468	16.39565	100	50	199.9	16.44433	90	1.5	170.0	-40.0
19	0.0	183.4003	-30.34830	-30.34830	100	50	202.8	11.21627	90	1.5	170.0	-40.0
20	0.0	183.7524	-29.50350	8.0	100	50	196.7	9.550721	90	1.5	170.0	-40.0
21	0.0	184.0184	-28.63510	7.541041	100	50	193.2	11.06531	90	1.5	170.0	-40.0
22	0.0	184.2452	-27.75890	7.029047	100	50	192.4	13.36929	90	1.5	170.0	-40.0
23	0.0	184.4564	-26.88280	6.518828	100	50	191.7	15.66527	90	1.5	170.0	-40.0
24	0.0	182.9296	-30.17756	17.72565	100	50	202.8	17.47752	90	1.5	170.0	-40.0
25	0.0	183.2649	-29.37622	16.29603	100	50	196.7	15.55072	90	1.5	170.0	-40.0

Fault segment	Fault rupture time	Epicenter		Focal depth (km)	Fault length (km)	Fault width (km)	Strike (degree)	Dip (degree)	Slip (degree)	Dislocation (meter)	Domain Origin	
		Lat	Lon								Lat	Lon
26	0.0	183.5294	-28.53444	17.13743	100	50	193.2	15.68844	90	1.5	170.0	-40.0
27	0.0	183.7629	-27.66506	18.59037	100	50	192.4	16.45643	90	1.5	170.0	-40.0
28	0.0	183.9816	-26.79510	20.01967	100	50	191.7	17.22176	90	1.5	170.0	-40.0

c. Kermadec ABC Mw = 8.7 earthquake (Scenario 6)

General Information
Total run time (second) : 86400.00
Time interval for output (second) : 1800.000
Time step size (second) : 2.313588
Total steps to run (steps) : 37345
Step interval for output (steps) : 778
Max. surface displacement output : ENABLED
Time history record output : ENABLED
Shoreline located at depth contour : 0.0000000E+00
Boundary condition : RADIATION (OPEN)

Initial Condition Information. Total number of fault segments : 28

Fault segment	Fault rupture time (second)	Epicenter		Focal depth (km)	Fault length (km)	Fault width (km)	Strike (degree)	Dip (degree)	Slip (degree)	Dislocation (meter)	Domain Origin	
		Lat	Lon								Lat	Lon
1	0.0	179.6930	-37.80790	3.970603	100	50	212.4	4.0	90	2	170.0	-40.0
2	0.0	180.2999	-37.05250	4.903464	100	50	212.3	4.602309	90	2	170.0	-40.0
3	0.0	180.8188	-36.26240	5.815893	100	50	202.9	5.210596	90	2	170.0	-40.0
4	0.0	179.2142	-37.56781	7.458427	100	50	212.4	6.0	90	2	170.0	-40.0
5	0.0	179.8257	-36.81326	8.915419	100	50	212.3	8.710391	90	2	170.0	-40.0
6	0.0	180.3078	-36.08834	10.35673	100	50	202.9	11.44768	90	2	170.0	-40.0
7	0.0	181.2725	-35.44100	6.691522	100	50	205.0	5.794348	90	2	170.0	-40.0
8	0.0	181.6950	-34.61180	7.310587	100	50	200.0	6.0	90	2	170.0	-40.0
9	0.0	182.0470	-33.75910	7.731237	100	50	197.5	6.0	90	2	170.0	-40.0
10	0.0	182.3678	-32.89860	8.0	100	50	196.9	6.582	90	2	170.0	-40.0
11	0.0	182.6807	-32.03810	8.0	100	50	197.0	8.122018	90	2	170.0	-40.0
12	0.0	183.0170	-31.18540	8.0	100	50	199.9	9.666493	90	2	170.0	-40.0
13	0.0	180.7754	-35.25214	11.73943	100	50	205.0	14.07456	90	2	170.0	-40.0
14	0.0	181.1850	-34.45902	12.53701	100	50	200.0	14.68941	90	2	170.0	-40.0
15	0.0	181.5346	-33.62477	12.95766	100	50	197.5	14.26876	90	2	170.0	-40.0
16	0.0	181.859	-32.76889	13.73125	100	50	196.9	14.388	90	2	170.0	-40.0
17	0.0	182.1791	-31.90809	15.06408	100	50	197.0	15.41468	90	2	170.0	-40.0
18	0.0	182.5303	-31.03468	16.39565	100	50	199.9	16.44433	90	2	170.0	-40.0
19	0.0	183.4003	-30.34830	-30.34830	100	50	202.8	11.21627	90	2	170.0	-40.0
20	0.0	183.7524	-29.50350	8.0	100	50	196.7	9.550721	90	2	170.0	-40.0
21	0.0	184.0184	-28.63510	7.541041	100	50	193.2	11.06531	90	2	170.0	-40.0
22	0.0	184.2452	-27.75890	7.029047	100	50	192.4	13.36929	90	2	170.0	-40.0
23	0.0	184.4564	-26.88280	6.518828	100	50	191.7	15.66527	90	2	170.0	-40.0
24	0.0	182.9296	-30.17756	17.72565	100	50	202.8	17.47752	90	2	170.0	-40.0
25	0.0	183.2649	-29.37622	16.29603	100	50	196.7	15.55072	90	2	170.0	-40.0

Fault segment	Fault rupture time	Epicenter		Focal depth (km)	Fault length (km)	Fault width (km)	Strike (degree)	Dip (degree)	Slip (degree)	Dislocation (meter)	Domain Origin	
		Lat	Lon								Lat	Lon
26	0.0	183.5294	-28.53444	17.13743	100	50	193.2	15.68844	90	2	170.0	-40.0
27	0.0	183.7629	-27.66506	18.59037	100	50	192.4	16.45643	90	2	170.0	-40.0
28	0.0	183.9816	-26.79510	20.01967	100	50	191.7	17.22176	90	2	170.0	-40.0

d. **Kermadec ABC Mw = 8.8 earthquake (Scenario 6)**

General Information
Total run time (second) : 86400.00
Time interval for output (second) : 1800.000
Time step size (second) : 2.313588
Total steps to run (steps) : 37345
Step interval for output (steps) : 778
Max. surface displacement output : ENABLED
Time history record output : ENABLED
Shoreline located at depth contour : 0.0000000E+00
Boundary condition : RADIATION (OPEN)

Initial Condition Information. Total number of fault segments : 28

Fault segment	Fault rupture time (second)	Epicenter		Focal depth (km)	Fault length (km)	Fault width (km)	Strike (degree)	Dip (degree)	Slip (degree)	Dislocation (meter)	Domain Origin	
		Lat	Lon								Lat	Lon
1	0.0	179.6930	-37.80790	3.970603	100	50	212.4	4.0	90	2.8	170.0	-40.0
2	0.0	180.2999	-37.05250	4.903464	100	50	212.3	4.602309	90	2.8	170.0	-40.0
3	0.0	180.8188	-36.26240	5.815893	100	50	202.9	5.210596	90	2.8	170.0	-40.0
4	0.0	179.2142	-37.56781	7.458427	100	50	212.4	6.0	90	2.8	170.0	-40.0
5	0.0	179.8257	-36.81326	8.915419	100	50	212.3	8.710391	90	2.8	170.0	-40.0
6	0.0	180.3078	-36.08834	10.35673	100	50	202.9	11.44768	90	2.8	170.0	-40.0
7	0.0	181.2725	-35.44100	6.691522	100	50	205.0	5.794348	90	2.8	170.0	-40.0
8	0.0	181.6950	-34.61180	7.310587	100	50	200.0	6.0	90	2.8	170.0	-40.0
9	0.0	182.0470	-33.75910	7.731237	100	50	197.5	6.0	90	2.8	170.0	-40.0
10	0.0	182.3678	-32.89860	8.0	100	50	196.9	6.582	90	2.8	170.0	-40.0
11	0.0	182.6807	-32.03810	8.0	100	50	197.0	8.122018	90	2.8	170.0	-40.0
12	0.0	183.0170	-31.18540	8.0	100	50	199.9	9.666493	90	2.8	170.0	-40.0
13	0.0	180.7754	-35.25214	11.73943	100	50	205.0	14.07456	90	2.8	170.0	-40.0
14	0.0	181.1850	-34.45902	12.53701	100	50	200.0	14.68941	90	2.8	170.0	-40.0
15	0.0	181.5346	-33.62477	12.95766	100	50	197.5	14.26876	90	2.8	170.0	-40.0
16	0.0	181.859	-32.76889	13.73125	100	50	196.9	14.388	90	2.8	170.0	-40.0
17	0.0	182.1791	-31.90809	15.06408	100	50	197.0	15.41468	90	2.8	170.0	-40.0
18	0.0	182.5303	-31.03468	16.39565	100	50	199.9	16.44433	90	2.8	170.0	-40.0
19	0.0	183.4003	-30.34830	-30.34830	100	50	202.8	11.21627	90	2.8	170.0	-40.0
20	0.0	183.7524	-29.50350	8.0	100	50	196.7	9.550721	90	2.8	170.0	-40.0
21	0.0	184.0184	-28.63510	7.541041	100	50	193.2	11.06531	90	2.8	170.0	-40.0
22	0.0	184.2452	-27.75890	7.029047	100	50	192.4	13.36929	90	2.8	170.0	-40.0
23	0.0	184.4564	-26.88280	6.518828	100	50	191.7	15.66527	90	2.8	170.0	-40.0
24	0.0	182.9296	-30.17756	17.72565	100	50	202.8	17.47752	90	2.8	170.0	-40.0
25	0.0	183.2649	-29.37622	16.29603	100	50	196.7	15.55072	90	2.8	170.0	-40.0

Fault segment	Fault rupture time	Epicenter		Focal depth (km)	Fault length (km)	Fault width (km)	Strike (degree)	Dip (degree)	Slip (degree)	Dislocation (meter)	Domain Origin	
		Lat	Lon								Lat	Lon
26	0.0	183.5294	-28.53444	17.13743	100	50	193.2	15.68844	90	2.8	170.0	-40.0
27	0.0	183.7629	-27.66506	18.59037	100	50	192.4	16.45643	90	2.8	170.0	-40.0
28	0.0	183.9816	-26.79510	20.01967	100	50	191.7	17.22176	90	2.8	170.0	-40.0

e. Kermadec ABC Mw = 8.9 earthquake (Scenario 6)

General Information
Total run time (second) : 86400.00
Time interval for output (second) : 1800.000
Time step size (second) : 2.313588
Total steps to run (steps) : 37345
Step interval for output (steps) : 778
Max. surface displacement output : ENABLED
Time history record output : ENABLED
Shoreline located at depth contour : 0.0000000E+00
Boundary condition : RADIATION (OPEN)

Initial Condition Information. Total number of fault segments : 28

Fault segment	Fault rupture time (second)	Epicenter		Focal depth (km)	Fault length (km)	Fault width (km)	Strike (degree)	Dip (degree)	Slip (degree)	Dislocation (meter)	Domain Origin	
		Lat	Lon								Lat	Lon
1	0.0	179.6930	-37.80790	3.970603	100	50	212.4	4.0	90	4	170.0	-40.0
2	0.0	180.2999	-37.05250	4.903464	100	50	212.3	4.602309	90	4	170.0	-40.0
3	0.0	180.8188	-36.26240	5.815893	100	50	202.9	5.210596	90	4	170.0	-40.0
4	0.0	179.2142	-37.56781	7.458427	100	50	212.4	6.0	90	4	170.0	-40.0
5	0.0	179.8257	-36.81326	8.915419	100	50	212.3	8.710391	90	4	170.0	-40.0
6	0.0	180.3078	-36.08834	10.35673	100	50	202.9	11.44768	90	4	170.0	-40.0
7	0.0	181.2725	-35.44100	6.691522	100	50	205.0	5.794348	90	4	170.0	-40.0
8	0.0	181.6950	-34.61180	7.310587	100	50	200.0	6.0	90	4	170.0	-40.0
9	0.0	182.0470	-33.75910	7.731237	100	50	197.5	6.0	90	4	170.0	-40.0
10	0.0	182.3678	-32.89860	8.0	100	50	196.9	6.582	90	4	170.0	-40.0
11	0.0	182.6807	-32.03810	8.0	100	50	197.0	8.122018	90	4	170.0	-40.0
12	0.0	183.0170	-31.18540	8.0	100	50	199.9	9.666493	90	4	170.0	-40.0
13	0.0	180.7754	-35.25214	11.73943	100	50	205.0	14.07456	90	4	170.0	-40.0
14	0.0	181.1850	-34.45902	12.53701	100	50	200.0	14.68941	90	4	170.0	-40.0
15	0.0	181.5346	-33.62477	12.95766	100	50	197.5	14.26876	90	4	170.0	-40.0
16	0.0	181.859	-32.76889	13.73125	100	50	196.9	14.388	90	4	170.0	-40.0
17	0.0	182.1791	-31.90809	15.06408	100	50	197.0	15.41468	90	4	170.0	-40.0
18	0.0	182.5303	-31.03468	16.39565	100	50	199.9	16.44433	90	4	170.0	-40.0
19	0.0	183.4003	-30.34830	-30.34830	100	50	202.8	11.21627	90	4	170.0	-40.0
20	0.0	183.7524	-29.50350	8.0	100	50	196.7	9.550721	90	4	170.0	-40.0
21	0.0	184.0184	-28.63510	7.541041	100	50	193.2	11.06531	90	4	170.0	-40.0
22	0.0	184.2452	-27.75890	7.029047	100	50	192.4	13.36929	90	4	170.0	-40.0
23	0.0	184.4564	-26.88280	6.518828	100	50	191.7	15.66527	90	4	170.0	-40.0
24	0.0	182.9296	-30.17756	17.72565	100	50	202.8	17.47752	90	4	170.0	-40.0
25	0.0	183.2649	-29.37622	16.29603	100	50	196.7	15.55072	90	4	170.0	-40.0

Fault segment	Fault rupture time	Epicenter		Focal depth (km)	Fault length (km)	Fault width (km)	Strike (degree)	Dip (degree)	Slip (degree)	Dislocation (meter)	Domain Origin	
		Lat	Lon								Lat	Lon
26	0.0	183.5294	-28.53444	17.13743	100	50	193.2	15.68844	90	4	170.0	-40.0
27	0.0	183.7629	-27.66506	18.59037	100	50	192.4	16.45643	90	4	170.0	-40.0
28	0.0	183.9816	-26.79510	20.01967	100	50	191.7	17.22176	90	4	170.0	-40.0

f. Kermadec ABC Mw = 9.0 earthquake (Scenario 6)

General Information
Total run time (second) : 86400.00
Time interval for output (second) : 1800.000
Time step size (second) : 2.313588
Total steps to run (steps) : 37345
Step interval for output (steps) : 778
Max. surface displacement output : ENABLED
Time history record output : ENABLED
Shoreline located at depth contour : 0.0000000E+00
Boundary condition : RADIATION (OPEN)

Initial Condition Information. Total number of fault segments : 28

Fault segment	Fault rupture time (second)	Epicenter		Focal depth (km)	Fault length (km)	Fault width (km)	Strike (degree)	Dip (degree)	Slip (degree)	Dislocation (meter)	Domain Origin	
		Lat	Lon								Lat	Lon
1	0.0	179.6930	-37.80790	3.970603	100	50	212.4	4.0	90	5.6	170.0	-40.0
2	0.0	180.2999	-37.05250	4.903464	100	50	212.3	4.602309	90	5.6	170.0	-40.0
3	0.0	180.8188	-36.26240	5.815893	100	50	202.9	5.210596	90	5.6	170.0	-40.0
4	0.0	179.2142	-37.56781	7.458427	100	50	212.4	6.0	90	5.6	170.0	-40.0
5	0.0	179.8257	-36.81326	8.915419	100	50	212.3	8.710391	90	5.6	170.0	-40.0
6	0.0	180.3078	-36.08834	10.35673	100	50	202.9	11.44768	90	5.6	170.0	-40.0
7	0.0	181.2725	-35.44100	6.691522	100	50	205.0	5.794348	90	5.6	170.0	-40.0
8	0.0	181.6950	-34.61180	7.310587	100	50	200.0	6.0	90	5.6	170.0	-40.0
9	0.0	182.0470	-33.75910	7.731237	100	50	197.5	6.0	90	5.6	170.0	-40.0
10	0.0	182.3678	-32.89860	8.0	100	50	196.9	6.582	90	5.6	170.0	-40.0
11	0.0	182.6807	-32.03810	8.0	100	50	197.0	8.122018	90	5.6	170.0	-40.0
12	0.0	183.0170	-31.18540	8.0	100	50	199.9	9.666493	90	5.6	170.0	-40.0
13	0.0	180.7754	-35.25214	11.73943	100	50	205.0	14.07456	90	5.6	170.0	-40.0
14	0.0	181.1850	-34.45902	12.53701	100	50	200.0	14.68941	90	5.6	170.0	-40.0
15	0.0	181.5346	-33.62477	12.95766	100	50	197.5	14.26876	90	5.6	170.0	-40.0
16	0.0	181.859	-32.76889	13.73125	100	50	196.9	14.388	90	5.6	170.0	-40.0
17	0.0	182.1791	-31.90809	15.06408	100	50	197.0	15.41468	90	5.6	170.0	-40.0
18	0.0	182.5303	-31.03468	16.39565	100	50	199.9	16.44433	90	5.6	170.0	-40.0
19	0.0	183.4003	-30.34830	-30.34830	100	50	202.8	11.21627	90	5.6	170.0	-40.0
20	0.0	183.7524	-29.50350	8.0	100	50	196.7	9.550721	90	5.6	170.0	-40.0
21	0.0	184.0184	-28.63510	7.541041	100	50	193.2	11.06531	90	5.6	170.0	-40.0
22	0.0	184.2452	-27.75890	7.029047	100	50	192.4	13.36929	90	5.6	170.0	-40.0
23	0.0	184.4564	-26.88280	6.518828	100	50	191.7	15.66527	90	5.6	170.0	-40.0
24	0.0	182.9296	-30.17756	17.72565	100	50	202.8	17.47752	90	5.6	170.0	-40.0
25	0.0	183.2649	-29.37622	16.29603	100	50	196.7	15.55072	90	5.6	170.0	-40.0

Fault segment	Fault rupture time	Epicenter		Focal depth (km)	Fault length (km)	Fault width (km)	Strike (degree)	Dip (degree)	Slip (degree)	Dislocation (meter)	Domain Origin	
		Lat	Lon								Lat	Lon
26	0.0	183.5294	-28.53444	17.13743	100	50	193.2	15.68844	90	5.6	170.0	-40.0
27	0.0	183.7629	-27.66506	18.59037	100	50	192.4	16.45643	90	5.6	170.0	-40.0
28	0.0	183.9816	-26.79510	20.01967	100	50	191.7	17.22176	90	5.6	170.0	-40.0

g. Kermadec ABC Mw = 9.1 earthquake (Scenario 6)

General Information
Total run time (second) : 86400.00
Time interval for output (second) : 1800.000
Time step size (second) : 2.313588
Total steps to run (steps) : 37345
Step interval for output (steps) : 778
Max. surface displacement output : ENABLED
Time history record output : ENABLED
Shoreline located at depth contour : 0.0000000E+00
Boundary condition : RADIATION (OPEN)

Initial Condition Information. Total number of fault segments : 28

Fault segment	Fault rupture time (second)	Epicenter		Focal depth (km)	Fault length (km)	Fault width (km)	Strike (degree)	Dip (degree)	Slip (degree)	Dislocation (meter)	Domain Origin	
		Lat	Lon								Lat	Lon
1	0.0	179.6930	-37.80790	3.970603	100	50	212.4	4.0	90	8	170.0	-40.0
2	0.0	180.2999	-37.05250	4.903464	100	50	212.3	4.602309	90	8	170.0	-40.0
3	0.0	180.8188	-36.26240	5.815893	100	50	202.9	5.210596	90	8	170.0	-40.0
4	0.0	179.2142	-37.56781	7.458427	100	50	212.4	6.0	90	8	170.0	-40.0
5	0.0	179.8257	-36.81326	8.915419	100	50	212.3	8.710391	90	8	170.0	-40.0
6	0.0	180.3078	-36.08834	10.35673	100	50	202.9	11.44768	90	8	170.0	-40.0
7	0.0	181.2725	-35.44100	6.691522	100	50	205.0	5.794348	90	8	170.0	-40.0
8	0.0	181.6950	-34.61180	7.310587	100	50	200.0	6.0	90	8	170.0	-40.0
9	0.0	182.0470	-33.75910	7.731237	100	50	197.5	6.0	90	8	170.0	-40.0
10	0.0	182.3678	-32.89860	8.0	100	50	196.9	6.582	90	8	170.0	-40.0
11	0.0	182.6807	-32.03810	8.0	100	50	197.0	8.122018	90	8	170.0	-40.0
12	0.0	183.0170	-31.18540	8.0	100	50	199.9	9.666493	90	8	170.0	-40.0
13	0.0	180.7754	-35.25214	11.73943	100	50	205.0	14.07456	90	8	170.0	-40.0
14	0.0	181.1850	-34.45902	12.53701	100	50	200.0	14.68941	90	8	170.0	-40.0
15	0.0	181.5346	-33.62477	12.95766	100	50	197.5	14.26876	90	8	170.0	-40.0
16	0.0	181.859	-32.76889	13.73125	100	50	196.9	14.388	90	8	170.0	-40.0
17	0.0	182.1791	-31.90809	15.06408	100	50	197.0	15.41468	90	8	170.0	-40.0
18	0.0	182.5303	-31.03468	16.39565	100	50	199.9	16.44433	90	8	170.0	-40.0
19	0.0	183.4003	-30.34830	-30.34830	100	50	202.8	11.21627	90	8	170.0	-40.0
20	0.0	183.7524	-29.50350	8.0	100	50	196.7	9.550721	90	8	170.0	-40.0
21	0.0	184.0184	-28.63510	7.541041	100	50	193.2	11.06531	90	8	170.0	-40.0
22	0.0	184.2452	-27.75890	7.029047	100	50	192.4	13.36929	90	8	170.0	-40.0
23	0.0	184.4564	-26.88280	6.518828	100	50	191.7	15.66527	90	8	170.0	-40.0
24	0.0	182.9296	-30.17756	17.72565	100	50	202.8	17.47752	90	8	170.0	-40.0
25	0.0	183.2649	-29.37622	16.29603	100	50	196.7	15.55072	90	8	170.0	-40.0

Fault segment	Fault rupture time	Epicenter		Focal depth (km)	Fault length (km)	Fault width (km)	Strike (degree)	Dip (degree)	Slip (degree)	Dislocation (meter)	Domain Origin	
		Lat	Lon								Lat	Lon
26	0.0	183.5294	-28.53444	17.13743	100	50	193.2	15.68844	90	8	170.0	-40.0
27	0.0	183.7629	-27.66506	18.59037	100	50	192.4	16.45643	90	8	170.0	-40.0
28	0.0	183.9816	-26.79510	20.01967	100	50	191.7	17.22176	90	8	170.0	-40.0

h. Kermadec ABC Mw = 9.2 earthquake (Scenario 6)

General Information
Total run time (second) : 86400.00
Time interval for output (second) : 1800.000
Time step size (second) : 2.313588
Total steps to run (steps) : 37345
Step interval for output (steps) : 778
Max. surface displacement output : ENABLED
Time history record output : ENABLED
Shoreline located at depth contour : 0.0000000E+00
Boundary condition : RADIATION (OPEN)

Initial Condition Information. Total number of fault segments : 28

Fault segment	Fault rupture time (second)	Epicenter		Focal depth (km)	Fault length (km)	Fault width (km)	Strike (degree)	Dip (degree)	Slip (degree)	Dislocation (meter)	Domain Origin	
		Lat	Lon								Lat	Lon
1	0.0	179.6930	-37.80790	3.970603	100	50	212.4	4.0	90	10	170.0	-40.0
2	0.0	180.2999	-37.05250	4.903464	100	50	212.3	4.602309	90	10	170.0	-40.0
3	0.0	180.8188	-36.26240	5.815893	100	50	202.9	5.210596	90	10	170.0	-40.0
4	0.0	179.2142	-37.56781	7.458427	100	50	212.4	6.0	90	10	170.0	-40.0
5	0.0	179.8257	-36.81326	8.915419	100	50	212.3	8.710391	90	10	170.0	-40.0
6	0.0	180.3078	-36.08834	10.35673	100	50	202.9	11.44768	90	10	170.0	-40.0
7	0.0	181.2725	-35.44100	6.691522	100	50	205.0	5.794348	90	10	170.0	-40.0
8	0.0	181.6950	-34.61180	7.310587	100	50	200.0	6.0	90	10	170.0	-40.0
9	0.0	182.0470	-33.75910	7.731237	100	50	197.5	6.0	90	10	170.0	-40.0
10	0.0	182.3678	-32.89860	8.0	100	50	196.9	6.582	90	10	170.0	-40.0
11	0.0	182.6807	-32.03810	8.0	100	50	197.0	8.122018	90	10	170.0	-40.0
12	0.0	183.0170	-31.18540	8.0	100	50	199.9	9.666493	90	10	170.0	-40.0
13	0.0	180.7754	-35.25214	11.73943	100	50	205.0	14.07456	90	10	170.0	-40.0
14	0.0	181.1850	-34.45902	12.53701	100	50	200.0	14.68941	90	10	170.0	-40.0
15	0.0	181.5346	-33.62477	12.95766	100	50	197.5	14.26876	90	10	170.0	-40.0
16	0.0	181.859	-32.76889	13.73125	100	50	196.9	14.388	90	10	170.0	-40.0
17	0.0	182.1791	-31.90809	15.06408	100	50	197.0	15.41468	90	10	170.0	-40.0
18	0.0	182.5303	-31.03468	16.39565	100	50	199.9	16.44433	90	10	170.0	-40.0
19	0.0	183.4003	-30.34830	-30.34830	100	50	202.8	11.21627	90	10	170.0	-40.0
20	0.0	183.7524	-29.50350	8.0	100	50	196.7	9.550721	90	10	170.0	-40.0
21	0.0	184.0184	-28.63510	7.541041	100	50	193.2	11.06531	90	10	170.0	-40.0
22	0.0	184.2452	-27.75890	7.029047	100	50	192.4	13.36929	90	10	170.0	-40.0
23	0.0	184.4564	-26.88280	6.518828	100	50	191.7	15.66527	90	10	170.0	-40.0
24	0.0	182.9296	-30.17756	17.72565	100	50	202.8	17.47752	90	10	170.0	-40.0
25	0.0	183.2649	-29.37622	16.29603	100	50	196.7	15.55072	90	10	170.0	-40.0

Fault segment	Fault rupture time	Epicenter		Focal depth (km)	Fault length (km)	Fault width (km)	Strike (degree)	Dip (degree)	Slip (degree)	Dislocation (meter)	Domain Origin	
		Lat	Lon								Lat	Lon
26	0.0	183.5294	-28.53444	17.13743	100	50	193.2	15.68844	90	10	170.0	-40.0
27	0.0	183.7629	-27.66506	18.59037	100	50	192.4	16.45643	90	10	170.0	-40.0
28	0.0	183.9816	-26.79510	20.01967	100	50	191.7	17.22176	90	10	170.0	-40.0

i. Kermadec ABC Mw = 9.3 earthquake (Scenario 6)

General Information
Total run time (second) : 86400.00
Time interval for output (second) : 1800.000
Time step size (second) : 2.313588
Total steps to run (steps) : 37345
Step interval for output (steps) : 778
Max. surface displacement output : ENABLED
Time history record output : ENABLED
Shoreline located at depth contour : 0.0000000E+00
Boundary condition : RADIATION (OPEN)

Initial Condition Information. Total number of fault segments : 28

Fault segment	Fault rupture time (second)	Epicenter		Focal depth (km)	Fault length (km)	Fault width (km)	Strike (degree)	Dip (degree)	Slip (degree)	Dislocation (meter)	Domain Origin	
		Lat	Lon								Lat	Lon
1	0.0	179.6930	-37.80790	3.970603	100	50	212.4	4.0	90	15	170.0	-40.0
2	0.0	180.2999	-37.05250	4.903464	100	50	212.3	4.602309	90	15	170.0	-40.0
3	0.0	180.8188	-36.26240	5.815893	100	50	202.9	5.210596	90	15	170.0	-40.0
4	0.0	179.2142	-37.56781	7.458427	100	50	212.4	6.0	90	15	170.0	-40.0
5	0.0	179.8257	-36.81326	8.915419	100	50	212.3	8.710391	90	15	170.0	-40.0
6	0.0	180.3078	-36.08834	10.35673	100	50	202.9	11.44768	90	15	170.0	-40.0
7	0.0	181.2725	-35.44100	6.691522	100	50	205.0	5.794348	90	15	170.0	-40.0
8	0.0	181.6950	-34.61180	7.310587	100	50	200.0	6.0	90	15	170.0	-40.0
9	0.0	182.0470	-33.75910	7.731237	100	50	197.5	6.0	90	15	170.0	-40.0
10	0.0	182.3678	-32.89860	8.0	100	50	196.9	6.582	90	15	170.0	-40.0
11	0.0	182.6807	-32.03810	8.0	100	50	197.0	8.122018	90	15	170.0	-40.0
12	0.0	183.0170	-31.18540	8.0	100	50	199.9	9.666493	90	15	170.0	-40.0
13	0.0	180.7754	-35.25214	11.73943	100	50	205.0	14.07456	90	15	170.0	-40.0
14	0.0	181.1850	-34.45902	12.53701	100	50	200.0	14.68941	90	15	170.0	-40.0
15	0.0	181.5346	-33.62477	12.95766	100	50	197.5	14.26876	90	15	170.0	-40.0
16	0.0	181.859	-32.76889	13.73125	100	50	196.9	14.388	90	15	170.0	-40.0
17	0.0	182.1791	-31.90809	15.06408	100	50	197.0	15.41468	90	15	170.0	-40.0
18	0.0	182.5303	-31.03468	16.39565	100	50	199.9	16.44433	90	15	170.0	-40.0
19	0.0	183.4003	-30.34830	-30.34830	100	50	202.8	11.21627	90	15	170.0	-40.0
20	0.0	183.7524	-29.50350	8.0	100	50	196.7	9.550721	90	15	170.0	-40.0
21	0.0	184.0184	-28.63510	7.541041	100	50	193.2	11.06531	90	15	170.0	-40.0
22	0.0	184.2452	-27.75890	7.029047	100	50	192.4	13.36929	90	15	170.0	-40.0
23	0.0	184.4564	-26.88280	6.518828	100	50	191.7	15.66527	90	15	170.0	-40.0
24	0.0	182.9296	-30.17756	17.72565	100	50	202.8	17.47752	90	15	170.0	-40.0
25	0.0	183.2649	-29.37622	16.29603	100	50	196.7	15.55072	90	15	170.0	-40.0

Fault segment	Fault rupture time	Epicenter		Focal depth (km)	Fault length (km)	Fault width (km)	Strike (degree)	Dip (degree)	Slip (degree)	Dislocation (meter)	Domain Origin	
		Lat	Lon								Lat	Lon
26	0.0	183.5294	-28.53444	17.13743	100	50	193.2	15.68844	90	15	170.0	-40.0
27	0.0	183.7629	-27.66506	18.59037	100	50	192.4	16.45643	90	15	170.0	-40.0
28	0.0	183.9816	-26.79510	20.01967	100	50	191.7	17.22176	90	15	170.0	-40.0

j. Kermadec ABC Mw = 9.4 earthquake (Scenario 6)

General Information
Total run time (second) : 86400.00
Time interval for output (second) : 1800.000
Time step size (second) : 2.313588
Total steps to run (steps) : 37345
Step interval for output (steps) : 778
Max. surface displacement output : ENABLED
Time history record output : ENABLED
Shoreline located at depth contour : 0.0000000E+00
Boundary condition : RADIATION (OPEN)

Initial Condition Information. Total number of fault segments : 28

Fault segment	Fault rupture time (second)	Epicenter		Focal depth (km)	Fault length (km)	Fault width (km)	Strike (degree)	Dip (degree)	Slip (degree)	Dislocation (meter)	Domain Origin	
		Lat	Lon								Lat	Lon
1	0.0	179.6930	-37.80790	3.970603	100	50	212.4	4.0	90	22	170.0	-40.0
2	0.0	180.2999	-37.05250	4.903464	100	50	212.3	4.602309	90	22	170.0	-40.0
3	0.0	180.8188	-36.26240	5.815893	100	50	202.9	5.210596	90	22	170.0	-40.0
4	0.0	179.2142	-37.56781	7.458427	100	50	212.4	6.0	90	22	170.0	-40.0
5	0.0	179.8257	-36.81326	8.915419	100	50	212.3	8.710391	90	22	170.0	-40.0
6	0.0	180.3078	-36.08834	10.35673	100	50	202.9	11.44768	90	22	170.0	-40.0
7	0.0	181.2725	-35.44100	6.691522	100	50	205.0	5.794348	90	22	170.0	-40.0
8	0.0	181.6950	-34.61180	7.310587	100	50	200.0	6.0	90	22	170.0	-40.0
9	0.0	182.0470	-33.75910	7.731237	100	50	197.5	6.0	90	22	170.0	-40.0
10	0.0	182.3678	-32.89860	8.0	100	50	196.9	6.582	90	22	170.0	-40.0
11	0.0	182.6807	-32.03810	8.0	100	50	197.0	8.122018	90	22	170.0	-40.0
12	0.0	183.0170	-31.18540	8.0	100	50	199.9	9.666493	90	22	170.0	-40.0
13	0.0	180.7754	-35.25214	11.73943	100	50	205.0	14.07456	90	22	170.0	-40.0
14	0.0	181.1850	-34.45902	12.53701	100	50	200.0	14.68941	90	22	170.0	-40.0
15	0.0	181.5346	-33.62477	12.95766	100	50	197.5	14.26876	90	22	170.0	-40.0
16	0.0	181.859	-32.76889	13.73125	100	50	196.9	14.388	90	22	170.0	-40.0
17	0.0	182.1791	-31.90809	15.06408	100	50	197.0	15.41468	90	22	170.0	-40.0
18	0.0	182.5303	-31.03468	16.39565	100	50	199.9	16.44433	90	22	170.0	-40.0
19	0.0	183.4003	-30.34830	-30.34830	100	50	202.8	11.21627	90	22	170.0	-40.0
20	0.0	183.7524	-29.50350	8.0	100	50	196.7	9.550721	90	22	170.0	-40.0
21	0.0	184.0184	-28.63510	7.541041	100	50	193.2	11.06531	90	22	170.0	-40.0
22	0.0	184.2452	-27.75890	7.029047	100	50	192.4	13.36929	90	22	170.0	-40.0
23	0.0	184.4564	-26.88280	6.518828	100	50	191.7	15.66527	90	22	170.0	-40.0
24	0.0	182.9296	-30.17756	17.72565	100	50	202.8	17.47752	90	22	170.0	-40.0
25	0.0	183.2649	-29.37622	16.29603	100	50	196.7	15.55072	90	22	170.0	-40.0

Fault segment	Fault rupture time	Epicenter		Focal depth (km)	Fault length (km)	Fault width (km)	Strike (degree)	Dip (degree)	Slip (degree)	Dislocation (meter)	Domain Origin	
		Lat	Lon								Lat	Lon
26	0.0	183.5294	-28.53444	17.13743	100	50	193.2	15.68844	90	22	170.0	-40.0
27	0.0	183.7629	-27.66506	18.59037	100	50	192.4	16.45643	90	22	170.0	-40.0
28	0.0	183.9816	-26.79510	20.01967	100	50	191.7	17.22176	90	22	170.0	-40.0

k. Kermadec ABC Mw = 9.5 earthquake (Scenario 6)

General Information
Total run time (second) : 86400.00
Time interval for output (second) : 1800.000
Time step size (second) : 2.313588
Total steps to run (steps) : 37345
Step interval for output (steps) : 778
Max. surface displacement output : ENABLED
Time history record output : ENABLED
Shoreline located at depth contour : 0.0000000E+00
Boundary condition : RADIATION (OPEN)

Initial Condition Information. Total number of fault segments : 28

Fault segment	Fault rupture time (second)	Epicenter		Focal depth (km)	Fault length (km)	Fault width (km)	Strike (degree)	Dip (degree)	Slip (degree)	Dislocation (meter)	Domain Origin	
		Lat	Lon								Lat	Lon
1	0.0	179.6930	-37.80790	3.970603	100	50	212.4	4.0	90	30	170.0	-40.0
2	0.0	180.2999	-37.05250	4.903464	100	50	212.3	4.602309	90	30	170.0	-40.0
3	0.0	180.8188	-36.26240	5.815893	100	50	202.9	5.210596	90	30	170.0	-40.0
4	0.0	179.2142	-37.56781	7.458427	100	50	212.4	6.0	90	30	170.0	-40.0
5	0.0	179.8257	-36.81326	8.915419	100	50	212.3	8.710391	90	30	170.0	-40.0
6	0.0	180.3078	-36.08834	10.35673	100	50	202.9	11.44768	90	30	170.0	-40.0
7	0.0	181.2725	-35.44100	6.691522	100	50	205.0	5.794348	90	30	170.0	-40.0
8	0.0	181.6950	-34.61180	7.310587	100	50	200.0	6.0	90	30	170.0	-40.0
9	0.0	182.0470	-33.75910	7.731237	100	50	197.5	6.0	90	30	170.0	-40.0
10	0.0	182.3678	-32.89860	8.0	100	50	196.9	6.582	90	30	170.0	-40.0
11	0.0	182.6807	-32.03810	8.0	100	50	197.0	8.122018	90	30	170.0	-40.0
12	0.0	183.0170	-31.18540	8.0	100	50	199.9	9.666493	90	30	170.0	-40.0
13	0.0	180.7754	-35.25214	11.73943	100	50	205.0	14.07456	90	30	170.0	-40.0
14	0.0	181.1850	-34.45902	12.53701	100	50	200.0	14.68941	90	30	170.0	-40.0
15	0.0	181.5346	-33.62477	12.95766	100	50	197.5	14.26876	90	30	170.0	-40.0
16	0.0	181.859	-32.76889	13.73125	100	50	196.9	14.388	90	30	170.0	-40.0
17	0.0	182.1791	-31.90809	15.06408	100	50	197.0	15.41468	90	30	170.0	-40.0
18	0.0	182.5303	-31.03468	16.39565	100	50	199.9	16.44433	90	30	170.0	-40.0
19	0.0	183.4003	-30.34830	-30.34830	100	50	202.8	11.21627	90	30	170.0	-40.0
20	0.0	183.7524	-29.50350	8.0	100	50	196.7	9.550721	90	30	170.0	-40.0
21	0.0	184.0184	-28.63510	7.541041	100	50	193.2	11.06531	90	30	170.0	-40.0
22	0.0	184.2452	-27.75890	7.029047	100	50	192.4	13.36929	90	30	170.0	-40.0
23	0.0	184.4564	-26.88280	6.518828	100	50	191.7	15.66527	90	30	170.0	-40.0
24	0.0	182.9296	-30.17756	17.72565	100	50	202.8	17.47752	90	30	170.0	-40.0
25	0.0	183.2649	-29.37622	16.29603	100	50	196.7	15.55072	90	30	170.0	-40.0

Fault segment	Fault rupture time	Epicenter		Focal depth (km)	Fault length (km)	Fault width (km)	Strike (degree)	Dip (degree)	Slip (degree)	Dislocation (meter)	Domain Origin	
		Lat	Lon								Lat	Lon
26	0.0	183.5294	-28.53444	17.13743	100	50	193.2	15.68844	90	30	170.0	-40.0
27	0.0	183.7629	-27.66506	18.59037	100	50	192.4	16.45643	90	30	170.0	-40.0
28	0.0	183.9816	-26.79510	20.01967	100	50	191.7	17.22176	90	30	170.0	-40.0

I. Kermadec A Mw = 8.5 earthquake (Scenario 1)

General Information
Total run time (second) : 86400.00
Time interval for output (second) : 1800.000
Time step size (second) : 2.313588
Total steps to run (steps) : 37345
Step interval for output (steps) : 778
Max. surface displacement output : ENABLED
Time history record output : ENABLED
Shoreline located at depth contour : 0.0000000E+00
Boundary condition : RADIATION (OPEN)

Initial Condition Information. Total number of fault segments : 6

Fault segment	Fault rupture time (second)	Epicenter		Focal depth (km)	Fault length (km)	Fault width (km)	Strike (degree)	Dip (degree)	Slip (degree)	Dislocation (meter)	Domain Origin	
		Lat	Lon								Lat	Lon
1	0.0	179.6930	-37.80790	3.970603	100	50	212.4	4.0	90	5	170.0	-40.0
2	0.0	180.2999	-37.05250	4.903464	100	50	212.3	4.602309	90	5	170.0	-40.0
3	0.0	180.8188	-36.26240	5.815893	100	50	202.9	5.210596	90	5	170.0	-40.0
4	0.0	179.2142	-37.56781	7.458427	100	50	212.4	6.0	90	5	170.0	-40.0
5	0.0	179.8257	-36.81326	8.915419	100	50	212.3	8.710391	90	5	170.0	-40.0
6	0.0	180.3078	-36.08834	10.35673	100	50	202.9	11.44768	90	5	170.0	-40.0

m. Kermadec B Mw = 8.9 earthquake (Scenario 2)

General Information
Total run time (second) : 86400.00
Time interval for output (second) : 1800.000
Time step size (second) : 2.313588
Total steps to run (steps) : 37345
Step interval for output (steps) : 778
Max. surface displacement output : ENABLED
Time history record output : ENABLED
Shoreline located at depth contour : 0.0000000E+00
Boundary condition : RADIATION (OPEN)

Initial Condition Information. Total number of fault segments : 12

Fault segment	Fault rupture time (second)	Epicenter		Focal depth (km)	Fault length (km)	Fault width (km)	Strike (degree)	Dip (degree)	Slip (degree)	Dislocation (meter)	Domain Origin	
		Lat	Lon								Lat	Lon
1	0.0	181.2725	-35.44100	6.691522	100	50	205.0	5.794348	90	10	170.0	-40.0
2	0.0	181.6950	-34.61180	7.310587	100	50	200.0	6.0	90	10	170.0	-40.0
3	0.0	182.0470	-33.75910	7.731237	100	50	197.5	6.0	90	10	170.0	-40.0
4	0.0	182.3678	-32.89860	8.0	100	50	196.9	6.582	90	10	170.0	-40.0
5	0.0	182.6807	-32.03810	8.0	100	50	197.0	8.122018	90	10	170.0	-40.0
6	0.0	183.0170	-31.18540	8.0	100	50	199.9	9.666493	90	10	170.0	-40.0
7	0.0	180.7754	-35.25214	11.73943	100	50	205.0	14.07456	90	10	170.0	-40.0
8	0.0	181.1850	-34.45902	12.53701	100	50	200.0	14.68941	90	10	170.0	-40.0
9	0.0	181.5346	-33.62477	12.95766	100	50	197.5	14.26876	90	10	170.0	-40.0
10	0.0	181.859	-32.76889	13.73125	100	50	196.9	14.388	90	10	170.0	-40.0
11	0.0	182.1791	-31.90809	15.06408	100	50	197.0	15.41468	90	10	170.0	-40.0
12	0.0	182.5303	-31.03468	16.39565	100	50	199.9	16.44433	90	10	170.0	-40.0

n. Kermadec C Mw = 8.8 earthquake (Scenario 3)

General Information
Total run time (second) : 86400.00
Time interval for output (second) : 1800.000
Time step size (second) : 2.313588
Total steps to run (steps) : 37345
Step interval for output (steps) : 778
Max. surface displacement output : ENABLED
Time history record output : ENABLED
Shoreline located at depth contour : 0.0000000E+00
Boundary condition : RADIATION (OPEN)

Initial Condition Information. Total number of fault segments : 10

Fault segment	Fault rupture time (second)	Epicenter		Focal depth (km)	Fault length (km)	Fault width (km)	Strike (degree)	Dip (degree)	Slip (degree)	Dislocation (meter)	Domain Origin	
		Lat	Lon								Lat	Lon
1	0.0	183.4003	-30.34830	-30.34830	100	50	202.8	11.21627	90	8	170.0	-40.0
2	0.0	183.7524	-29.50350	8.0	100	50	196.7	9.550721	90	8	170.0	-40.0
3	0.0	184.0184	-28.63510	7.541041	100	50	193.2	11.06531	90	8	170.0	-40.0
4	0.0	184.2452	-27.75890	7.029047	100	50	192.4	13.36929	90	8	170.0	-40.0
5	0.0	184.4564	-26.88280	6.518828	100	50	191.7	15.66527	90	8	170.0	-40.0
6	0.0	182.9296	-30.17756	17.72565	100	50	202.8	17.47752	90	8	170.0	-40.0
7	0.0	183.2649	-29.37622	16.29603	100	50	196.7	15.55072	90	8	170.0	-40.0
8	0.0	183.5294	-28.53444	17.13743	100	50	193.2	15.68844	90	8	170.0	-40.0
9	0.0	183.7629	-27.66506	18.59037	100	50	192.4	16.45643	90	8	170.0	-40.0
10	0.0	183.9816	-26.79510	20.01967	100	50	191.7	17.22176	90	8	170.0	-40.0

o. Kermadec AB Mw9.2 earthquake (Scenario 4)

General Information
Total run time (second) : 86400.00
Time interval for output (second) : 1800.000
Time step size (second) : 2.313588
Total steps to run (steps) : 37345
Step interval for output (steps) : 778
Max. surface displacement output : ENABLED
Time history record output : ENABLED
Shoreline located at depth contour : 0.0000000E+00
Boundary condition : RADIATION (OPEN)

Initial Condition Information. Total number of fault segments : 18

Fault segment	Fault rupture time (second)	Epicenter		Focal depth (km)	Fault length (km)	Fault width (km)	Strike (degree)	Dip (degree)	Slip (degree)	Dislocation (meter)	Domain Origin	
		Lat	Lon								Lat	Lon
1	0.0	179.6930	-37.80790	3.970603	100	50	212.4	4.0	90	22	170.0	-40.0
2	0.0	180.2999	-37.05250	4.903464	100	50	212.3	4.602309	90	22	170.0	-40.0
3	0.0	180.8188	-36.26240	5.815893	100	50	202.9	5.210596	90	22	170.0	-40.0
4	0.0	179.2142	-37.56781	7.458427	100	50	212.4	6.0	90	22	170.0	-40.0
5	0.0	179.8257	-36.81326	8.915419	100	50	212.3	8.710391	90	22	170.0	-40.0
6	0.0	180.3078	-36.08834	10.35673	100	50	202.9	11.44768	90	22	170.0	-40.0
7	0.0	181.2725	-35.44100	6.691522	100	50	205.0	5.794348	90	22	170.0	-40.0
8	0.0	181.6950	-34.61180	7.310587	100	50	200.0	6.0	90	22	170.0	-40.0
9	0.0	182.0470	-33.75910	7.731237	100	50	197.5	6.0	90	22	170.0	-40.0
10	0.0	182.3678	-32.89860	8.0	100	50	196.9	6.582	90	22	170.0	-40.0
11	0.0	182.6807	-32.03810	8.0	100	50	197.0	8.122018	90	22	170.0	-40.0
12	0.0	183.0170	-31.18540	8.0	100	50	199.9	9.666493	90	22	170.0	-40.0
13	0.0	180.7754	-35.25214	11.73943	100	50	205.0	14.07456	90	22	170.0	-40.0
14	0.0	181.1850	-34.45902	12.53701	100	50	200.0	14.68941	90	22	170.0	-40.0
15	0.0	181.5346	-33.62477	12.95766	100	50	197.5	14.26876	90	22	170.0	-40.0
16	0.0	181.859	-32.76889	13.73125	100	50	196.9	14.388	90	22	170.0	-40.0
17	0.0	182.1791	-31.90809	15.06408	100	50	197.0	15.41468	90	22	170.0	-40.0
18	0.0	182.5303	-31.03468	16.39565	100	50	199.9	16.44433	90	22	170.0	-40.0

p. Kermadec BC Mw = 9.3 earthquake (Scenario 5)

General Information
Total run time (second) : 86400.00
Time interval for output (second) : 1800.000
Time step size (second) : 2.313588
Total steps to run (steps) : 37345
Step interval for output (steps) : 778
Max. surface displacement output : ENABLED
Time history record output : ENABLED
Shoreline located at depth contour : 0.0000000E+00
Boundary condition : RADIATION (OPEN)

Initial Condition Information. Total number of fault segments : 22

Fault segment	Fault rupture time (second)	Epicenter		Focal depth (km)	Fault length (km)	Fault width (km)	Strike (degree)	Dip (degree)	Slip (degree)	Dislocation (meter)	Domain Origin	
		Lat	Lon								Lat	Lon
1	0.0	181.2725	-35.44100	6.691522	100	50	205.0	5.794348	90	22	170.0	-40.0
2	0.0	181.6950	-34.61180	7.310587	100	50	200.0	6.0	90	22	170.0	-40.0
3	0.0	182.0470	-33.75910	7.731237	100	50	197.5	6.0	90	22	170.0	-40.0
4	0.0	182.3678	-32.89860	8.0	100	50	196.9	6.582	90	22	170.0	-40.0
5	0.0	182.6807	-32.03810	8.0	100	50	197.0	8.122018	90	22	170.0	-40.0
6	0.0	183.0170	-31.18540	8.0	100	50	199.9	9.666493	90	22	170.0	-40.0
7	0.0	180.7754	-35.25214	11.73943	100	50	205.0	14.07456	90	22	170.0	-40.0
8	0.0	181.1850	-34.45902	12.53701	100	50	200.0	14.68941	90	22	170.0	-40.0
9	0.0	181.5346	-33.62477	12.95766	100	50	197.5	14.26876	90	22	170.0	-40.0
10	0.0	181.859	-32.76889	13.73125	100	50	196.9	14.388	90	22	170.0	-40.0
11	0.0	182.1791	-31.90809	15.06408	100	50	197.0	15.41468	90	22	170.0	-40.0
12	0.0	182.5303	-31.03468	16.39565	100	50	199.9	16.44433	90	22	170.0	-40.0
13	0.0	183.4003	-30.34830	-30.34830	100	50	202.8	11.21627	90	22	170.0	-40.0
14	0.0	183.7524	-29.50350	8.0	100	50	196.7	9.550721	90	22	170.0	-40.0
15	0.0	184.0184	-28.63510	7.541041	100	50	193.2	11.06531	90	22	170.0	-40.0
16	0.0	184.2452	-27.75890	7.029047	100	50	192.4	13.36929	90	22	170.0	-40.0
17	0.0	184.4564	-26.88280	6.518828	100	50	191.7	15.66527	90	22	170.0	-40.0
18	0.0	182.9296	-30.17756	17.72565	100	50	202.8	17.47752	90	22	170.0	-40.0
19	0.0	183.2649	-29.37622	16.29603	100	50	196.7	15.55072	90	22	170.0	-40.0
20	0.0	183.5294	-28.53444	17.13743	100	50	193.2	15.68844	90	22	170.0	-40.0
21	0.0	183.7629	-27.66506	18.59037	100	50	192.4	16.45643	90	22	170.0	-40.0
22	0.0	183.9816	-26.79510	20.01967	100	50	191.7	17.22176	90	22	170.0	-40.0

q. Kermadec Mw7.6 earthquake (Real event on 7 July 2011)

General Information
Total run time (second) : 86400.00
Time interval for output (second) : 1800.000
Time step size (second) : 2.313588
Total steps to run (steps) : 37345
Step interval for output (steps) : 778
Max. surface displacement output : ENABLED
Time history record output : ENABLED
Shoreline located at depth contour : 0.0000000E+00
Boundary condition : RADIATION (OPEN)

Initial Condition Information. Total number of fault segments : 22

Fault segment	Fault rupture time (second)	Epicenter		Focal depth (km)	Fault length (km)	Fault width (km)	Strike (degree)	Dip (degree)	Slip (degree)	Dislocation (meter)	Domain Origin	
		Lat	Lon								Lat	Lon
1	0.0	175.76	-29.18	20	118	22	171	33	-105	1.43	170.0	-40.0

Appendix 2: Tsunami spectra

a. Scenario 1

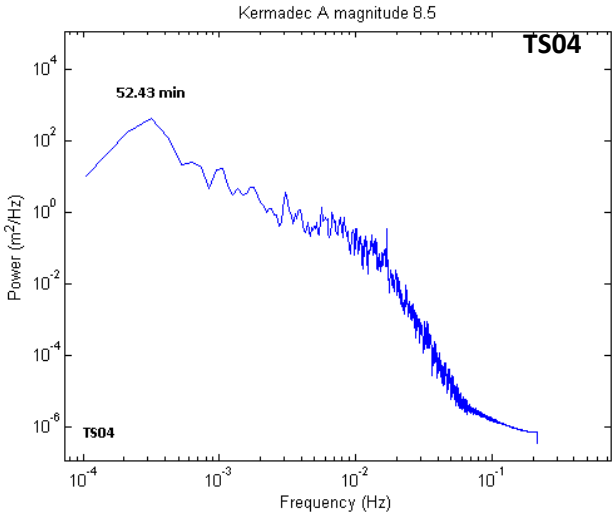

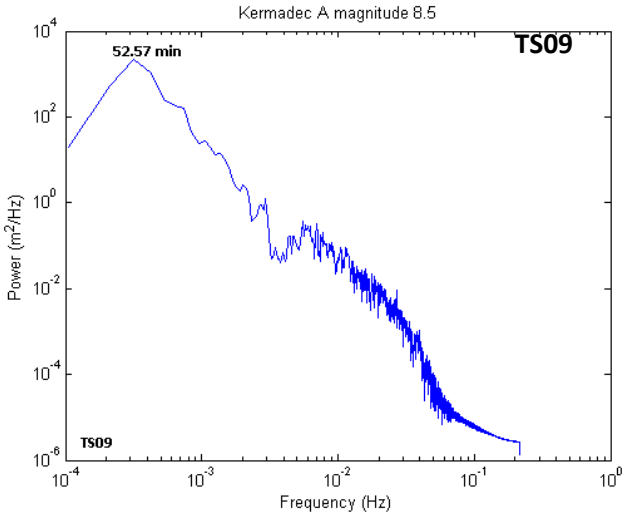

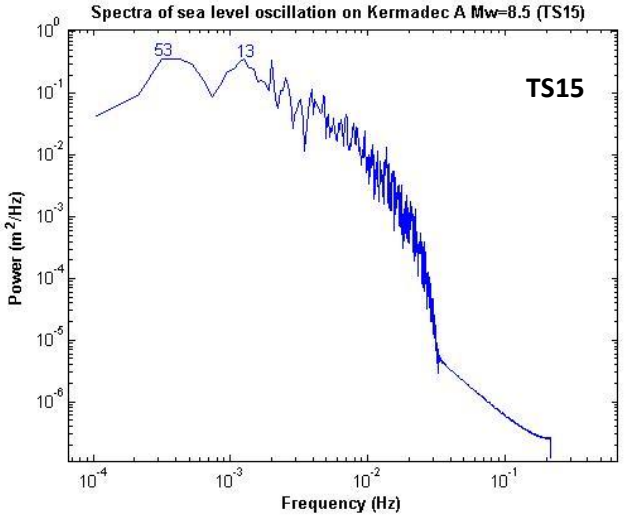

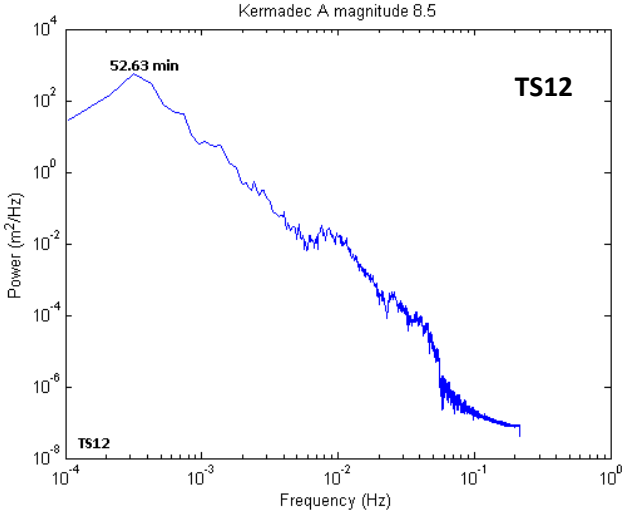

b. Scenario 2

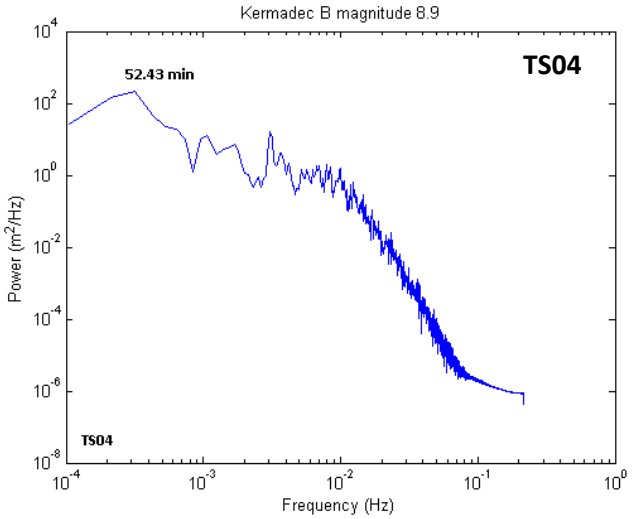
Kermadec B magnitude 8.9
52.43 min
TS04
TS04
Power (m²/Hz)
Frequency (Hz)

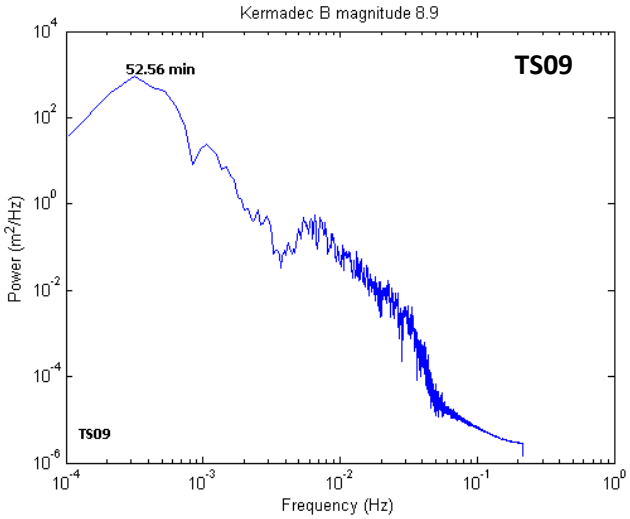
Kermadec B magnitude 8.9
52.56 min
TS09
TS09
Power (m²/Hz)
Frequency (Hz)

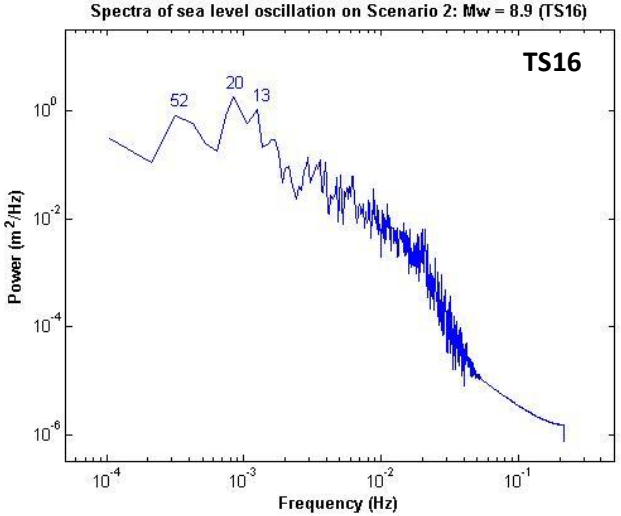
Spectra of sea level oscillation on Scenario 2: Mw = 8.9 (TS16)
TS16
52
20
13
Power (m²/Hz)
Frequency (Hz)

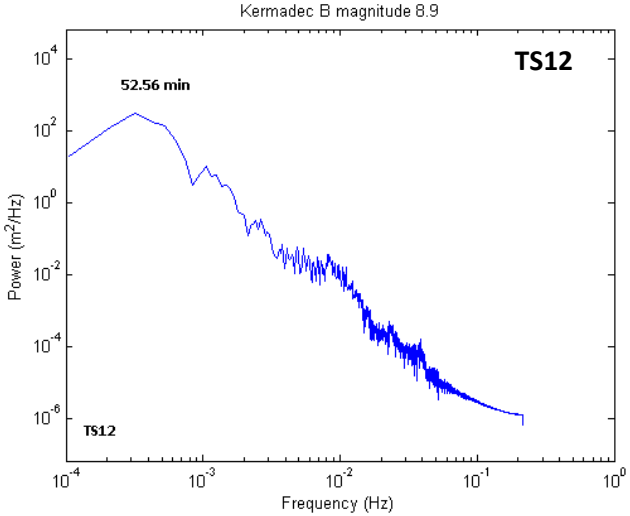
Kermadec B magnitude 8.9
52.56 min
TS12
TS12
Power (m²/Hz)
Frequency (Hz)

c. Scenario 3

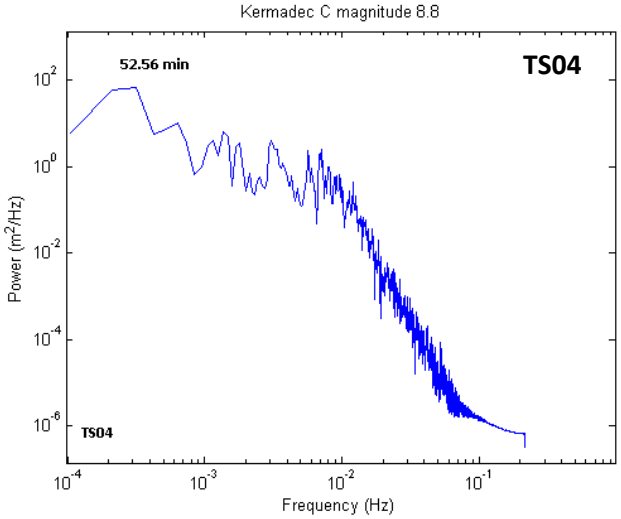
Kermadec C magnitude 8.8
52.56 min
TS04
TS04
Power (m²/Hz)
Frequency (Hz)

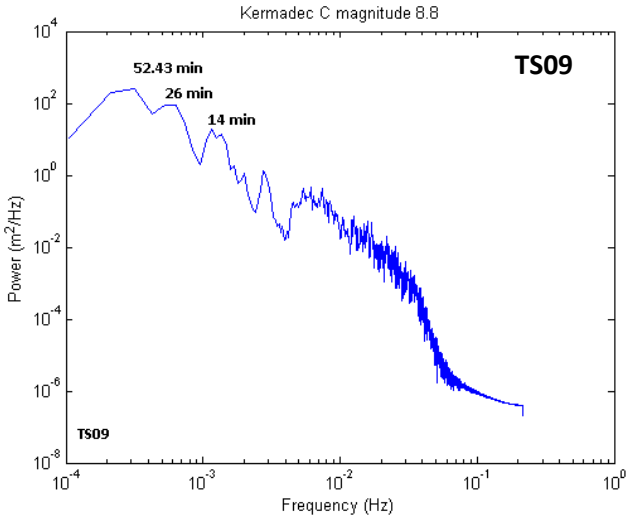
Kermadec C magnitude 8.8
52.43 min
26 min
14 min
TS09
TS09
Power (m²/Hz)
Frequency (Hz)

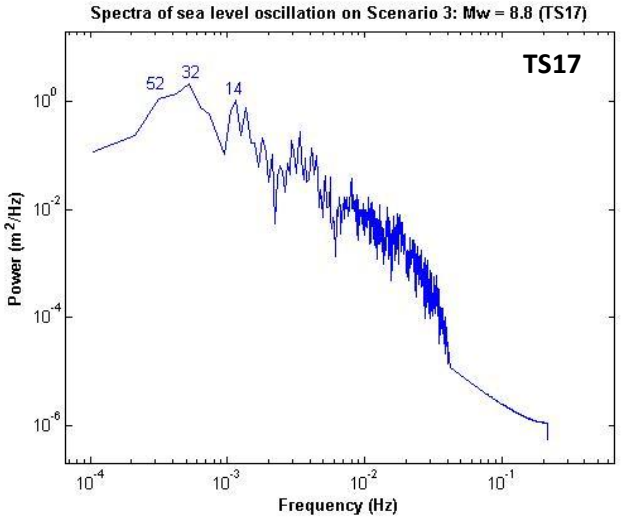
Spectra of sea level oscillation on Scenario 3: Mw = 8.8 (TS17)
52
32
14
TS17
Power (m²/Hz)
Frequency (Hz)

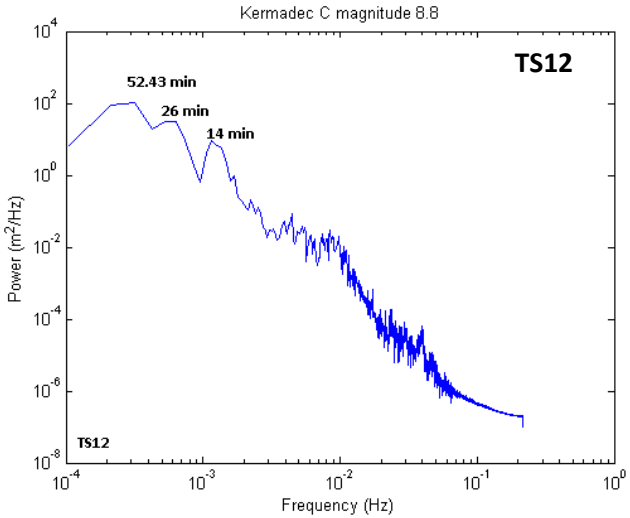
Kermadec C magnitude 8.8
52.43 min
26 min
14 min
TS12
TS12
Power (m²/Hz)
Frequency (Hz)

d. Scenario 4

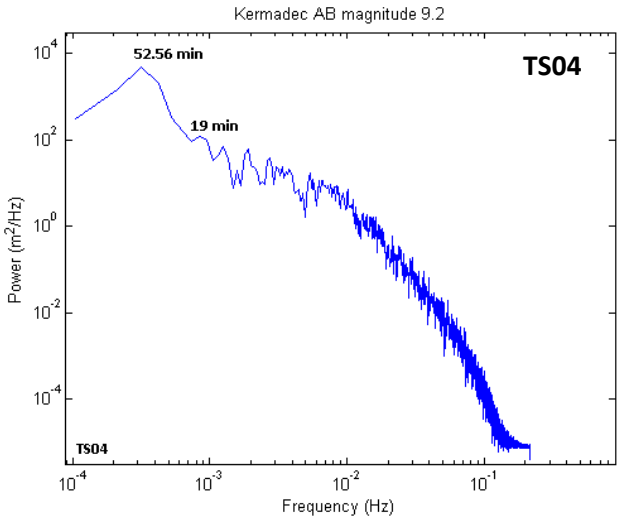
Kermadec AB magnitude 9.2
52.56 min
19 min
TS04
TS04
Power (m²/Hz)
Frequency (Hz)

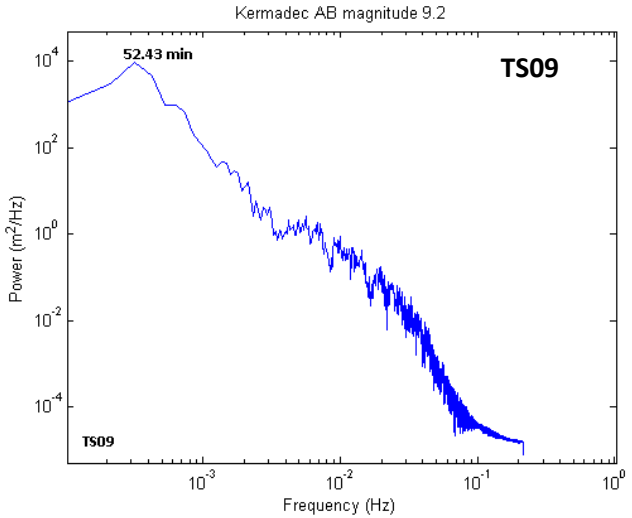
Kermadec AB magnitude 9.2
52.43 min
TS09
TS09
Power (m²/Hz)
Frequency (Hz)

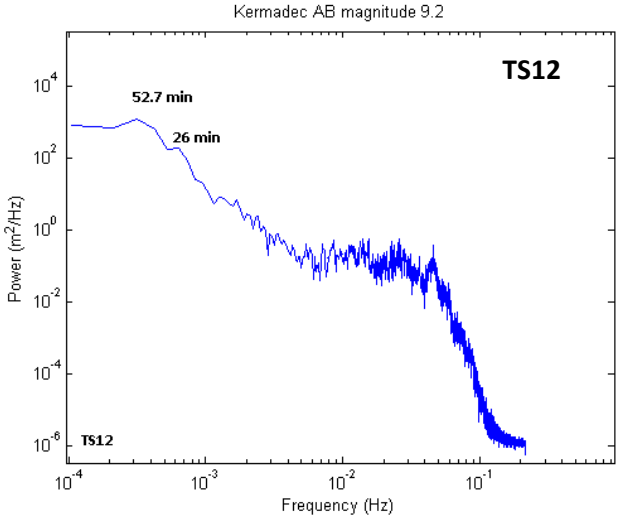
Kermadec AB magnitude 9.2
52.7 min
26 min
TS12
TS12
Power (m²/Hz)
Frequency (Hz)

e. Scenario 5

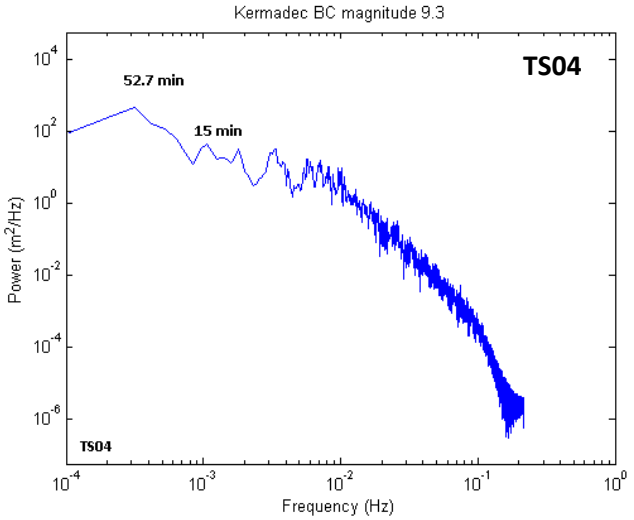
Kermadec BC magnitude 9.3
TS04
52.7 min
15 min
TS04
Power (m²/Hz)
Frequency (Hz)

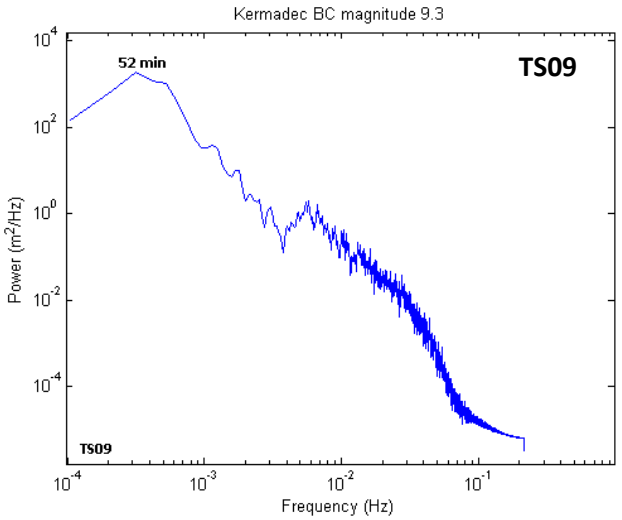
Kermadec BC magnitude 9.3
TS09
52 min
TS09
Power (m²/Hz)
Frequency (Hz)

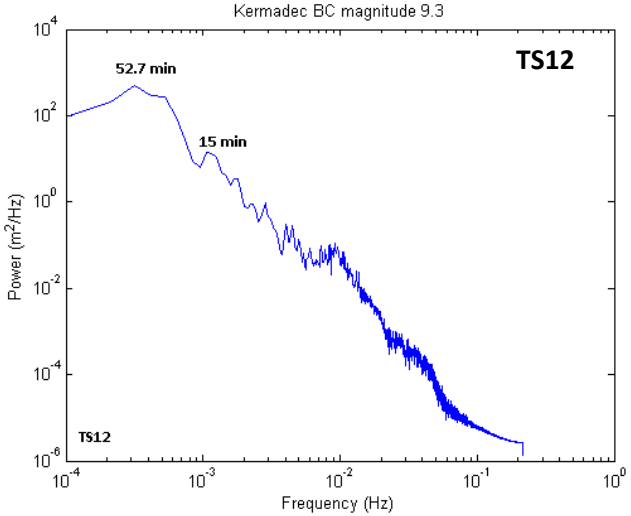
Kermadec BC magnitude 9.3
TS12
52.7 min
15 min
TS12
Power (m²/Hz)
Frequency (Hz)

f. Scenario 6: M_w = 8.5

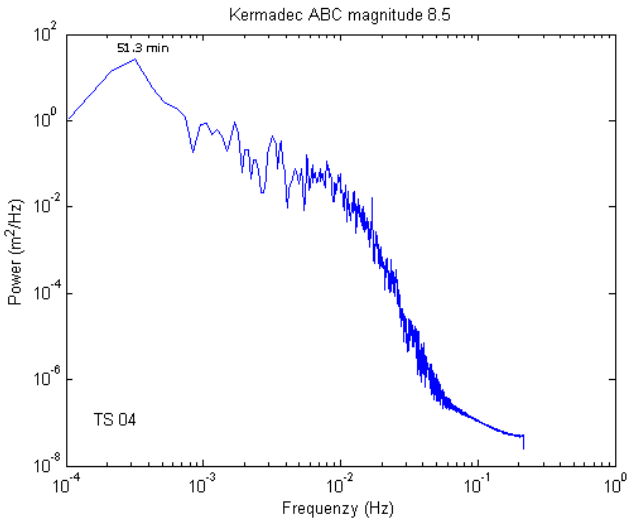

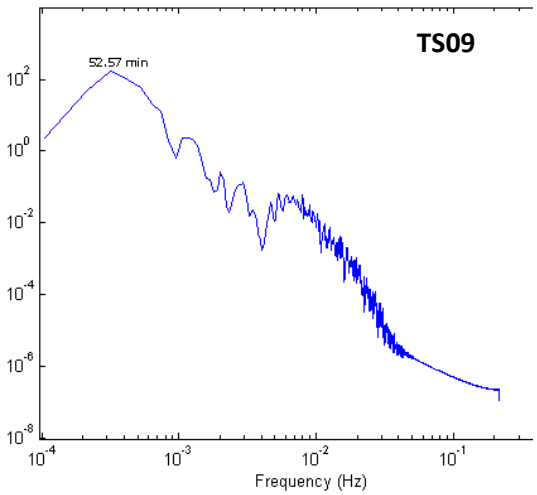

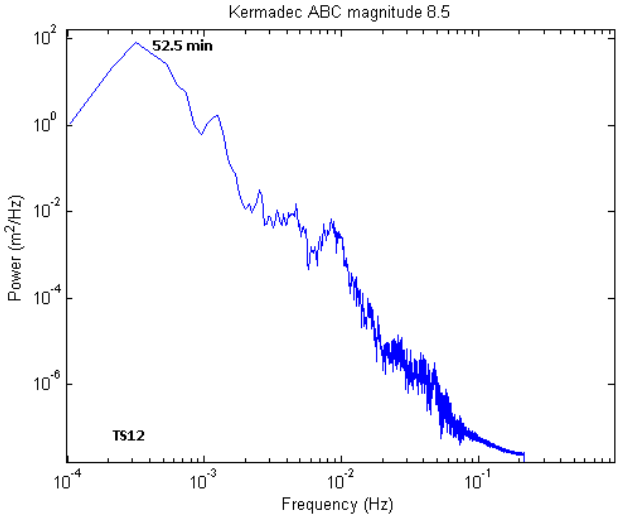

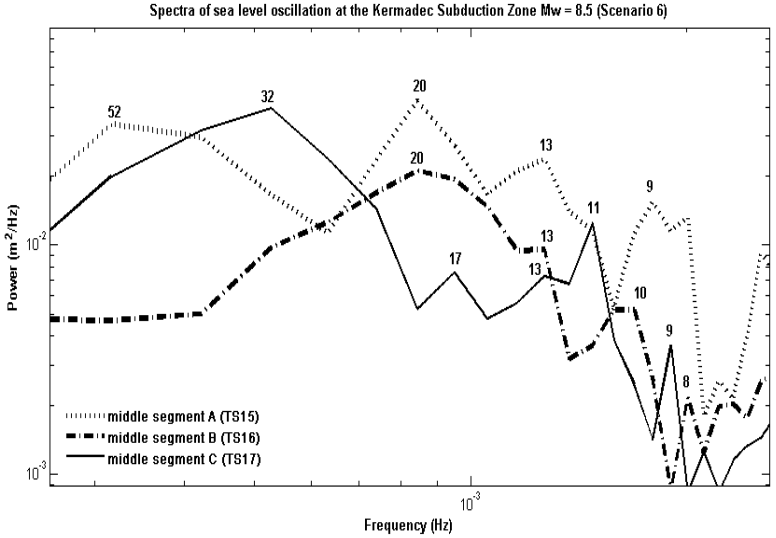

g. Scenario 6: M_w = 8.6

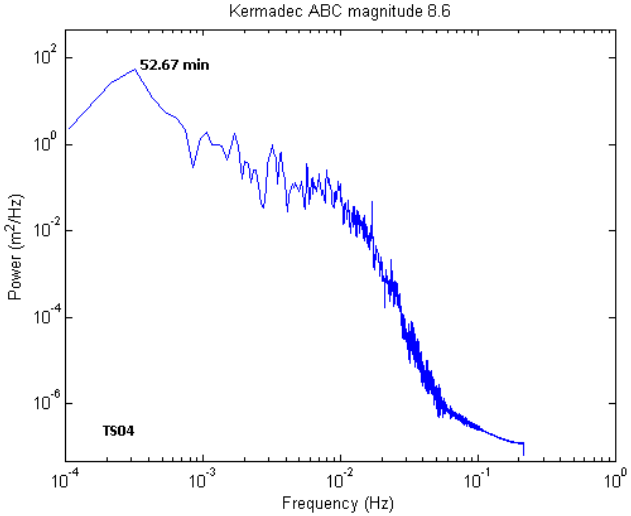

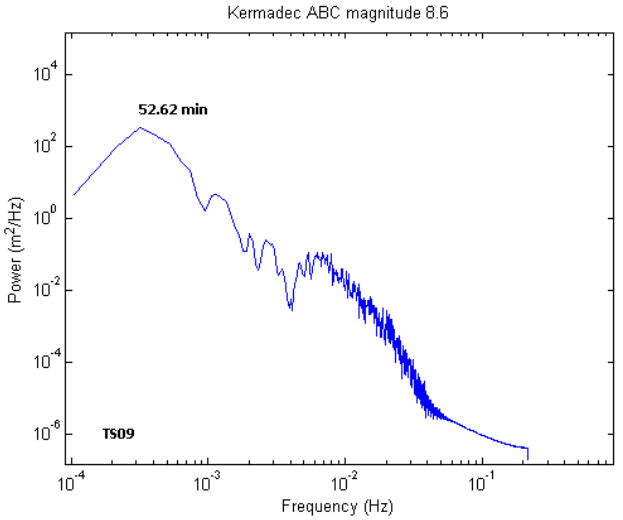

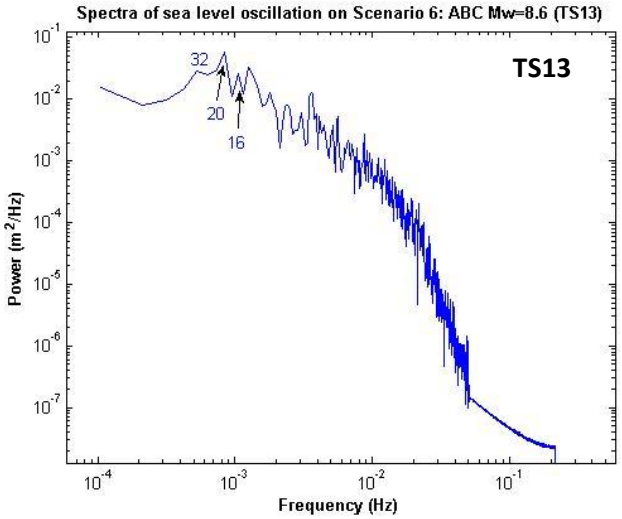

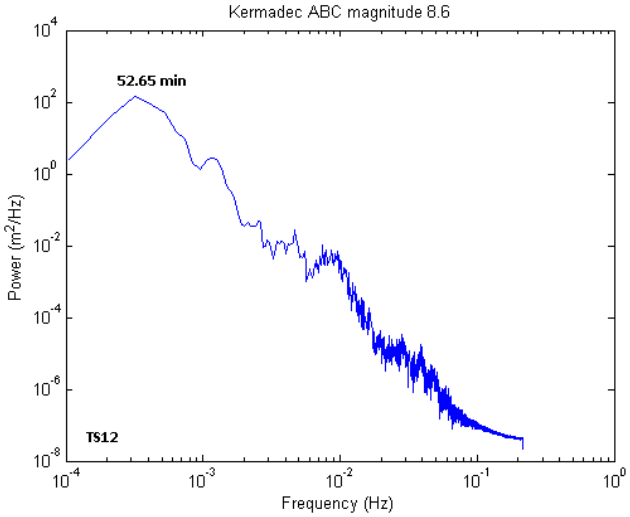

h. Scenario 6: M_w = 8.7

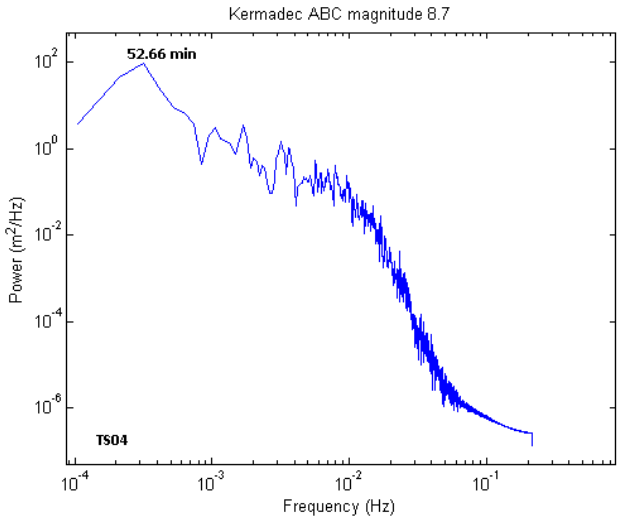

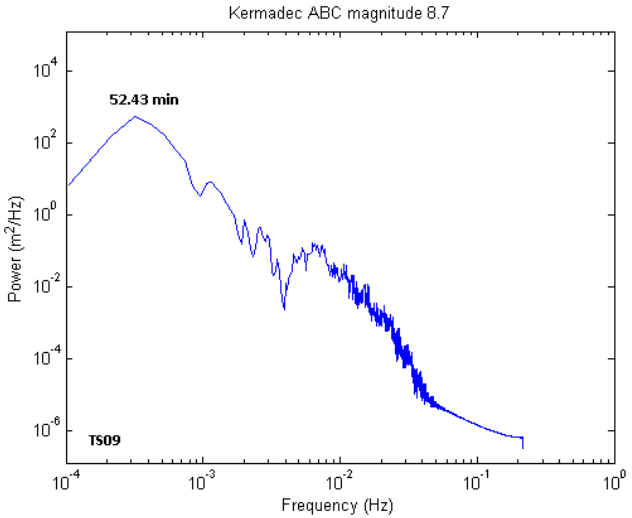

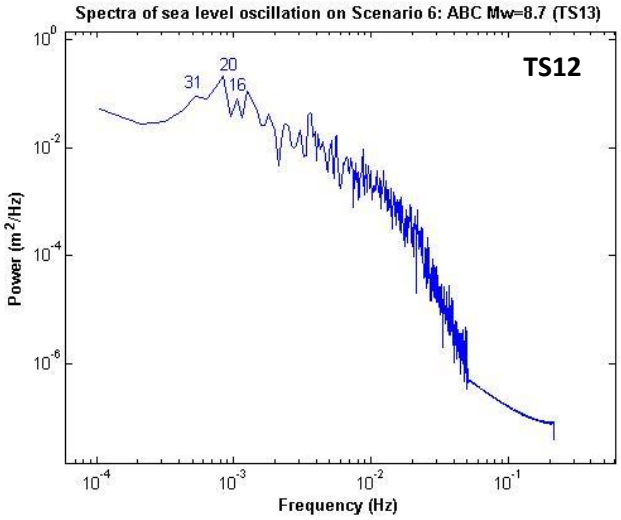

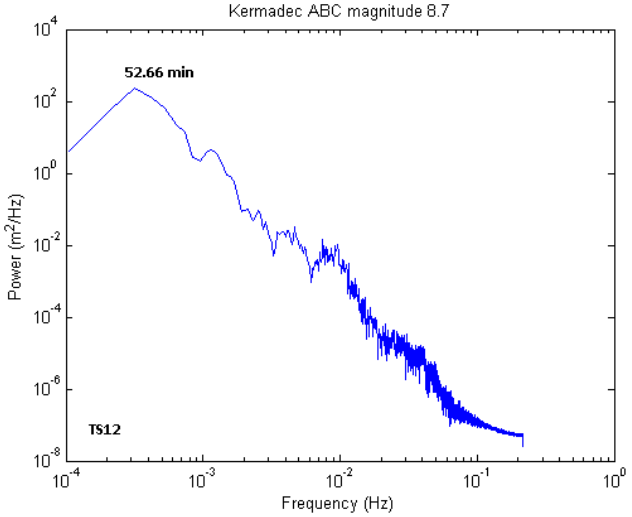

i. Scenario 6: M_w = 8.8

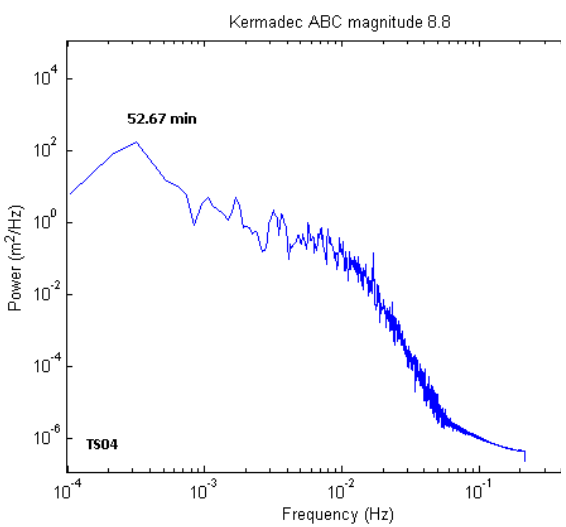

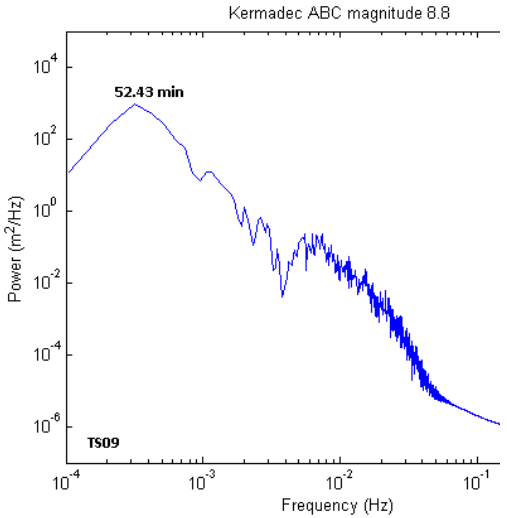

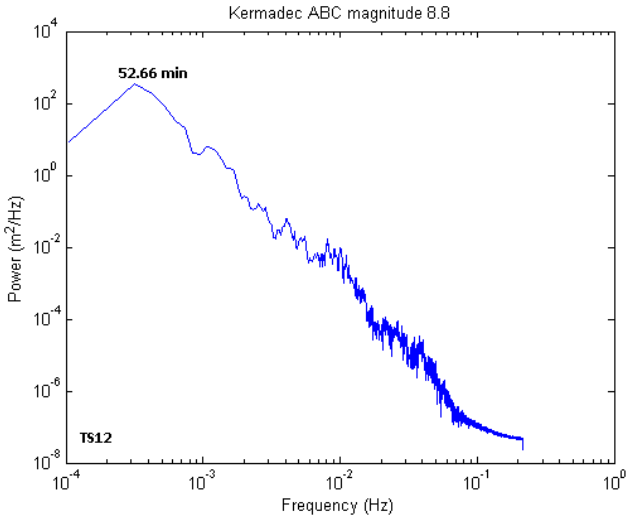

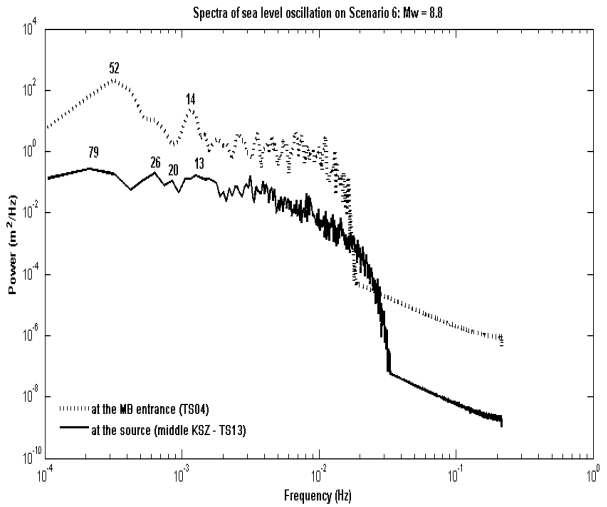

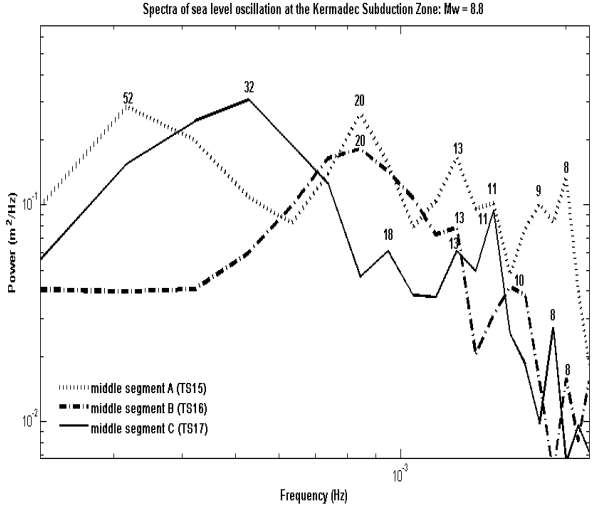

j. Scenario 6: M_w = 8.9

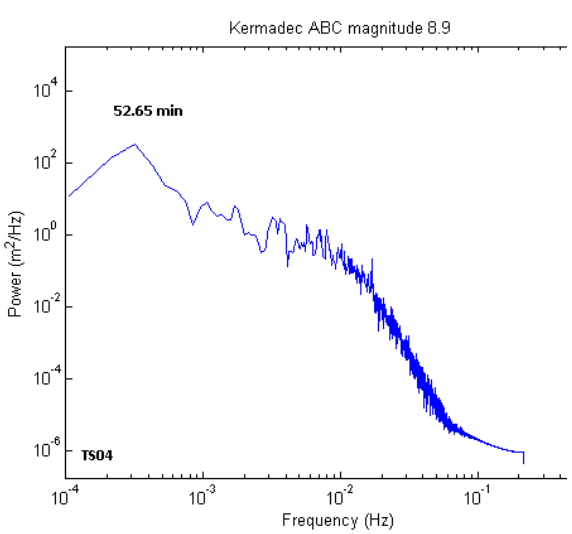

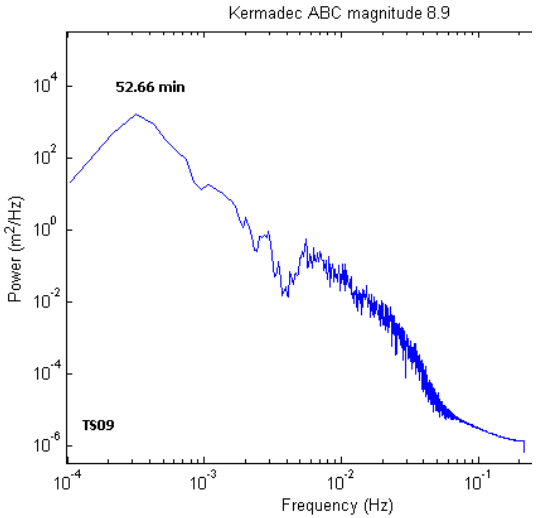

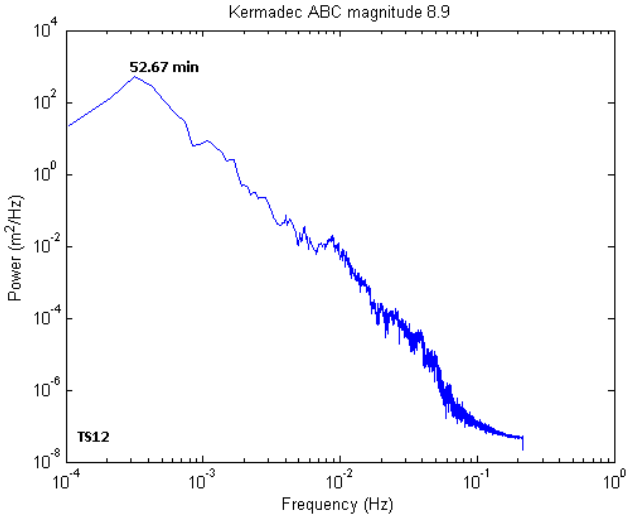

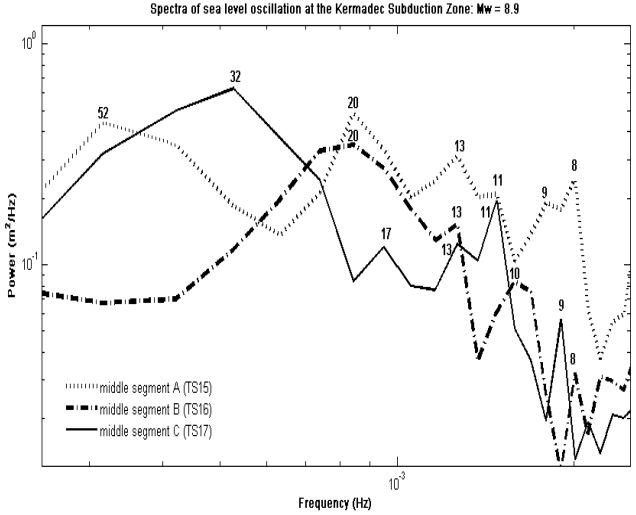

k. Scenario 6: M_w = 9.0

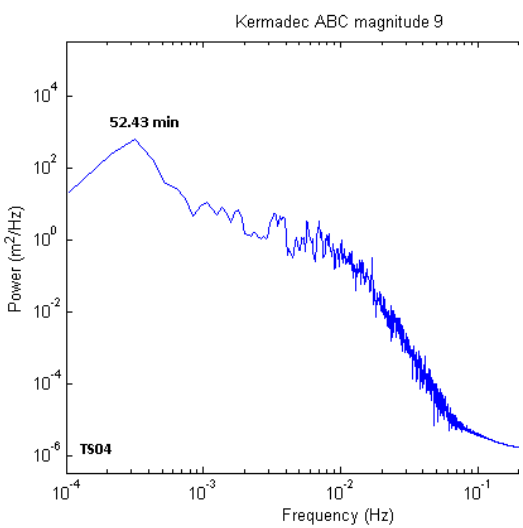

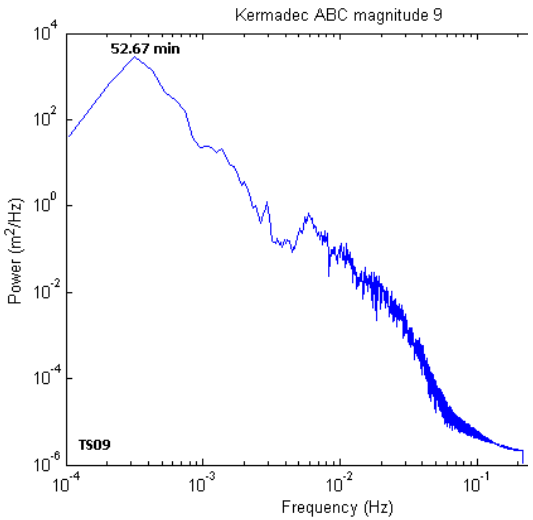

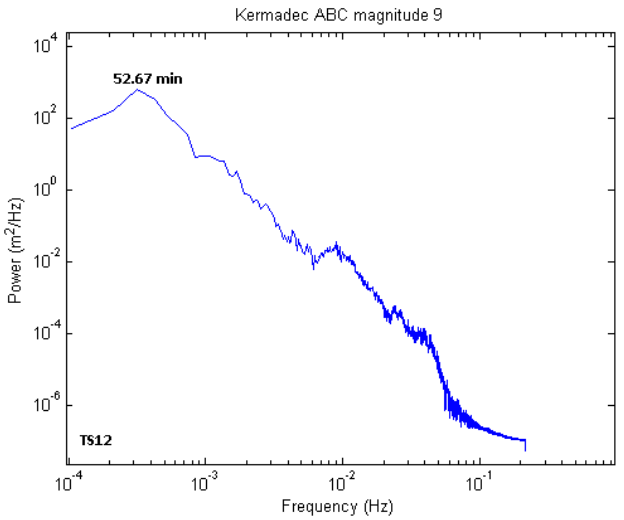

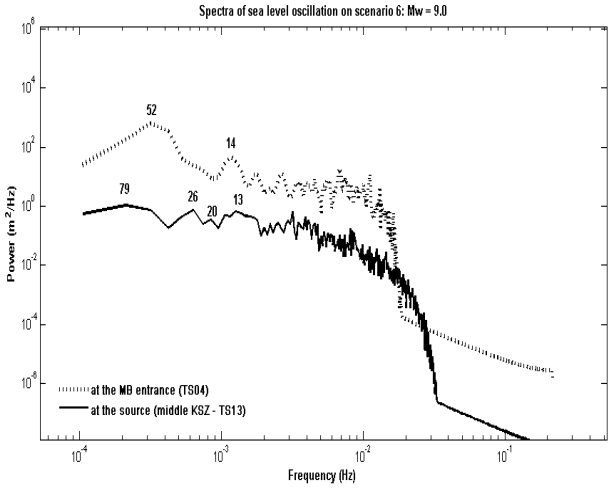

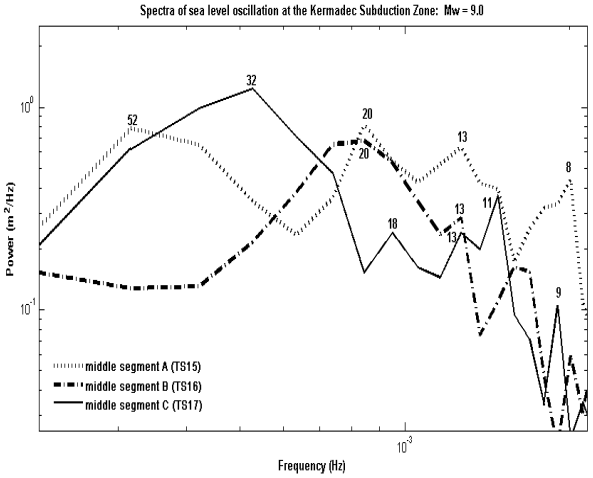

I. Scenario 6: M_w = 9.1

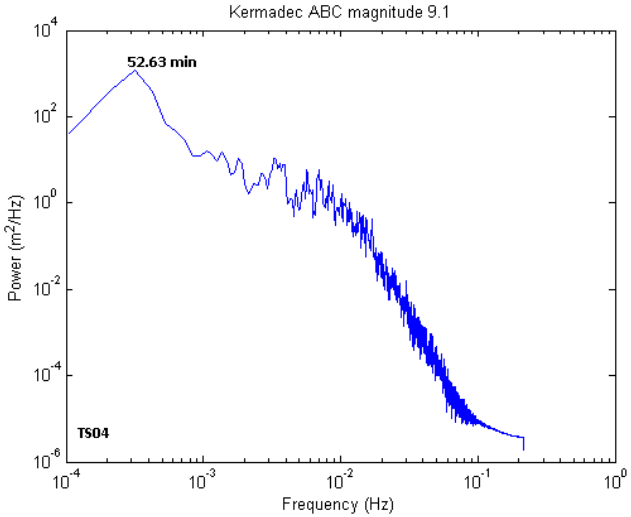

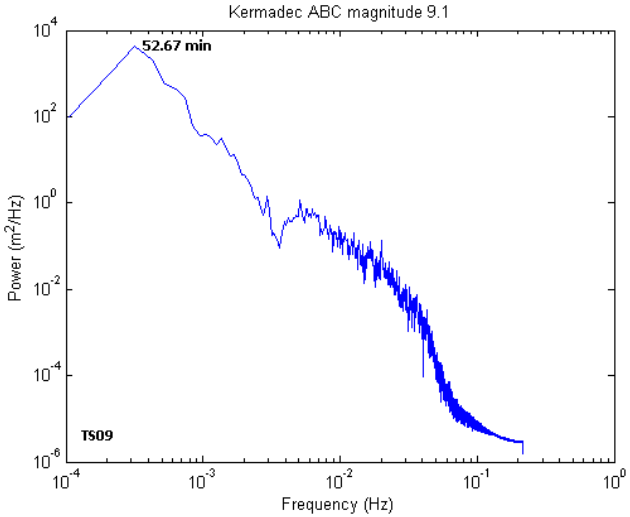

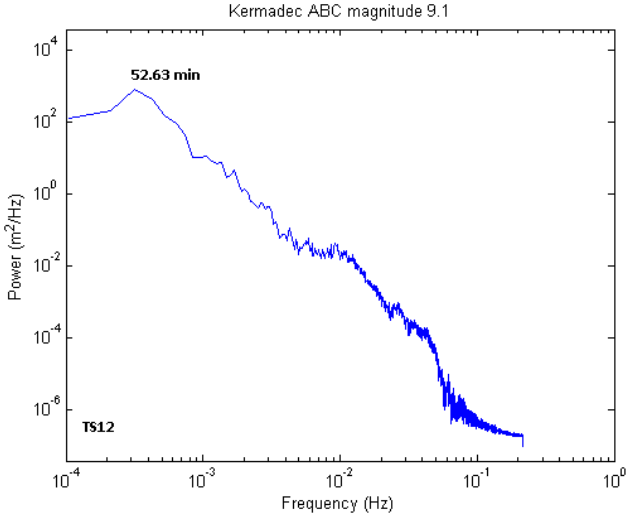

m. scenario 6: M_w = 9.2

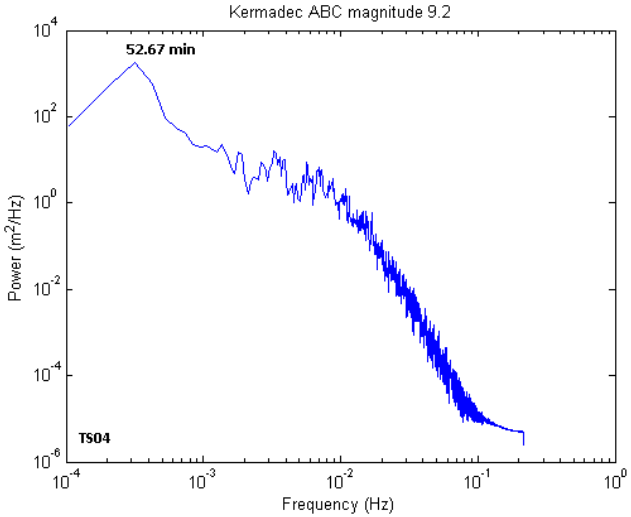

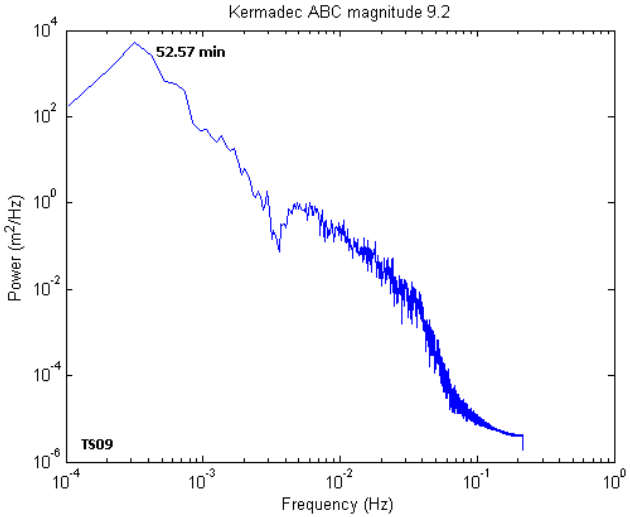

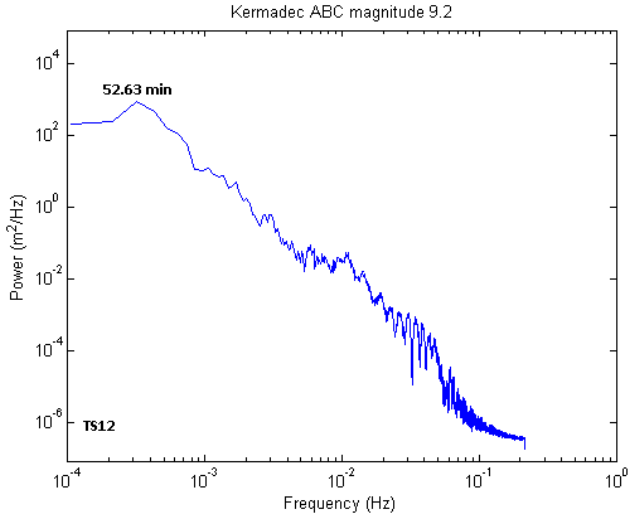

n. scenario 6: M_w = 9.3

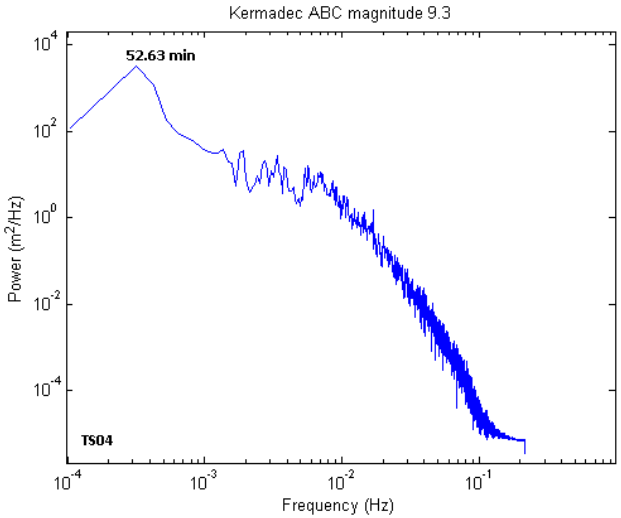

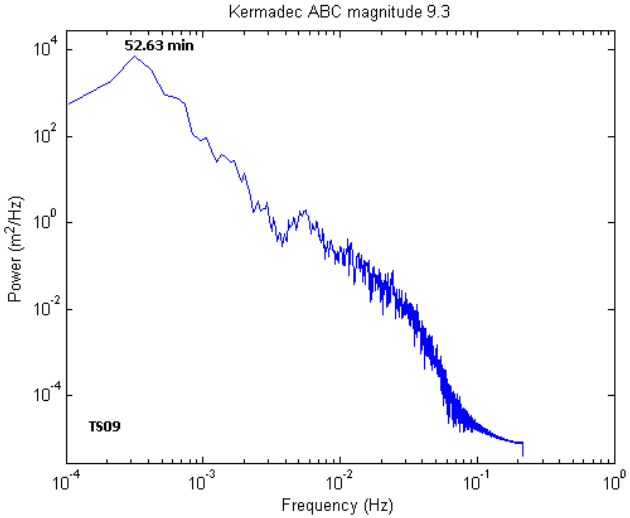

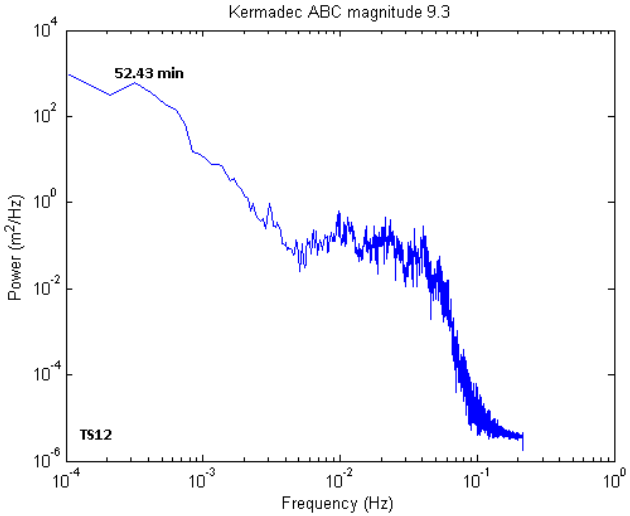

o. scenario 6: M_w = 9.4

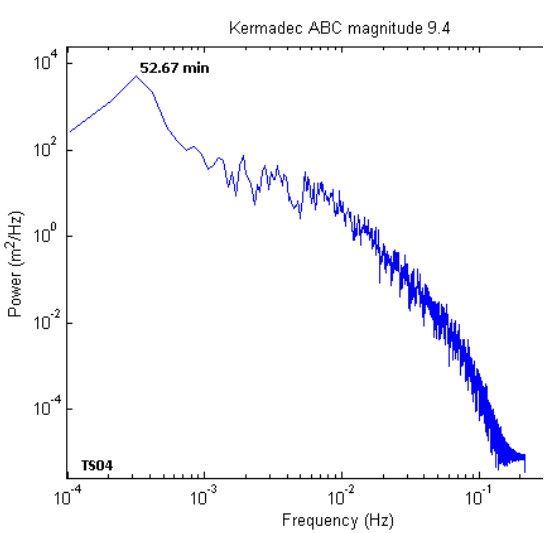

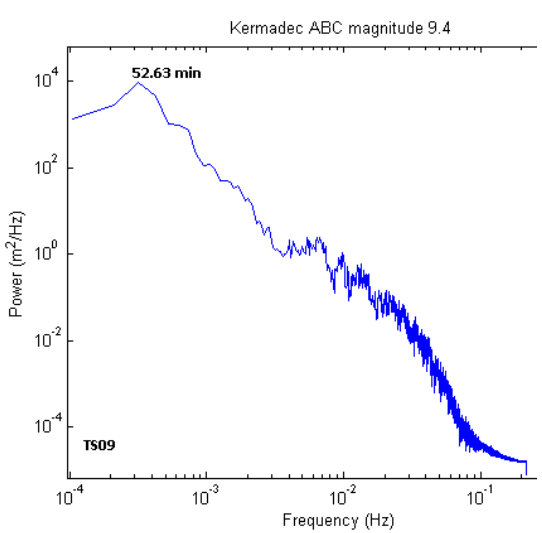

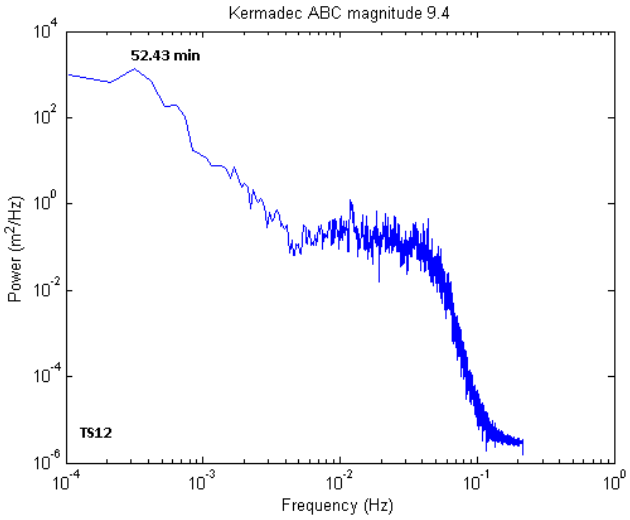

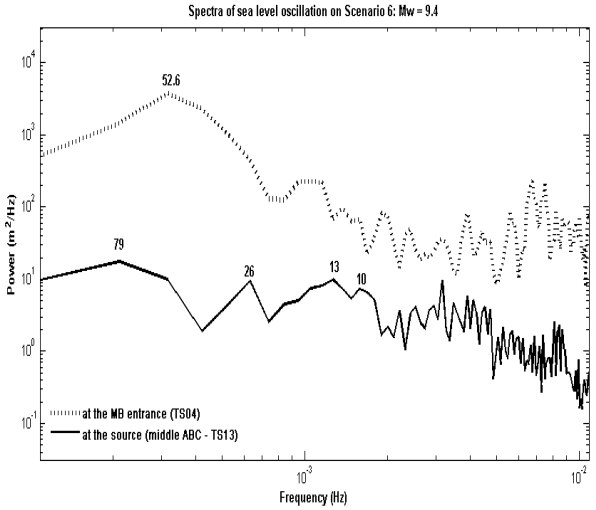

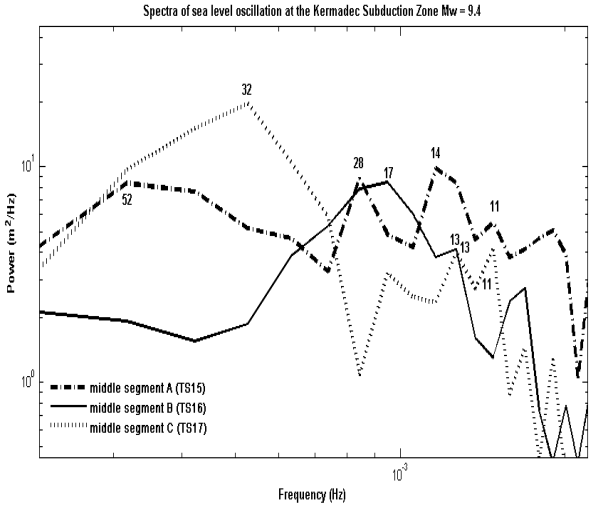

p. Scenario 6: M_w = 9.5